Phytochemical Investigations, Antibacterial and Antioxidant Activities, and *In Silico* Molecular Docking Studies of Stem Bark Constituents of *Dodonaea angustifolia* L. f

Adane Mulisa Risa

A Thesis Submitted to the Department of Applied Chemistry

School of Applied Natural Sciences

Presented in Partial Fulfillment of the Requirements for the Degree of Master's in Applied Chemistry (Specialization in Medicinal Chemistry)

Office of Graduate Studies

Adama Science and Technology University

May, 2023

Adama, Ethiopia

Phytochemical Investigations, Antibacterial and Antioxidant Activities and *In Silico* Molecular Docking Studies of Stem Bark Constituents of *Dodonaea angustifolia* L. f

Adane Mulisa Risa

Advisor: Yadessa Melaku (PhD)
Co-Advisor: Ankita Garg (PhD)

A Thesis Submitted to the Department of Applied Chemistry
School of Applied Natural Sciences
Presented in Partial Fulfillment of the Requirements for the Degree of Master's in Applied Chemistry (Specialization in Medicinal Chemistry)

Office of Graduate Studies
Adama Science and Technology University

May, 2023
Adama, Ethiopia

DECLARATION

I hereby declare that this thesis entitled **"**Phytochemical investigations, antibacterial and antioxidant activities and *in silico* molecular docking studies of stem bark constituents of *Dodonaea angustifolia* L. f**"** is my original work. That is, it has not been submitted for the award of any academic degree, diploma or certificate to any other university. All sources of materials that are used for this thesis have been duly acknowledged through citations.

Adane Mulisa Risa	_____	_____
Name of student	Signature	Date

RECOMMENDATION OF ADVISORS

We, the advisors of this thesis, hereby certify that we have read the revised version of the thesis entitled **"**Phytochemical investigations, antibacterial and antioxidant activities and *in silico* molecular docking studies of stem bark constituents of *Dodonaea angustifolia* L. f**"** prepared under our guidance by Adane Mulisa, submitted in partial fulfillment of the requirements for the degree of masters of science in applied chemistry (Medicinal Chemistry). Therefore, we recommend the submission of revised version of the thesis to the department following the applicable procedures.

Yadessa Melaku (PhD)	_____	_____
Major Advisor	Signature	Date
Ankita Garg (PhD)	_____	_____
Co-Advisor	Signature	Date

APPROVAL PAGE

We, the advisors of the thesis entitled "Phytochemical investigations, antibacterial and antioxidant activities and *in silico* molecular docking studies of stem bark constituents of *Dodonaea angustifolia* L. f" and developed by Adane Mulisa, hereby certify that the recommendation and suggestions made by the board of examiners are appropriately incorporated into the final version of the thesis.

_____	_____	_____
Major Advisor	Signature	Date
_____	_____	_____
Co-Advisor	Signature	Date

APPROVAL OF BOARD OF EXAMINERS

We, the undersigned, members of the Board of Examiners of the thesis by Adane Mulisa have read and evaluated the thesis entitled "Phytochemical investigations, antibacterial and antioxidant activities and *in silico* molecular docking studies of stem bark constituents of *Dodonaea angustifolia* L. f" and examined the candidate during the open defense. This is, therefore, to certify that the thesis is accepted for partial fulfillment of the requirement of the degree of Master of Science in applied chemistry (Medicinal Chemistry).

Chairperson	Signature	Date
Internal Examiner	Signature	Date
External Examiner	Signature	Date

Final approval and acceptance of the thesis are contingent upon the submission of its final copy to the Office of Postgraduate Studies (OPGS) through the Department Graduate Council (DGC) and School Graduate Committee (SGC).

Department Head	Signature	Date
School Dean	Signature	Date
Office of Postgraduate Studies, Dean	Signature	Date

ACKNOWLEDGEMENT

Above all, I thank the Almighty God and His mother St. Virgin Marry for giving me strength and courage in my life. I sincerely thank Dr. Yadessa Melaku, who has been kindly supervising me with continuous guidance, suggestions, valuable practical support and encouragement as an advisor in this thesis work. I express my sincerest gratitude to him for his kindness, respect and exemplary work habits. Also, I would like to thank my co-advisor Dr. Ankita Garg for her unreserved help and guidance.

I would like to express my deepest gratitude to Dr. R. Venkatesha Perumal (Department of Applied Chemistry, ASTU) for the molecular docking analysis. I extremely thank Addis Ababa University, Department of Chemistry for helping me with NMR analysis; Adama Science and Technology University, department of Biology for providing space for antibacterial activity test in their laboratory. My special gratitude also goes to Mr. Leta Guta for carrying out the antibacterial tests and training me valuable technical skills.

I am grateful to my classmates Mrs. Bethlehem Behailu, Mr. Yalew Amare, Terfo Yilma and my beloved friends for their advice and encouragement. My heartfelt thanks also extend to Mr. Tolosa Gutema, Hadush Gebrehiwot, Bihon Abera, Urgessa, Kebede Shenkute, Mrs. Emebet Getaneh and Merima for their special professional experience sharing, unreserved help and cooperation. I would like to express my deepest gratitude to my beloved mother W/ro Tsehay G/Hana for her prayer and encouragement, all my families for their never ending support throughout my life and to my friend Mrs. Peacock Mulugeta, who worked hard with me and gave me strength.

Finally, I thank my academic instructors and supervisors at department of Applied Chemistry, Adama Science and Technology University, who have been an example to me during my MSc studies. Last, but not least I would like to thank Adama Science and Technology University, Applied Chemistry department for giving the opportunity to pursue my MSc studies and Dilla University for leave of absence.

TABLE OF CONTENTS

PAGE

LIST OF TABLES

TABLE PAGE

LIST OF FIGURES

FIGURE PAGE

LIST OF APPENDIXES

ACRONYMS AND ABBREVIATIONS

ADMET	Absorption, Distribution, Metabolism, Excretion and Toxicity
ATCC	American Type Culture Collection
AMR	Antimicrobial resistance
BBB	Blood Brain Barrier
CLSI	Clinical and Laboratory Standards Institute
$CDCl_3$	Deuterated chloroform
COPD	Chronic obstructive pulmonary disease
DMSO	Dimethyl Sulfoxide
DNA	Deoxyribose Nucleic Acid
DPPH	1,1-diphenyl-2-picrylhydrazyl
GI	Gastrointestinal
IC_{50}	50 % Inhibition Concentration
MHA	Mueller–Hinton agar
MIC	Minimum Inhibitory Concentration
MRSA	Methicillin-resistant Staphylococcus aureus
NMR	Nuclear Magnetic Resonance
PDB	Protein Data Base
P-gp	P-glycoprotein
R_f	Retention Factor
SAR	Structural Activity Relationship
TLC	Thin Layer Chromatography
TMS	Tetramethylsilane
ROS	Reactive oxygen species
UV-Vis	Ultra Violet and Visible
WHO	World Health Organization

ABSTRACT

*Plant derived therapies that mitigate infectious disease and oxidative stress may be beneficial in the treatment of wide range of diseases. D. angustifolia is commonly known as Hitacha in Afan Oromo, Kitkita in Amharic, traditionally used for the treatment of variety conditions. This study was aimed to identify antibacterial and antioxidant compounds from the extracts of D. angustifolia. In view of this, stem bark of D. angustifolia was extracted with dichloromethane and dichloromethane:methanol (1:1) and the later extract was further partitioned. The dichloromethane extract after silica gel column chromatography afford six compounds identified as stigmasterol (**45**), stigmasterol derivatives (**46**), 2-hydroxy-3-(stearoyloxy) propanoic acid (**47**), 2,3-dihydroxypropyl stearate (**48**), stearic acid (**49**) and hexacosane (**50**). The structures of the isolated compounds were characterized using NMR spectroscopic techniques. Additionally, five compounds previously isolated from ethyl acetate leaves extract of D. angustifolia, including 2-hydroxy-15,16-epoxyceloda-3,13(16),14-trien-18-oic acid (**6**), santin (**25**), pinocembrin (**26**), 5,7,4'-trihydroxy-3,6-dimethoxyflavone (**28**) and 5,6,5'-trihydroxy-3,7,4'-trimethoxyflavone (**51**) were included herein for bioassay and in silico computational studies. The antibacterial and antioxidant activities were evaluated using agar disc diffusion method against four strains of bacteria and DPPH methods, respectively. The antibacterial evaluation showed highest activity with the aqueous methanol soluble portion of stem bark extract against E. coli (13.00±2.52 mm at 100 mg/mL); compound **45** against P. aeruginosa (13.33±0.88 mm); pinocembrin (**26**) against E. coli and S. pyogenes (12.67±0.88 mm and 11.00±0.58 mm) and compound **28** against S. aureus (12.00±1.00 mm) each at 2 mg/mL, compared with ciprofloxacin (ranging from 16.83±0.70 – 21.67±1.20 mm at 30 μg/mL). The highest percent inhibition of the DPPH radical were observed with aqueous methanol soluble portion (IC_{50}: 13.15 μg/mL); pinocembrin (**26**) (IC_{50}: 0.089 μg/mL), compared with ascorbic acid (IC_{50} of 0.11 μg/mL). Molecular docking study was done using Auto-Dock Vina, where pinocembrin (**26**) and compound **45** exhibited highest binding affinity (-8.1 and -7.4 kcal/mol) with the target DNA gyrase B and Santin (**25**) (-5.1 kcal/mole) with S. aureus pyruvate kinase. Additionally, compounds **6**, **25, 26, 28, 45** and **51** showed higher binding affinity with the target human peroxiredoxins 5. The current study revealed that the plant is promising source of antimicrobial and antioxidant compounds which support the traditional use of D. angustifolia for the treatment of infections.*

***Key words**: Dodonaea angustifolia, Antibacterial, Antioxidant, Molecular docking, ADMET*

1. INTRODUCTION

1.1 Background

Human beings have been dependent on herbs and medicinal plants as sources of food and treatment from time immemorial. Plants are the sources of different chemical constituents, which in general have nutritional, medicinal and pharmaceutical uses (Abate *et al*., 2022). Medicinal systems around the world, which has been developed thousands of years ago heavily relied on natural products, which is the backbone of traditional system of healing throughout the globe (Wink, 2015). The plant crude extracts or pure compounds are significantly used to treat diverse ailments by generations of indigenous practitioners (Dekebo, 2019; Stéphane *et al*., 2012). The medicinal value of those plants is due to the presence of a variety of secondary metabolites such as alkaloids, flavonoids, terpenoids etc., which are synthesized naturally in different parts of the plant body tissue including the bark, root, leaves, stem, flower, fruits, and seeds (Ates & Yalcin, 2022).

The World Health Organization (WHO, 2013) estimates that 80% of Asian and African populations rely on traditional medicine for their primary health care needs and in the developed countries 70%–80% of the population use some form of complementary and alternative medicine (Bultum *et al*., 2019). Ethiopia is one of the six plant-rich countries in Africa (Abate *et al*., 2022), which estimated to contain between 6500 and 7000 species of higher plants of which about 12% are endemic. It is estimated that about 80% of the Ethiopian population, predominantly in rural areas uses traditional medicine, due to the cultural acceptability of healers, local pharmacopeias, the relatively low cost and difficult access to modern health facilities (Ayele, 2018).

A wide range of microbes, including bacteria, viruses and fungi become resistant to standard commercial drugs used to treat infections. The problem is aggravated by the emergence of multidrug microbial resistance to standard drugs on the market (Desai *et al*., 2017; Singh *et al*., 2021). In developing countries such as Ethiopia, the load is so serious. Therefore, there is still needed to discover and investigate new and effective antimicrobial drugs (Hailemariam *et al*., 2021).

Highly reactive free radicals and oxygen species are found in biological systems (Sies *et al*., 2017). The oxidative stress leads to the production of reactive oxygen species (ROS). Their

removal leads to oxidative damage of cell membranes, mitochondria, lipids and proteins. Free radical damage related to oxidative stress causes various diseases, including atherosclerosis, chronic obstructive pulmonary disease (COPD), Alzheimer's disease, and cancer. Antioxidants have been used to avoid oxidative stress (Makhaeva *et al*., 2017; Raghu, 2019).

Dodonaea is one of the 150 genera found in the family of *Sapindaceae*, also known as the soapberry family. The genus comprises about 60-70 species widely distributed in the warmer parts of most countries (Beshah *et al*., 2020; Saeidnejad, 2021). *D. angustifolia* is one of the well-known species of this genus commonly known as Hitacha in Afan Oromo, Kitkita in Amharic and Sarka in Gamogofa (Ethiopia) (Berhan *et al*., 2006) and Sand Olive, sticky hop-bush in English (Orwa *et al*., 2009). Various parts of the plant *i.e.* stems, leaves, seeds, roots, barks, and aerial parts have been traditionally used for the treatment of fever, swellings, colds, oral thrush, measles, as an antipruritic in skin rashes (Naidoo *et al*., 2012; Van Wyk *et al*., 2002), viral dermal infections caused by herpes zoster (Tegen *et al*., 2021; Teklay *et al*., 2013), rheumatism, uterine colic and other disorders involving smooth muscles, toothache, skin burn, tumor and wound healing (Getie *et al*., 2003). It is also used as analgesic, antimalarial, antioxidant, antiulcer and anti-inflammatory (Berhan *et al*., 2006; Muhammad *et al*., 2012, 2016). In addition, the leaf have been also used to treat human and livestock diseases, like evil eye, ticks and diarrhea by means of boiling, grinding and squeezing (Banchiamlak & Young-dongKim, 2019).

Moreover, the genus *Dodonaea* contained number of secondary metabolites isolated by different researchers. Among which terpenoids, flavonoids, phenolics are major isolated classes of compounds which possess remarkable pharmacological activities (B.Anilreddy, 2009; Beshah *et al*., 2020). In this context, the identification and biological assay of phytochemicals plays great role. In view of the above mentioned facts this study was undertaken to identify antibacterial and antioxidant compounds from the extracts of *D. angustifolia* (Sapindaceae), with their *in silico* molecular docking studies, ADMET and drug likeness predictions.

1.2 Statement of the problem

Infectious disease caused by a variety of microbes including bacteria, viruses, and fungi has been a serious challenge. The problem is exacerbated by the emergence of multidrug microbial resistance to standard commercial drugs (Digafie *et al*., 2021). Genomic studies on various microorganisms indicate that prolonged use of antimicrobials and antibiotics makes these microorganisms more resistant to drugs (Ellington *et al*., 2017). Therefore, there is a need to discover new antimicrobial compounds or extracts to address the crucial problem of increasing microbial resistance.

Oxidative stress may act as either primary (e.g. radiation) or secondary (e.g. COPD, hypertension and Alzheimer disease) cause of diseases. Thus, plant derived therapies that mitigates oxidative stress may be beneficial in the treatment of wide range of diseases (Makhaeva *et al*., 2017; Raghu, 2019). Owing to this fact, the identification and characterization of natural products with antioxidant activity has received much interest over the past few years.

Medicinal plants plays significant role in the treatment of various human and livestock ailments. In Africa up to 80% of the population uses traditional medicine to help meet their health care needs. The use of traditional medicine also remains huge unfold in Ethiopia and yet majority stays scientifically neglected and undiscovered (Wolde-mariam *et al.*, 2015).

The selected plant species have been traditionally used for the treatment of variety of conditions. However, to the best of our knowledge the stem bark of *D. angustifolia* has not been studied for isolation of compounds and biological activities. There have been also few scientific reports on the antimicrobial and antioxidant activities of compounds isolated from the leaves, aerial and leaf surface exudate parts of the plant species (Getie *et al*., 2003; T. Ngabaza *et al*., 2017; Thamsanqa Ngabaza, 2016; L. Omosa *et al*., 2016; L. K. Omosa *et al*., 2014; Teffo *et al*., 2010). The plant was selected for this study on the basis of medical importance and their genera are rich source of variety classes of secondary metabolites with different biological properties.

In addition, as continuity proof of research findings on the selected medicinal plant, this study also contained of bioassay and *in silico* computational studies of five compounds, which were previously isolated from ethyl acetate leaves extract of *D. angustifolia* by Yadessa Melaku (PhD) and his coworkers. Among which santin (**25**) and pinocembrin (**26**) have minimal

reports for their antimicrobial and antioxidant activities (L. K. Omosa *et al*., 2014; Teffo *et al*., 2010), while compounds **6, 28** and **51** had no prior reports of antibacterial and antioxidant activities. Therefore, this study was aimed at identification of antibacterial and antioxidant compounds from the stem bark and leave extracts of *D. angustifolia*.

1.3 Objectives

1.3.1 General objective

- The general objective of this study was to identify antibacterial and antioxidant compounds from the stem bark and leave extracts of *D. angustifolia*.

1.3.2 Specific objectives

- Conduct phytochemical screenings on the dichloromethane, dichloromethane:methanol and methanol soluble portion stem bark extracts of *D. angustifolia*.
- Isolate compounds from the stem bark extract of *D. angustifolia* using silica gel column chromatography.
- Characterize the structure of compounds isolated from the stem bark extract of *D. angustifolia* using spectroscopic method (^{1}H-NMR, ^{13}C-NMR, and DEPT-135) and in comparison with literature data.
- Evaluate the antibacterial activities of the extracts and isolated compounds from stem bark and leaves extracts of *D. angustifolia* using disk diffusion method against selected Gram-negative (*E. coli* and *P. aeruginosa*) and Gram-positive (*S. aureus* and *S. pyogenes*) pathogenic bacteria.
- ✓ Evaluate the antioxidant activity of the extracts and isolated compounds using DPPH method.
- ✓ Conduct *in silico* molecular docking analysis of the isolated compounds using Auto-Dock Vina (MGLTools-1.5.6) software program on selected protein targets (*E. coli* DNA gyrase (PDB ID: 6F86), *S. aureus* pyruvate kinase (PDB ID: 3T07), Human peroxiredoxin 5 (PDB ID: 1HD2) and human topoisomerase II β (PDB ID: 3QX3).
- ✓ Predict *in silico* drug likeness and ADMET profile of the isolated compound using Swiss ADME, PreADMET and ProTox-II tools.

1.4 Significance of the study

Continuing scientific evidences on the phytochemicals, structural elucidation and bioactive constituents of plant origin may help the sustainable use of natural products in the drug discovery and development research. Therefore, the finding of this study might help to:

- Provide documented information about ethnomedicinal uses, chemical constituents and biological activity of *D. angustifolia.*
- Arrive at promising bioactive compounds to use as lead compound for drug discovery.
- Provide compounds or extracts with antimicrobial activity that might help to address the crucial problem of increasing microbial resistance.
- Provide valuable information observed from promising *in vitro* activity with *in silico* molecular docking analysis on target protein of selected strain of microorganisms, disease target and their pharmacokinetic & drug likeness predictions.
- Finally, enhance interest, confidence, knowledge and development toward phytochemical studies and computational approaches.

2. LITERATURE REVIEW

Medicinal plants and their bioactive constituents have been used for hundreds of years as source of a biologically active novel compounds. Statistically around 50 % of the new chemical entities are either obtained from natural products or natural product analogues (Li & Vederas, 2009; Stéphane *et al*., 2012). Natural products are currently of considerable significance due to their unique attributes as a significant source of therapeutic phytochemicals and their efficacy, safety, and minimal side effects (Nn, 2015).

2.1 The Family Sapindaceae and the Genus *Dodonaea*

Sapindaceae, also referred to as the soapberry family, is a family of flowering plants that comprise of about 150 genera with 2000 species distributed in temperate to tropical regions, many in laurel habitat, throughout the world (S.Veliyil., 2019). They exist as trees and shrubs, and tendril-bearing vines which are one of the most important forest species to be conserved and valued due to their multiple uses, high nutritional content and medicinal value (Temitope & Ogundipe, 2012). About fourteen genera belonging to the family Sapindaceae (*Dodonaea*, *Paullinia, Pappea*, *Filicium*, *Erythrophsa*, *Zanha*, *Cardiospermum*, *Allophylus, Deinbollia*, *Lepisanthes*, *Bottegoa*, *Lecanidiscus*, *Haplocoelum* and *Blighia*) and nineteen species are registered in the flora of Ethiopia (Hedgerg & Edwards, 1989; Melaku, 2015).

The genus *Dodonaea* comprises about 60-70 species and used for various activities. *Dodonaea viscosa, D. spatulate, D. angustifolia, D. polyandra and D. ceratocarpa* are well-known species of this genus (Beshah *et al*., 2020; Saeidnejad, 2021). Most of the Dodonaea genus are restricted to continental Australia (approximately 60 species), one in New Guinea (*D. polyandra*), one species endemic to Madagascar (*D. madagascariensis*) and one species (*D. angustifolia*) widely distributed in all continents (Harrington & Gadek, 2009; Melaku, 2015).

2.1.1 Taxonomic classification:

Kingdom: Plantae,
Subkingdom: Viridiplantae,
Infrakingdom: Streptophyta,
Superdivision: Embryophyta,
Division: Tracheophyta,
Subdivision: Spermatophytina,

Class: Magnoliopsida,

Superorder: Rosanae,

Order: Sapindales,

Family: Sapindaceae,

Genus: *Dodonaea*,

Species: *Dodonaea angustifolia* (Al-Snafi, 2017).

2.2 Ethnobotanical Uses of the genus *Dodonaea*

Several *Dodonaea* species were used extensively and regularly by traditional practitioners for different ailments. The stem, roots, leaves and sometimes the fruits parts are used in the formulation of traditional medicine (Beshah *et al*., 2020).

Dodonaea has been traditionally used in the treatment of inflammation, kidney pain, sore throat, intestinal parasite, herpes, wounds burn, rheumatism, cough, toothache, skin burn, skin infection, tumor and wound healing (Getie *et al*., 2003). The infusions of the plant have been used in traditional medicine in different parts of the world as carminative, diuretic, anti-epileptic, anti-rheumatic and pain reliever especially in nervous headache and migraine (Hajhashemi *et al*., 2003).

The aerial parts, leaves and tips of *Dodonaea viscosa var. angustifolia* are traditionally used in folk medicine of Latin America, China, Africa, and India for the treatment of fever, swellings, colds, oral thrush, measles and as an antipruritic in skin rashes (Naidoo *et al*., 2012; Van Wyk *et al*., 2002). The powdered leave juice is used for the treatment of trachoma and to expel roundworms (Rani, M. S et al., 2009). The plant is gargled for oral thrush and the twigs are chewed to clean the teeth (Akhalwaya *et al*., 2018).

In Ethiopia, the dry leaves of *D. angustifolia* alone or mixed with other plant (e.g. *Clematis hirsute*) have been used to treat viral dermal infections caused by herpes zoster (Tegen *et al*., 2021; Teklay *et al*., 2013). The crushed fruit and seeds mixed with honey is eaten as a remedy against malaria in different areas of Ethiopia (Berhan *et al*., 2006; Teklay *et al*., 2013). Furthermore, the shoot apex is charred on an open fire and the powder is mixed with butter and applied to treat the affected area called chife in local names. And to treat any broken part of body, the leaves are crushed and applied as bandage being held by bamboo (Kerkeha), Shembeko and tied by a rope, practiced in different part of the country (Wolde-mariam *et al*.,

2015). The stems are used as fumigants to treat rheumatism (Rani, M. S *et al*., 2009). In addition, the leaf have been also used to treat human and livestock diseases, like evil eye, ticks and diarrhea by means of boiling, grinding and squeezing (Banchiamlak & Young-dongKim, 2019).

2.3 *Dodonaea angustifolia*

The genus *Dodonaea* become named after Rambert Dodoaens, a well-known sixteenth century physician and writer on plants (Orwa *et al*., 2009). *D. angustifolia*, commonly known as Kitkita in Amharic, Hitacha in Afan Oromo, and Sarka in Gamogofa (Ethiopia) (Berhan *et al*., 2006), and referred as Sand Olive, sticky hop-bush in English (Orwa *et al*., 2009), is a variable shrub or tree, usually 2-8 m tall; branchlets rusty red and resinous; the bark dark grey, fissured and peeling. All parts of the plant are hairless. The taxonomy of the species has been confusing due to its big distribution and similarity to the closely related *D. viscosa* (Orwa *et al*., 2009).

It is widely distributed in four continents namely Australia, Africa, Asia and South America (L. K. Omosa *et al*., 2010). The greatest center of diversity appears to be the Southeast Asian region. It occurs naturally in different African countries including Ethiopia, Kenya, Somalia, Senegal, Nigeria, Mozambique, Madagascar, Democratic Republic of Congo, and South Africa. *D. angustifolia* is a hedge plant in East Africa which reproduces itself from seed very freely and grows on dry rocky slopes between 1500 and 2100 m throughout Ethiopia (Cunningham *et al*., 2004; Melaku, 2015).

Figure 1: Picture of *Dodonaea angustifolia* L. f from the outskirts of Adama Science and Technology University, Adama, Ethiopia (Picture taken by Adane Mulisa on 04/04/2022).

2.4 Phytochemical studies

Knowledge about chemical constituents of a medicinal plant is important for optimizing extraction procedures, understanding pharmacological activity as well as potential toxicity and interaction with pharmaceutical drugs (Anode et al., 2018). Phytochemicals are produced by plants via primary and secondary metabolism. The latter are produced either as a result of the organism adapting to its surrounding environment or for its own survival and defense against predators.

Phytochemical screening done by Anode *et al.,* on the leaves, stem and bark extracts of *D. angustifolia* using ethanol, methanol and diethyl ether were reported the presence of diverse groups of plant metabolites such us, volatile oil, anthraquinones, terpenoids, saponins, tannins, glycosides, steroids, phenolics etc. The study also indicates flavonoids are detected in leaf and ethanolic stem extracts, but not detected in the bark extracts. Steroids was present in ethanolic leaf extract and in bark extracts, while tannin was present only in methanolic leaf and bark extracts (Anode et al., 2018). Though, little work has been conducted on the stem bark of *D. angustifolia* found in Ethiopia where it grows in a variety of habitats.

Other studies on *Dodonaea* species especially *D. viscosa* had reported low concentration of steroids in the ethanolic leaf extracts and absence in bark and stem of the plant extracts (Anode et al., 2018; Saranya & Divyabharathi, 2019). Overall, phytochemical screenings on the extracts from the genus *Dodonaea* was found to contain secondary metabolites like flavonoids, terpenoids, tannins, steroids, phenolics, and saponins abundantly (Anode et al., 2018; Khurram et al., 2011; Riaz et al., 2012).

2.4.1 Chemical constituents of the genus *Dodonaea*

The genus *Dodonaea* contained number of secondary metabolites isolated by different researchers. The leaf, aerial and leaf surface exudate parts of plant are frequently considered for investigation, while the stem bark and root parts of the plant were the least investigated one. In general, more than eighty (80) compounds have been isolated from Dodonaea genus, out of these one fourth (¼) of bioactive compounds were isolated from *D. angustifolia* species. Among which terpenoids, flavonoids, phenolics are major isolated compounds along with minimal report for inositols, steroids and saponins which possess remarkable pharmacological

activities. The alkaloids, anthraquinones, essential oils and others are under-investigated (B.Anilreddy, 2009; Beshah *et al*., 2020).

Though, there has been much phytochemical works done on the *Dodonaea* genus, but to the best of our knowledge compound isolation from the stem bark of *D. angustifolia* species are not investigated yet. The summaries for the phytochemical investigation from the genus are presented in Table 1.

Table 1: Summary of chemical constituents isolated from the genus of *Dodonaea*

Isolated Compounds	Species	Structure number	References
Terpenoids			
Mkapwanin (neoclerodan-3,13-diene-16,15,18,19-diolide)	D. a	**1**	(L. K. Omosa *et al*., 2010)
15-Methoxymkapwanin	"	**2**	"
(Ent-3β,8α)-15,16-epoxy-13(16),14-labdadiene-3,8-diol	"	**3**	(L. K. Omosa *et al*., 2014)
Dodonic acid		**4**	"
2β-Hydroxyhardwickiic acid	"	**5**	"
2-Hydroxy-15,16-epoxyceloda-3,13(16),14-triene-18-oic acid	"	**6**	(Melaku *et al*., 2017)
Ent-16-hydroxylabdan-3α,8β-dihydroxy-13(14)-en-15,16-olide	"	**7**	"
(-)-6α-Hydroxy-5α,8α,9α,10α-cleroda-3,13-dien-15,16-olid-18-oic acid	D. v	**8**	(Mostafa *et al*., 2014)
13,14-Dihydroxy-15,16-dimethoxy-(-)-6α-hydroxy-5α,8α,9α, 10α-cleroda-3-en-18-oic acid	"	**9**	"
hautriwaic lactone	"	**10**	(Muhammad *et al*., 2016)
6*β*-Hydroxy-15,16-epoxy-5*β*,8*β*,9*β*,10*α*-cleroda-3,13(16),14-trien-18-oic acid	"	**11**	"
stictic acid	"	**12**	(Huang et al., 2010; Ortega et al., 2001)
hautriwaic acid	"	**13**	
Visclerodol acid	"	**14**	(Huang et al., 2010)
Carboxylic acid functionalized ent-Labdane diterpenoids	D.v	**15, 16**	(Deans *et al.*, 2018; Olivier *et al*., 2016)

13,17-epoxy-13-methyl-15-oxo-labda-7-ene	D. p	**17**	(Simpson *et al*., 2012)
17-Hydroxy-13-methyl-labda-7,13Z-diene-15-oic acid	"	**18**	"
Flavonoids			
5-Hydroxy-3,4′,7-trimethoxyflavone	D. a	**19**	(L. K. Omosa *et al*., 2014)
3,5-Dihydroxy-4′7-dimethoxyflavone	"	**20**	"
3,4′,5,7-Tetrahydroxy-6-ethoxyflavone	"	**21**	"
Isokaempferide (4′,5,7-trihydroxy-3-methoxyflavone)	"	**22**	"
Kumatakenin (3,5,7,4′-tetrahydroxy-3,7-dimethoxyflavone)	"	**23**	"
Rhamnocitrin (3,5,7,4′-tetrahydroxy-7-methoxyflavone)	"	**24**	"
Santin (5,7-dihydroxy-3,6,4′-trimethoxyflavone)	"	**25**	(Melaku *et al*., 2017; L. K. Omosa *et al*., 2014)
Pinocembrin (5,7-dihydroxyflavone)	"	**26**	(Melaku *et al*., 2017; L. K. Omosa *et al*., 2014)
5,6,7-Trihydroxy-3,4′-dimethoxyflavone	"	**27**	(Melaku *et al*., 2017)
5,7,4′-Trihydroxy-3,6-dimethoxyflavone	"	**28**	(Melaku *et al*., 2017)
Visconataflavonol	D. v	**29**	(Uddin *et al*., 2017)
Viscosine (7,4′-dihydroxy-3,6-dimethoxyflavone)	"	**30**	(Muhammad *et al*., 2015; Uddin *et al*., 2017)
Kaempferol-3-methylether	"	**31**	(Muhammad *et al*., 2015)
(2S,3S)-3,5,7,4'-Tetrahydroxyflavanone (aromadendrin)	"	**32**	"
5-Hydroxy-7,3',4'-trimethoxy-6-acetoxy-3-prenylflavone	"	**33**	(Al-Aamri & Hossain, 2016)
5,6,8-Trihydroxy-7-methoxy-2-(4-methoxyphenyl)-4H-chromen-4-one	"	**34**	(T. Ngabaza *et al*., 2017)

5,7,4'-Trihydroxy-3'(3-methylbut-2-enyl)-3-methoxy flavones	D. p	**35**	(Simpson *et al*., 2011)
5,7-Dihydroxy-3'(3-methylbut-2-enyl)-3,4'-dimethoxyflavone	"	**36**	"
5,7,4'-Trihydroxy-3',5'(3-methylbuyt-2-enyl)-3-methoxyflavone	"	**37**	"
Phenolics			
Nebrodenside A	*D. v*	**38**	(Muhammad *et al*., 2012)
Vanillic acid	"	**39**	"
Docosyl caffeate	"	**40**	"
3,4-dihydroxybenzoic acid	"	**41**	(Muhammad *et al*., 2016)
Other constituent			
4-Methoxylstigmasterol	D. v	**42**	(Al Habsi & Hossain, 2018)
1-L-1-O-methyl-2-acetyl-3-P-Z-coumarylmyoinositol	"	**43**	(Mostafa *et al*., 2014)
1-L-1-O-methyl-2-acetyl-3-P-E-coumarylmyoinositol	"	**44**	"

D. a- *D. angustifolia*; **D. v**- *D. viscosa*; **D. p**- *D. polyandra*

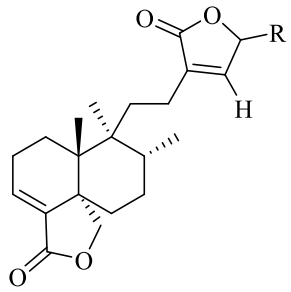

1 R = H
2 R = OMe

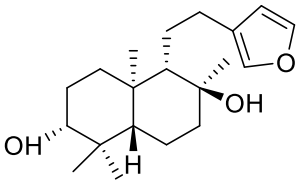

3

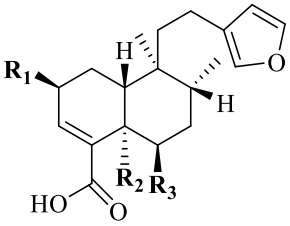

	R_1	R_2	R_3
4	H	Me	OH
5	OH	Me	H

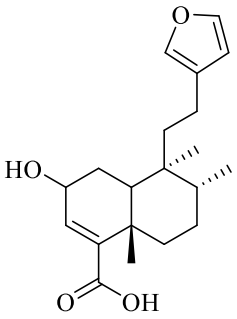

6

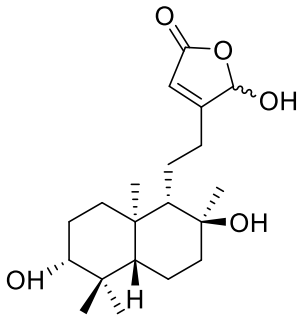

7

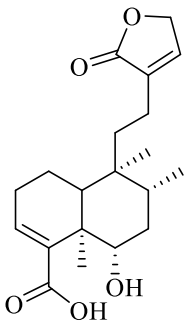

8

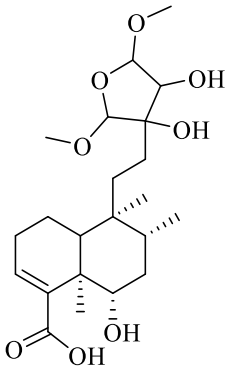

9

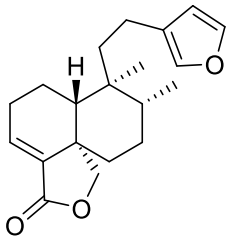

10

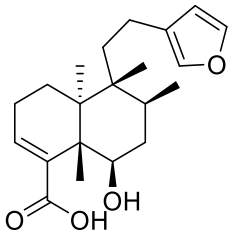

11

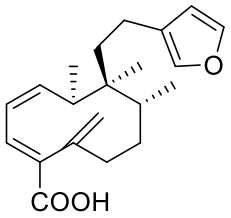

12

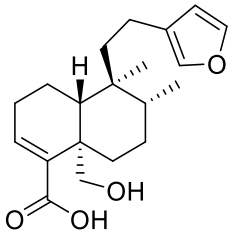

13

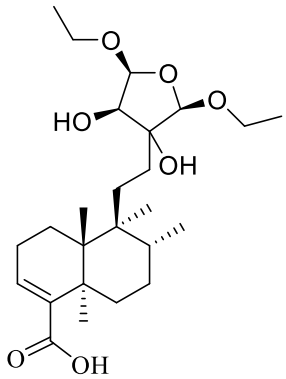

14

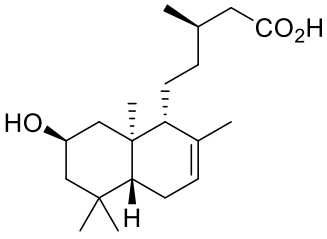

15

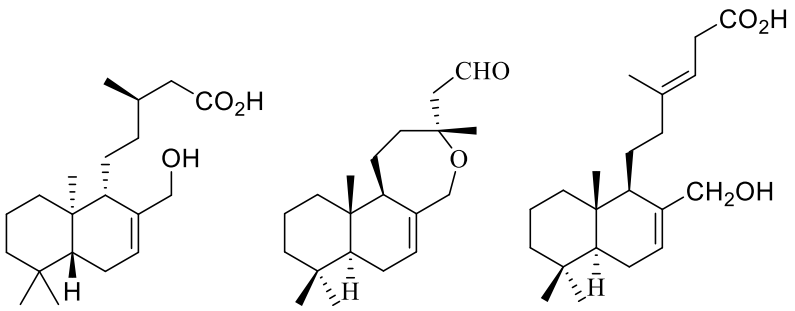

16 **17** **18**

Figure 1: Structures of terpenoids (1-18) isolated from genus *Dodonaea*

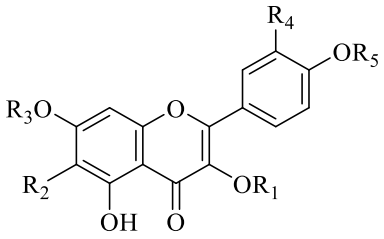

	R_1	R_2	R_3	R_4	R_5
19	Me	H	Me	H	Me
20	H	H	Me	H	Me
21	H	OMe	H	H	H
22	Me	H	H	H	H
23	Me	H	Me	H	H
24	H	H	Me	H	H
25	Me	OMe	H	H	Me

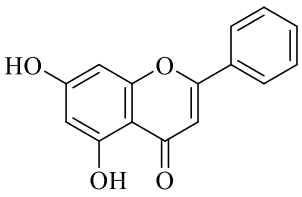

26

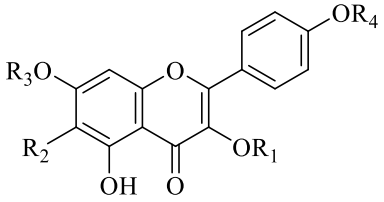

	R_1	R_2	R_3	R_4
27	Me	OH	OH	Me
28	Me	Me	OH	H

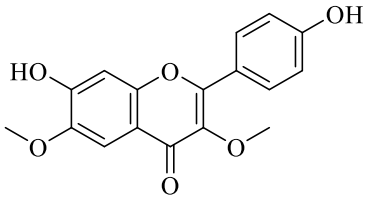

30

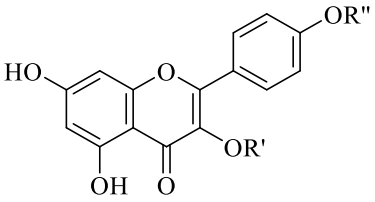

	R'	R''
31	CH_3	CH_3
32	H	H

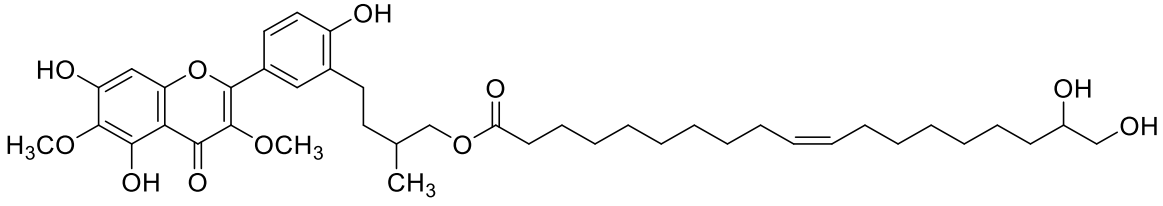

29

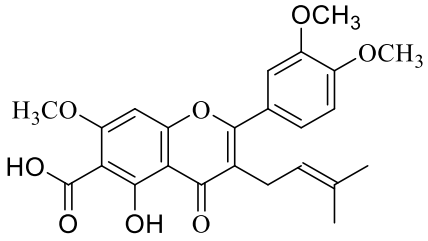

33

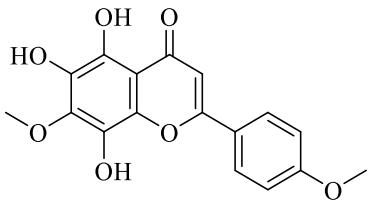

34

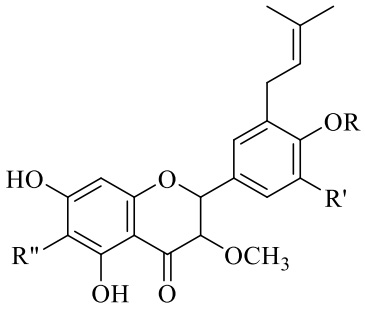

(35) R, R' and R" = H
(36) R = CH_3, R' and R" = H
(37) R = H; R' = 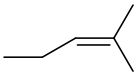 R" = H

Figure 2: Structures of flavonoids (19-37) isolated from genus *Dodonaea*

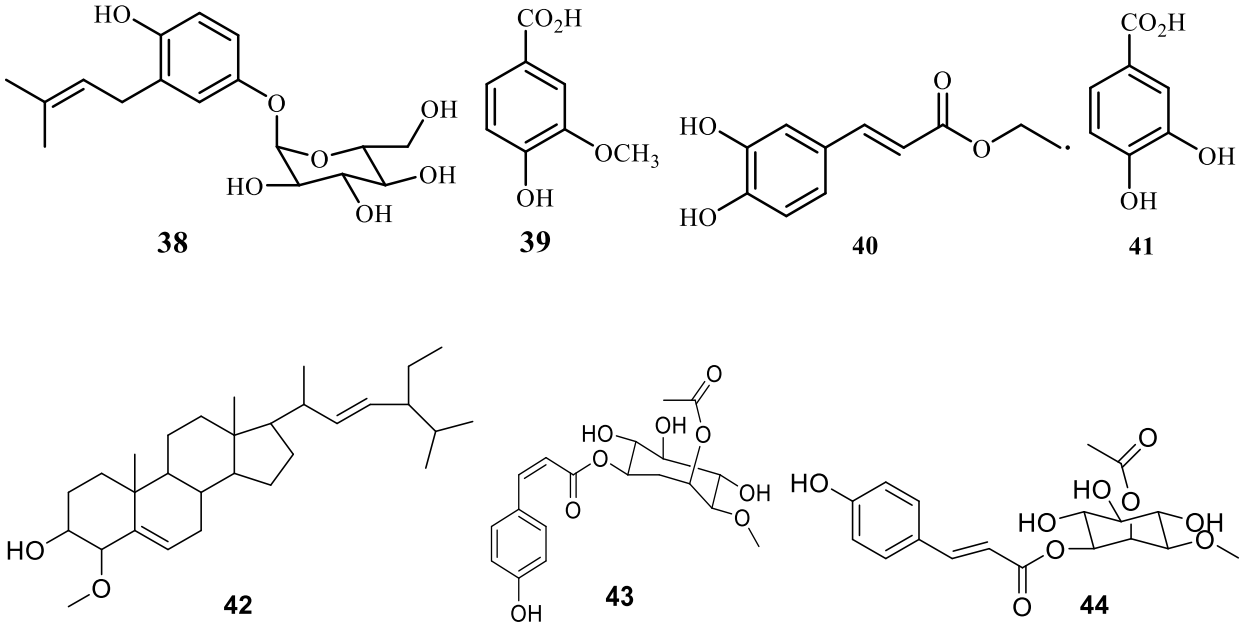

Figure 3: Structures of phenolic and other constituents (38-44) isolated from genus *Dodonaea*

2.5 Biological activities of the Genus *Dodonaea*

The genus *Dodonaea* shows various biological activities. Thus, the antimicrobial and antioxidant of *Dodonaea* genus (extracts and isolated compounds) were reviewed here in this literature. The leaf, aerial and leaf surface exudate parts of plant are frequently considered for investigation, while root part was the least investigated and the stem bark is under investigated for biological activities.

2.5.1 Antimicrobial activity

Literature survey reveals that the *Dodonaea* genus collected in different countries demonstrates variable biological activity. The genus *Dodonaea* was suggested to have the potential to be used in controlling oral infections (for a toothache and sore throat), diarrhea, used as antipuritic in skin rashes and for the treatment dermatitis (Akhalwaya *et al*., 2018; Ayele, 2018; Getie *et al*., 2003). Mostly plant leaves and its methanolic extracts have been reported to exhibit the highest antimicrobial activities, while no prior reports for the stem bark extracts. The methanol leaves extracts of the Ethiopian *D. viscosa* species showed antibacterial activity against *S. pyogenes* and *S. aureus* with inhibition zone of 10 mm & 9 mm at 100 mg/mL concentration, respectively and not active against the Gram negative bacteria (*P. aeruginosea* and *E. coli*), suggesting the potential of these plants to treat bacterial infections of the skin (Getie *et al*., 2003).

Study done by *S. Zonyane et al.,(2013)* were reported the methanolic and chloroform extract of *D. viscosa* mixed with other plant extract showed enhanced antimicrobial efficacy with additive and synergy interaction. Thus, methanol extract showed MIC values of 49µg/ml for *Staphylococcus aureus* and *Bacillus subtilis* and 98µg/ml for *Klebsiella pneumoniae* and *Escherichia coli* (Zonyane *et al*., 2013).

Additionally, a study done by *Omosa et al., (2014)* was revealed that, the surface exudates crude extracts of *D. angustifolia* showed antibacterial activity against *E. coli, S. aureus* and *B. pumilus, with* minimum inhibition concentration (MIC) values less than 625µg/well or/and expressed as with zone of inhibition 8.97mm, 9.32mm, and 9.27mm, respectively. Different isolated compounds were also showed varied antimicrobial activities. For instance, a quercetin derivative (3,4′,5-trihydroxy-3′,7-dimethoxyflavone) isolated from *D. angustifolia* showed a broad spectrum of antibacterial activity against *E. coli* and *B. pumilus* with MIC values less than 31.25µg/well (inhibition zone of 9.08mm & 8.97mm respectively) and against *S. aureus* with MIC below 62.5µg/well (inhibition zone of 9.37 mm) (L. K. Omosa et al., 2014). Rhamnocitrin with a similar oxygenation pattern; except for the absence of a methoxy group at 3′ position; was also inactive (L. K. Omosa *et al.*, 2014).

Moreover, the report was indicated the importance of a 3′-methoxy (OMe) group in flavonoids for activity against *E. coli*. Also, it was implied that for good activity against *S. aureus*, hydroxyl group at C-3 position in the flavone skeleton (e.g quercetin derivative) were important. Furthermore, among the isolated compounds hautriwaic acid lactone (**13**) and Santin (**25**) were

reported to have good antifungal activity against *S. cerevisiae* with MIC values < 3.9 and 7.8µg/well respectively, and their lipophilic nature were postulated to be contributor for this activity. However, they exhibited poor antibacterial activity with MIC value > 250 µg/well (L. K. Omosa *et al*., 2014).

Furthermore, a flavone (5,6,8-Trihydroxy-7,4-dimethoxyflavone (5,6,8-Trihydroxy-7-methoxy-2-(4-methoxyphenyl)-4H-chromen-4-one)) isolated form *D. viscosa var. angustifolia* species have been also reported for its better antimicrobial activity with MIC values of 0.2 mg/ml against common pathogens (*S. aureus, E. coli*) and unicellular fungi (*C. parapsilosis*) in a safe condition (T. Ngabaza et al., 2017). The antibacterial effects of flavones are generally due to the interference with the DNA synthesis in the pathogens and the effect was not cell-wall related. It was suggested that the hydroxyl group at position C-5 and C-7 is important for antibacterial activity. A hydroxyl group at C-4' was reported for activity with *P. aeruginosa*, but this was apparently not the case with *S. aureus* (T. Ngabaza *et al*., 2017; Teffo *et al*., 2010).

2.5.2 Antioxidant activity

Teffo *et al*., (2010) studied the antioxidant activity of isolated compounds from leaves of *D. viscosa* by DPPH (2,2-diphenyl-1-picrylhydrazyl) method. Out of the isolated compounds, 4'-O-methylkaempferol (EC_{50} = 75.49 ± 1.76 µM) and kaempferol (35.06 ± 0.85 µM) showed significant antioxidant activity, but lower than L-ascorbic acid (EC_{50}=13.55±0.28 µM) used as a standard antioxidant agent. The presence of those free-OH groups of kaempferol could be linked to higher antioxidant activity of the compound compared to other derivatives with more methoxylated groups. Methylation of free-OH groups in flavonoids substantially reduces the antioxidant activity of the compounds (Teffo *et al*., 2010).

A study done by Muhammad *et al.*(2015) reported the antioxidant activity of flavonoids from *D. viscosa* through six complementary test i.e. *β*-carotene-linoleic acid for lipid peroxidation; DPPH free radical, ABTS cation radical, superoxide anion radical scavenging, metal chelating, and CUPRAC assays. Among the compounds viscosine and 5,7-dihydroxy-3-(4’’-acetoxy-3’’-methylbutyl)-3,6,4’-trimethoxy flavone showed higher antioxidant activity in all tests. The study indicates the importance of “OCH_3” at C-6 that lies between two OH located at C-5 and C-7 to increase the antioxidant activity of the flavonoids (Muhammad *et al*., 2015).

Tauchen *et al.* (2015) studied the antioxidant activities of ethanol extract of 18 Ethiopian wild medicinal plants, one of which is *D. angustifolia* that demonstrated a moderate effect with IC_{50} of 22.2±1.2 µg/mL. Interestingly, the root extracts of *D. angustifolia* also exhibited significant combinatory antioxidant and anti-proliferative effect with excreting low or minimal toxicity to normal cells (Tauchen *et al*., 2015).

Antioxidant activity of *D. viscosa* leaf extract was studied by Al Habsi and Hossain, (2018) using DPPH method. It has been reported that ethyl acetate extract showed the highest antioxidant activity with percentage of inhibition value of 95.01 ± 0.18 at 200 µg/mL concentration. The isolated compounds of leaves of *D. viscosa*, 3,3′,4′,5,7-pentahydroxyflavone (98.09 ± 0.17 at 200 µg/mL) and 4-methoxystigmasterol (**42)** (94.68 ± 0.15 at 200 µg/mL) showed potent antioxidant activity by DPPH method in comparison to the reference gallic acid (Al Habsi & Hossain, 2018).

3. MATERIAL AND METHODS

3.1 Plant Material Collection, Identification and Preparation

The stem bark of *D. angustifolia* L. f. was collected from the outskirts of Adama Science and Technology University, Adama, Ethiopia, in April, 2022. The geographical coordinates of the area were 8°34'02.4" North latitude, 39°17'24.9" East longitudes. The plant material was identified by botanist Melaku Wendaferash (AAU, Biology department) and deposited at the National Herbarium of Ethiopia, Addis Ababa University with voucher specimen number AD001/2014. The collected stem bark sample was transported to the research laboratory, ASTU, thoroughly cleaned and dried under the shade for 10 days. It was ground into powder using analytical mills (mortar and pestle, blender machine).

3.2 Chemicals and Reagents

The chemicals and reagents used for the extraction, isolation, phytochemical analysis, and other activities in this study were silica gel (230-400 mesh), anhydrous sodium sulphate, sulphuric acid, hydrochloric acid, acetic anhydride, potassium iodide (Samir Tech- Chem PVT. LTD., 99.8%), iodine (Alpha Chemika, 98.5%), KOH, NaOH, Wagner's reagent. Solvents used in this study were dichloromethane (Loba Chemie PVT. LTD. 99%), *n*-hexane (Loba Chemie PVT. LTD. 99%), ethanol (Favor trading PLC, 99.9%), ethyl acetate (Loba Chemie PVT. LTD., 99.5%), methanol and distilled water. Muller Hilton Agar (MHA), DMSO (Srlchem, 99.5%), and DPPH reagent were used for bioassay. Ciprofloxacin pharmaceutical tablet and ascorbic acid were used as positive control for antibacterial and antioxidant test, respectively.

3.3 Instruments

Analytical Thin Layer Chromatography (TLC) was run on a 0.25 mm thick layer of silica gel GF254 (Merck) on aluminum plate. Spots were detected by observation under UV light (254 and 366 nm) followed by dipping in vanillin/H_2SO_4. Column chromatography was performed using silica gel (230-400 mesh, Merck) for isolation and purification of compounds. Samples were applied on column by either adsorbing on silica gel or dissolving in appropriate solvent. Solvents were evaporated under reduced pressure using Rotavapor (BUCHI). The absorbance of extracts and isolated pure compounds at different concentration was measured by UV Visible

spectrophotometer (Shimadzu, Model 1800, Japan) for the determination of antioxidant activity. ^{1}H and ^{13}C NMR spectra were measured on Bruker Avance instrument (Bruker Avance 400 MHz spectrometer), with tetramethylsilane (TMS) as the internal standard. Deuterated $CDCl_3$ was used as solvent and chemical shifts values were given in δ (ppm).

3.4 Extraction

The stem bark powder of *D. angustifolia* (600 g) was extracted with dichloromethane (3 L) by using a maceration for 72hrs, with vigorous shaking using mechanical shaker at 120 revolutions per minute (RPM). The solvent was evaporated from the extract by using rotary evaporator under reduced pressure at a temperature of 40°C to give dichloromethane extract (7.67 g). The marc was further extracted in dichloromethane:methanol (1:1) (3 L) for 72 hrs, filtered, and concentrated to afford dichloromethane:methanol (DCM:MeOH) extract (22 g).

After TLC analysis, the dichloromethane extract presents good spots when visualized under UV light. Based on this, DCM:MeOH extract (22 g) was dissolved in methanol and diluted with water to furnish 80% aqueous methanol extract. This was fractionated with dichloromethane and separated using separatory funnel.

Then, the DCM soluble portion was dried over anhydrous Na_2SO_4 and filtered and concentrated using rotary evaporator to give dichloromethane soluble portion (10 g). The aqueous MeOH portion (12 g) was dried. All the prepared extracts from the stem bark powder of *D. angustifolia* were used for the determination of their antibacterial and antioxidant activities.

3.5 Phytochemical screening

The dichloromethane, DCM:MeOH and aqueous MeOH extracts were analyzed for the presence of flavonoids, alkaloids, coumarin, saponins, tannins, steroids, flavonoids, anthraquinones, glycosides, phenolics and terpenoids based on the protocols available in the literature.

Test for Flavonoids (Shinoda Test (Magnesium hydrochloride reduction test)):

Each extracts (10 mg) was dissolved in 5 mL of methanol. The solution was warmed and magnesium ribbon was added. To this solution 2-3 drops of concentrated Hydrochloric acid was added. The appearance of pink, scarlet, crimson red or occasionally green to blue color after few minutes indicates the presence of flavonoids (Anode *et al*., 2018).

Tests for alkaloids (Wagner's test): The prepared extracts (10 mg) was separately stirred with 1% HCl (0.5 mL) in a water bath for 5 min and filtered into a test tube. 2 drops of Wagner's

reagent (iodine in potassium iodide) was added; the formation of a brown/reddish precipitate indicates the presence of alkaloids (Praiwala *et al*., 2019).

Test for steroids (*Libermann Burchard* test):

10 mg of prepared extracts was separately mixed with 5mL chloroform. To this 2 ml acetic anhydride and 2 drops of concentrated sulphuric acid was added from the side of test tube. First red, then blue and finally green colour appearance indicates the presence of a steroids (Nwodo & Nkwocha, 2015).

Test for Glycoside (*Keller-Killiani* Test):

The plant extracts (10mg) from each solvent was dissolved in 3 mL of glacial acetic acid containing 1 drop of ferric chloride solution. This was underlayed with 1 mL concentrated sulphuric acid. A brown ring at the interface was indicating the presence of deoxysugar characteristic of cardenolides. A violet ring may appear below the ring while in the acetic acid layer, a greenish ring may form (Anode *et al*., 2018).

Test for Coumarins

The plant extracts (10 mg) was dissolved in 5 mL ethanol and alcoholic KOH is added. Yellow colour which disappears on adding few drops of conc. HCl indicates the presence of coumarins (Anode *et al*., 2018).

Test for Terpenoids (*Salkowski's* test):

10 mg of the extracts was treated with 1 mL chloroform followed by few drops of concentrated H_2SO_4. Shaken well and allowed to stand for 5 min. Red color in the lower layer indicates the presence of sterols and the formation of yellow colored lower layer indicates the presence of triterpenoids (Santhi & Sengottuvel, 2016).

Test for Tannins (*Ferric Chloride* Test):

10 mg of the extracts was dissolved in distilled water to this solution 2 mL of 5% ferric chloride solution was added. Formation of blue green indicates presence of tannins.

Test for anthraquinones

20 mg of plant extracts from each solvent was put in a dry test tube and 5 mL of chloroform added and shaken for 5 min. The extract solution was filtered and the filtrate shaken with 5 mL of 10% v/v ammonia solution. A pink violet or red colour in the ammonical layer indicates the presence of anthraquinones (Anode *et al*., 2018).

Test for Phenols: The prepared extracts (10 mg) were dissolved in 5 mL of distilled water. To this, a few drops of 5% ferric chloride solution was added. A dark green color indicated the presence of phenolic compounds (Bargah & Rohit, 2015).

Test for Saponins (*Froth test*)*:*

10 mg of each extracts was diluted with 6 mL of distilled water in a test tube. The mixture was shaken vigorously while heating to boil. The formation of persistent foam indicates the presence of saponins (Anode *et al*., 2018).

3.6 Isolation of compounds

The extracts of dichloromethane and dichloromethane soluble portion obtained from DCM:MeOH extracts showed very close TLC profile and hence mixed together. The combined extract (**15** g) was adsorbed on silica gel and chromatographed over silica gel (160 g), using *n*-hexane for packing. Elution was carried out through gradual increment of polarity of ethyl acetate in *n*-hexane and in methanol as eluent. A total of 270 fractions (first three fractions with 100 mL and later each 20 mL) were collected through gradient elution following the color band (Table 2) and left to dry at room temperature. Fractions that showed the same TLC profiles were combined to afford 10 subfractions (F1-24, 25-49, 50-59, 60-69, 70-89, 90-119, 120-130, 131-159, 160-190 and 191-270).

Table 2: Column chromatographic fractionation of the dichloromethane extract of the stem bark of *D. angustifolia*

Solvent system	Gradient Ratio	Fractions number	Solvent system	Gradient Ratio	Fractions number
n-hexane	100 %	F_1–F_3	*n*-hexane/ ethyl acetate	40:60	F_{184}–F_{192}
n-hexane/ ethyl acetate	95:5	F_4–F_{12}		40:60	F_{193}–F_{200}
	90:10	F_{13}–F_{31}		30:70	F_{201}–F_{216}
	90:10	F_{32}–F_{39}		20:80	F_{217}–F_{224}
	85-15	F_{40}–F_{55}		10:90	F_{225}–F_{231}
	80:20	F_{56}–F_{78}	EtOAc	100	F_{232}–F_{251}
	75:25	F_{79}–F_{95}	EtOAc:methanol	90:10	F_{252}–F_{259}
	75:25	F_{96}–F_{113}		80:20	F_{260}
	70:30	F_{114}–F_{129}		70:30	F_{261}–F_{263}
	65:35	F_{130}– F_{144}		60:40	F_{264}–F_{269}
	60:40	F_{145}–F_{159}		50:50	F_{270}
	50:50	F_{160}–F_{174}			
	40:60	F_{175}–F_{183}			

Fractions **25-49** (6g) obtained from fractionation of dichloromethane extract (eluted with 9:1 and some fractions with 8.5:1.5, *n*-hexane:EtOAc), were rechromatographed over silica gel (120 g), using *n*-hexane for packing. Elution was carried out through gradual increment of polarity of ethyl acetate in *n*-hexane as eluent. A total of **161** fractions were collected, which were pooled together according to their TLC profile to afford **19** combined fractions. Elution started with *n*-hexane initially (200 mL, F1-10), followed with *n*-hexane:EtOAc gradient elutions (9.5:0.5, 120 mL, F11-24; 9:1, 90 mL, F25; **9:1, 60 mL, F26**; 8.5:1.5, 100 mL, F27; **8:2, 80 mL, F28**; **8:2, 90 mL, F29-33**; 7.5:2.5, F34-54; **7:3, 40 mL, F55**; **7:3, 20 mL, F56;** 7:3, F57-66; 6.5:3.5, F67-75; 6:4, F76-80; 5:5, F81-126; 4:6, F127-140; 3:7, F141-146; 2:8, F147-150; 1:9, F151-159; 100% EtOAc, F160-161).

Among the combined **19** fractions, **F26** (38mg) was diluted and applied on small column chromatography over silica gel (30 g) through isocratic elution of *n*-hexane:EtOAc (9:1) yielded compound **50** (28mg) as a solid.

F28 (80mg) was diluted and applied on small column chromatography over silica gel (20 g) by isocratic systems using 20% ethyl acetate in *n*-hexane. A total of 20 fractions were collocated. Out of the 20 fractions, sub-fraction **4** affords compound **48** (26 mg).

F29-33 (45mg) was diluted and applied on small column chromatography over silica gel (30 g), through isocratic elution using *n*-hexane:EtOAc (8:2), yielded compound **49** (22 mg) obtained as a white powder.

Fraction 55 (35 mg) obtained as white powder from combined fractions (eluted with 30 % EtOAc in *n*-hexane), was suspended in ethyl acetate (2 mL), shaken and the EtOAc soluble portion were decanted to afford compound **45** (21 mg). Likewise, **Fraction 56** (38 mg) was suspended in methanol (2 mL), shaken and the MeOH were decanted to afford compound **46** (11 mg). On the other hand, fraction **60-69 (300mg)** obtained from fractionation of dichloromethane extract, after rechromatographed over silica gel (60 g) afforded compound **47** (18 mg) as white crystal; R_f value of 0.42 (10% EtOAc in *n*-hexane as mobile phase).

3.7 Spectral data of isolated compounds

The spectroscopic techniques (^{1}H-NMR and ^{13}C-NMR) were employed to elucidate the structure of isolated compounds. The ^{1}H-NMR and ^{13}C-NMR were obtained in $CDCl_3$ on Bruker Avance 400 MHz spectrometer.

3.8 Evaluation of Biological Activities of the Extracts and Isolated compounds

Evaluation of the antibacterial and antioxidant activities of the stem bark extracts and isolated compounds from the leaves and stem bark of *D. angustifolia* were done in collaboration with the Department of Applied Biology, Adama Science and Technology University.

3.8.1 Antibacterial Activity

Antibacterial activity test was tested using Kirby–Bauer agar disc diffusion method originally described by Bauer *et al* (Bauer *et al*., 1966; Hudzicki, 2012) and currently recommended by the Clinical and Laboratory Standards Institute (CLSI) guideline, with slight modification to meet the present experimental conditions (CLSI, 2012).

All samples were evaluated for their antibacterial activity against two Gram-positive bacteria (*Staphylococcus aureus*, ATCC 25923 & *staphylococcus pyogenes* ATCC 19615) and two Gram-negative bacteria (*Escherichia coli* ATCC 25922 & *Pseudomonas aeruginosa* ATCC 27853) in comparison with ciprofloxacin as standard drug and DMSO as negative control. All bacterial strains are an American Type Culture Collection (ATCC) and obtained from Adama Public Health Research & Referral Laboratory Center. The bacteria were selected based on the availability and considering the likely bacterial strains that can cause bacterial infections.

The concentration of samples were prepared by dissolving required amounts in DMSO to give sets of four dilutions, 100, 50, 25, and 12.5 mg/mL for extracts and dilutions at 2, 1, 0.5, and 0.25 mg/mL for isolated compounds (Getie *et al*., 2003). Likewise, the reference antibiotics (Ciprofloxacin) were used at 30 µg/mL and DMSO as inert negative control (CLSI, 2012).

The bacterial cultures of each test organisms were prepared by taking 100 μ_L of bacterial subcultures and inoculated into 10 mL of sterile nutrient broth (inoculation medium) and grown overnight at 37°C. After incubation the turbidity of each bacterium was adjusted to 0.5 McFarland standards using nutrient broth solution. The prepared Muller Hinton Agar (MHA) media solution was poured (approximately 20 mL) to sterile petri-dishes aseptically and allowed to solidify. Then, the strains of bacteria were inoculated into the pre-labeled MHA plates using sterile cotton swab by streaking swabs over the entire sterile agar surface and the procedure was repeated 2 more times rotating the plates at 60˚ each time to ensure even distribution. A duplicate plate of each organism was prepared.

Sterile filter paper disks impregnated with test compounds, standard drug, with a diameter of 6 mm were placed over each MHA plate. Finally the plates were incubated at 37°C for 18 hr. The resulting diameters of zones of inhibition produced by the plant extracts, isolated compounds and standard antibiotic (ciprofloxacin) were measured using a ruler and expressed in millimeters. The experiment was performed in triplicate for each bacterium. The mean of zones of inhibition was calculated and expressed as mean ± SEM of triplicate (Table 10,Table 11 and Table 12).

3.8.2 Antioxidant Activity

The antioxidant activity of the extracts and isolated compounds of *Dodonaea angustifolia* was measured on the basis of the scavenging activity of the stable DPPH (1,1-diphenyl 2-picrylhyorazyl) free radical by measuring the absorbance at 517 nm according to the method used by *Al Habsi & Hossain* with modification (Al Habsi & Hossain, 2018). Serial dilutions were carried out with the stock solutions of 2 mg/mL for the plant extract and 0.4 mg/mL of isolated compounds to obtain concentrations of 1000, 500, 250, 125, 62.5 & 31.25 µg/mL and 400, 200, 100, 50, 25 & 12.5 µg/mL, respectively. The solutions were prepared using methanol as solvent. Each concentration of sample (2 mL) was placed in a clean test tube and DPPH solution (2 mL) was added to the same test tube (Al Habsi & Hossain, 2018). The DPPH solution was prepared by dissolving 4 mg of DPPH in 100 mL of MeOH.

The solution was shaken vigorously by hand and kept in a dark place for 30 minutes. Then, the absorbance was measured by using UV-Vis spectrophotometer at 517 nm. DPPH solution without the test sample was used as control and methanol solvent were used as blank. Whereas, the reference standard used in this method are L-ascorbic acid. The DPPH radical scavenging rate of each samples were calculated using the following formula from literature. The results are expressed as averages of three measurements (Sahu *et al*., 2013).

$$\text{Radical Scavenging Activity (\%)} = \frac{(Ac - As)}{Ac} \times 100$$

Where, Ac is the absorbance of the control (DPPH solution) and As is the absorbance of the sample (extracts and compounds) or standard (L-ascorbic acid).

The IC_{50} value is defined as the concentration of a substrate that causes 50 % loss of the DPPH activity. The lower the IC_{50} value, the higher is the scavenging potential (Riaz *et al*., 2012). The IC_{50} values of all samples were calculated by using GraphPad prism version 8, using nonlinear

regression analysis of the percentage radical scavenging activity against the concentration of the tested extracts/compounds.

3.9 *In silico* Pharmacokinetic and Drug likeness Prediction

The isolated compounds (**6, 25, 26, 28, 45, 47, 48, 49,** and **51**) were subjected to computational studies to predict their drug-likeness properties through determining the physicochemical properties required to become a drug like molecule, viz. Lipinski's rule of fine (ROF), i.e., MW ≤ 500 Daltons, cLog *P* ≤ 5, H-bond donors ≤5, and H-bond acceptors ≤10 (Lipinski *et al*., 1997) and Veber's parameters (Veber *et al*., 2002) (rotatable bonds ≤10 and topological polar surface area (TPSA ≤140 $Å^2$), as well as the pharmacokinetic parameters using SwissADME (Daina *et al*., 2017) and PreADMET (Lee *et al*., 2003) online tools. The online program ProTox-II (Banerjee *et al*., 2018) was used to predict the ligands' organ toxicity profiles and toxicological endpoints, as well as their LD_{50}. Furthermore, the cLogP and TPSA values of the compounds were plotted to predict human intestinal absorption (HIA) and blood brain barrier (BBB) access through BOILED-Egg model (Daina & Zoete, 2016).

3.10 *In silico* Molecular Docking

The chemical structures of the isolated compounds (**6, 25, 26, 28, 45, 47, 48, 49,** and **51**) and standards, such as ciprofloxacin (CPFX), ascorbic acid (AA) and etoposide (EVP) were drawn using ACD/ChemSketch, then optimized by the DFT/B3LYP method with 6–31G(d,p) basis sets using Gaussian09 software. The energy-minimized ligands were then input into the docking procedure. The targets, *E. coli* DNA gyrase (PDB ID: 6F86), *S. aureus* pyruvate kinase (PDB ID: 3T07), Human peroxiredoxin 5 (PDB ID: 1HD2) and human topoisomerase II*β* (PDB ID: 3QX3) were retrieved from the Protein Data Bank (https://www.rcsb.org/). Biovia Discovery Studio 2020 was used to prepare the targets (Pawar & Rohane, 2021). The protein complex's water molecules were removed, and the bound ligand was chosen to determine the characteristics of the binding site before being removed from the complex (Trott & Olson, 2009). Redocking of bound ligand with the target protein was carried out to validate the binding site. The target was augmented with polar hydrogen atoms and the necessary charges. Using Auto Dock Vina (MGLTools-1.5.6), the target and ligand were generated in the necessary format (pdbqt) for docking, and docking was performed (Trott & Olson, 2009). Nine conformers and their

associated binding energies were generated for each ligand during the docking procedure (Nguyen *et al*., 2020). Using Biovia Discovery Studio 2020, the conformation with the lowest binding energy was chosen to determine the interactions between the receptor and ligand. The binding site x, y, z values which attributes for each target given below:-

Binding site attributes for *E. coli* DNA gyrase (PDB ID: 6F86) are center_x = 61.680259, center_y = 28.330852, center_z = 64.290148; size_x = 28, size_y = 20, size_z = 28

Binding site attributes for *S. aureus pyruvate kinase* (PDB ID: 3T07) are center_x = -12.446889, center_y = 0.983556, center_z = 2.585889; size_x = 30, size_y = 25, size_z = 30

Binding site attributes for Human peroxiredoxin 5 (PDB ID: 1HD2) are center_x = 7.023778, center_y = 41.721111, center_z = 34.408556; size_x = 27, size_y = 21, size_z = 20

Binding site attributes for human TOP2β (PDB ID: 3QX3) are center_x = 33.025762, center_y = 95.765381, center_z = 51.567476; size_x = 20, size_y = 24, size_z = 22

3.11 Statistical Data Analysis

The data of antibacterial and antioxidant activities were the averages of triplicate analyses. Data were recorded as mean ± standard error of mean (SEM). The results are expressed as 50% inhibition concentration (IC_{50}). The sample concentration that provides 50% activity (IC_{50}) was calculated from nonlinear regression analysis of percent inhibitory activity versus sample concentration. All data were analyzed with the aid of Excel Microsoft office, and statistical package program Graphpad Prism version 8 for Windows (Graphpad Software Inc., San Diego, USA).

4. RESULTS AND DISCUSSION

4.1 Extract Yield

The finely powdered (600 g) stem-bark of *D. angustifolia* was extracted with dichloromethane and dichloromethane: methanol (1:1) yielded a green dichloromethane extract (7.67 g) and dark-green dichloromethane:methanol extract (22 g) with percentage yield of 1.28 % and 3.67 % w/w, respectively. On the other hand, the dichloromethane and methanol soluble portion which was partitioned from dichloromethane:methanol extract (22 g) yield 10 g (45.46 % w/w) and 12 g(54.5 % w/w), respectively. The highest yield was obtained from stem barks extracted with dichloromethane: methanol solvent (1:1). The results showed that the percentage yields increases with increasing the polarity of extractive solvents.

TLC profile of the Fractions

The column chromatographic fractions obtained from dichloromethane and dichloromethane soluble portion of the dichloromethane: methanol extract were analyzed using TLC with the results depicted in Appendix 11. The results of the TLC profile demonstrated the presence of different spots which confirmed the existence of different compounds in the extract. Therefore, the dichloromethane extract was subjected to silica gel column chromatography.

4.2 Phytochemical Screening

Qualitative phytochemicals screening were done to determine the class of compounds present in the extracts following standard experimental protocols. The result revealed that flavonoids, terpenoids, glycosides, coumarins, phenolics, and saponins were presents in the stem bark extracts of CH_2Cl_2, CH_2Cl_2:MeOH extracts and aqueous MeOH soluble portion (Table 3). However, anthraquinones was not detected in all extracts. On the other hand alkaloids was detected in DCM:MeOH extracts, but was not detected in dichloromethane extracts. Steroids was present in dichloromethane and DCM:MeOH extracts, while tannin was not detected in dichloromethane extracts. Table 3 below summarizes the results of various phytochemical identification tests done on the stem bark extracts of *D. angustifolia*.

Table 3: Phytochemicals screening result of the stem bark extracts of *D. angustifolia*

Phytochemicals tested	Extracts		
	Dichloromethane	**DCM:MeOH**	**MeOH**
Flavonoids (Shinoda test)	+	+	+
Terpenoids (*Salkowski's* test)	+	+	+
Alkaloids (Wagner's test)	–	+	+
Steroids (*Libermann Burchard*)	+	+	–
Glycosides (*Keller-Killiani*)	+	+	+
Coumarins	+	+	+
Anthraquinones	–	–	–
Phenols	+	+	+
Saponins (*Froth test*)	+	+	+
Tannins (*Ferric Chloride*)	–	+	+

DCM:MeOH = dichloromethane:methanol; + = indicates presence; – = indicates absence

Previous studies done on *D. angustifolia* had reported presence of steroids in ethanolic leaves and bark extracts and absence of flavonoids in bark of the plant extracts, while tannin was present only in methanolic leaves and bark extracts (Anode *et al*., 2018). In this study steroids were absent in polar solvent of aqueous MeOH extract, while flavonoids presents in all extracts. Additionally, in consistent with results presented in this study, it was reported that phytochemical screenings done on the extracts from the genus *Dodonaea* found to contain secondary metabolites like flavonoids, terpenoids, tannins, steroids, phenolics, and saponins abundantly (Anode *et al*., 2018; Khurram *et al*., 2011; Riaz *et al*., 2012). The variation in the production of metabolites (phytochemical profiles) might be attributed to difference on the parts of plant tested environmental factors and plant geographical location.

Overall, the qualitatively determined phytochemical constituents of the stem bark of *D. angustifolia* were reasonably suggests the presence of compounds which may contribute for medicinal importance the plants.

4.3 Characterization of compounds isolated from the stem bark of *D. angustifolia*

Compound 45

Compound **45** (21 mg) was obtained as a white solid from dichloromethane extract of the stem bark of *D. angustifolia*. TLC showed a spot at R_f 0.56 using 10% EtOAc in *n*-hexane as mobile phase, which was visualized after spraying with vanillin/H_2SO_4 followed by heating on hot plate. The ^{1}H-NMR (400 MHz, $CDCl_3$) spectrum (Table 4, Appendix 1) of compound **45** varied in the range of δ 0.71 to 5.36. The spectrum displayed proton signal at δ 3.53 (m, 1H, H-3) integrating for 1H was indicative of proton on hydroxyl bearing carbon (H-3). Two olefinic proton signals appeared as downfield in the ^{1}H-NMR spectrum at δ 5.35 (m, 1H, H-6), and δ 5.12 (m, 2H, H-22 and H-23), which are typical signals for three methine protons indicating double bond between C-5 & C-6 of the steroidal skeleton and C-22 and H-23 of sterol, respectively (Al Habsi & Hossain, 2018). The spectrum showed the presence of six methyl groups that appeared between δ 0.71–1.04. Two singlet peaks at δ 0.85 (s, 3H) and 0.69 (s, 3H) were assigned to two angular methyl groups attached to C-13 (H-18) and C-10 (H-19), respectively. The four methyl proton signals appeared at δ 0.89 (d, J = 6.5 Hz, 3H), δ 0.81 (bro. s, 3H), δ 1.02 (d, J = 8.2 Hz, 3H) and δ 0.79 (bro. s, 3H) corresponds to H-21, H-26, H-27 and H-29, respectively. The signal at δ 2.33 (m, 2H, H-4) and 1.99 (m, 2H, H-7) revealed that the two methylene proton adjacent to carbon attached to a hydroxyl group and double bond, respectively.

The ^{13}C-NMR ($CDCl_3$, 101 MHz) spectrum (Table 4, Appendix 2) of compound **45** analyzed with the aid of DEPT-135 (Appendix 3) established the presence of 29 carbon resonances, of which six methyl (CH_3) groups at δ 12.0, 18.9, 19.4, 19.4 (2-C), and 12.3; nine methylenes (CH_2) and eleven methine carbons (CH) were observed (including one oxymethine and three olefinic methine group). The peaks observed at δ 36.3 and 40.5 in the ^{13}C-NMR spectrum were suggesting the presence of two quaternary carbons accounted to C-10 and C-13, respectively. The signal at δ 71.8 is assignable to C-3, corresponding to hydroxylated carbon. The spectrum also displayed the most downfield signal at δ 140.74 (C-5) and 121.73 (C-6), 138.34 (C-22), and 129.26 (C-23) which are corresponding to olefinic carbons. Carbon signals at δ 65.04, 22.71, 24.51, 29.72, 34.11 and 14.41 were mixture/impurity, not considered here in the spectral analysis.

Based on the above spectral data, compound **45** was found to be comparable with data reported for stigmasterol, which was previously reported from wood bark extract of *Baccaurea*

macrocarpa miq. Mull. Arg (Erwin *et al*., 2020) and other biological sources including *Premna herbacea* Roxb (Shwe *et al*., 2019). Previously 4-methoxylstigmasterol (**42**) was reported from the hexane extract of *Dodonaea viscosa* (Al Habsi & Hossain, 2018). This is the first report of stigmasterol (**45**) from the extract of *D. angustifolia*.

Stigmasterol has been reported for its various pharmacological effects including anti-inflammatory, anti-diabetic, antioxidant, and blood cholesterol level lowering effects. Moreover, stigmasterol is recently reported with *in-vivo* and *in-vitro* anti-tumor potential in several cancers cells via inhibiting growth while promoting apoptosis in tumor cells (Zhang *et al*., 2022). Hence, evaluating the antibacterial and antioxidant activities of this compound plays great relevance.

Table 4: ^{1}H and ^{13}C NMR spectral data of compound **45**

Position	**NMR data of compound 45**		**Literature reported for stigmasterol (Erwin *et al*., 2020)**	
	δ_H (multiplicity) in ppm	δ_C in ppm	δ_H (multiplicity) in ppm	δ_C in ppm
1	1.84 (br.s, 2H)	37.3	1.85 (2H, s br.)	37.3
2	1.51 (brs, 2H)	31.7	1.52 (o), 1.84 (o)	31.6
3	3.53 (m, 1H)	71.8	3.52 (m)	71.9
4	2.33 (m, 2H)	42.3	2.24 (dd, *J*= 1.44; 1.06) and 2.38, t)	42.4
5	-	140.7	-	140.8
6	5.35 (m, 1H)	121.7	5.36 (t)	121.7
7	1.99 (m, 2H)	31.7	1.99 (m)	31.7
8	2.00 (m, 1H)	31.9	2.00(m)	31.9
9	-	50.2	0.94 (m)	50.2
10	-	36.3	-	36.6
11	1.01 (brs, 2H)	21.1	1.02 (m,)	21.2
12	-	39.7	1.16 (m)	39.8
13	-	40.03	-	42.4
14	1.02 (m, 1H)	56.9	1.00 (m)	56.9
15	1.29 (brs, 2H)	24.9	1.06 (m) and 1.58(m)	24.5
16	1.29 (brs, 2H)	29.4	1.66 (m)and 1.25(m)	29.1
17	-	55.9	1.12 (m)	56.1
18	0.85 (s, 3H)	12.1	0.85 (s)	12.1
19	0.69 (s, 3H)	19.4	0.680 (s)	19.5
20	-	40.5	1.16 (m)	40.7
21	0.89 (d, J = 6.5 Hz, 3H)	-	1.03 (d,*J*= 7.2 Hz,3H)	21.2
22	5.11 (m, 1H)	138.3	5.00 (dd, *J*=1.73 Hz and 1.72Hz)	138.5
23	5.12 (m, 1H)	129.3	5.15 (dd, j=1.75 Hz and 1.73 Hz)	129.4
24	1.51 (s, 1H)	51.3	1,55 (m)	51.4

25	-	31.9	1.45 (m)	32.0
26	0.81 (br s, 3H)	19.2	0.84 (br s)	19.9
27	1.02 (d, *J* = 8.2 Hz, 3H)	-	1.02 (d,*J*=13 Hz)	21.2
28	1.29 (brs, 2H)	25.2	1.16 (m)	25.6
29	0.79 (brs, 3H)	11.9	0.81 (t)	12.4

Based on the above spectral data in comparison with literature report, compound **45** was identified as stigmasterol whose strcuture is depicted in Figure 4.

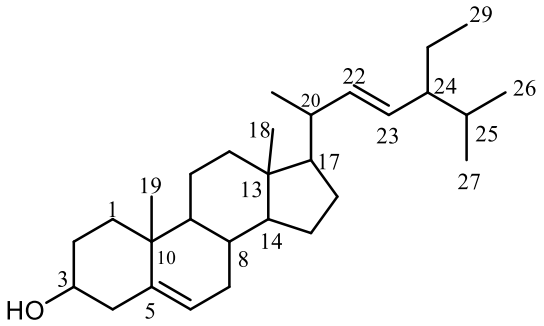

45

Figure 4: Proposed structure of compound **45**

Compound 46

Compound **46** (11 mg) was obtained as white solid from dichloromethane extract of the stem bark of *D. angustifolia*. TLC showed a spot at R_f 0.56 using 20% EtOAc in *n*-hexane as mobile phase (isolated from the same fraction to that of stigmasterol (**45)** and have similar R_f value). Its spot was visualized after spraying with vanillin/H_2SO_4 followed by heating on hot plate.

The ^{1}H-NMR (400 MHz, $CDCl_3$) spectrum (Table 5, Appendix 4) displayed the presence of two angular methyl singlets at δ 0.70 (s, 3H, H-18) and 0.72 (s, 3H, H-19); three methyl doublets that appeared at δ 1.04 (d, J = 7.6 Hz, 3H, H-21), δ 0.85 (d, J = 7.3 Hz, 3H, H-27), and δ 0.81 (d, J = 6.7 Hz, 3H, H-26); and a methyl triplet at δ 0.90 (t, J = 6.7 Hz, 3H, H-29). Proton signal at δ 3.55 (m, 1H, H-3), indicates a methine proton of H-3. The olefinic protons were appeared as downfield at δ 5.37 (d, J = 5.3 Hz, 1H, H-6), δ 5.10 (t, J = 5.1 Hz, 1H, H-22), and δ 5.03 (m, 1H, H-23). The spectrum also showed signals for aliphatic carboxylate substituted at C-3, with a triplet methylene proton signals at δ 2.36 (t, J = 7.6 Hz, 2H, H-2') and δ 1.63 (q, J = 7.3 Hz, 2H, H-3'). Furthermore, an up field triplet proton signal at δ 0.90 (t, J = 6.7 Hz, 3H, H-16'), is evident for the presence of terminal methyl proton in the compound. On the other hand, the

proton peaks at δ 4.13 – 4.34 (due to methylene protons (-C**H**$_2$OCO-) of triglyceride unit) and δ 1.27 are considered as a mixture/impurity.

The ^{13}C-NMR ($CDCl_3$, 101 MHz) spectrum (Table 5, Appendix 5) of the compound **46** with the aid of DEPT-135 (Appendix 6) displayed signals at δ 140.8 (C-5), 121.7 (C-6), 138.3 (C-22), and 129.3 (C-23), which corresponds to the double bond of stigmasterol. The spectrum also showed signals at δ 71.8 (C-3), attributed to carboxylated methine carbon. The up field signals of the methyl groups were evident at δ 12.0 (C-18), 12.1 (C-29), 18.9 (C-26 & C-27), 19.4 (C-19 & C-21) and 14.1 (C-16'). The most downfield carbon signal at δ 174.0 is assignable to carbonyl carbon (C-1′), whereas signals at δ 34.1 (C-2′), 25.4 (C-3′), 22.7 (C- 15′), and 14.1 (C-16′) represents the methylene and methyl group of the aliphatic carboxylate, respectively. However, the spectrum showed carbon signals resonated at δ 173.5 and δ 173.8, which were possibly secondary to carbonyl carbons (-CH$_2$O**OC** & -CHO**OC**) of triglyceride unit as mixture/impurity (Kundu & De, 2021). Carbon signals at δ 72.1, δ 68.37, 65.0, δ 62.0 and δ 61.6, are also not considered here in the spectral analysis.

Based on the above spectral data, the structure of compound **46** was in close agreement with reported in the literature for 29-benzoyl-3-octadecanoyl stigmasterol, which was previously isolated from the stem bark of *Albizia gummifera* (Ayele *et al.*, 2022). The difference is the signals for carboxyl of ester at C-1' appeared at δ 174.0 in compound **46** and at δ 178.5 in the literature and the benzoyl group at C-29 were absent in the case of compound **46** (Table 5). Previously 4-methoxylstigmasterol (**42**) was reported from the hexane extract of *Dodonaea viscosa*. This is the first report of compound **46** from the dichloromethane extract of *D. angustifolia*.

Table 5: ^{1}H and ^{13}C NMR spectral data of compound **46**

Position	**NMR data of compound 46**		**Literature reported for stigmasterol** (Ayele et al., 2022)	
	δ_H (multiplicity) in ppm	δ_C in ppm	δ_H (multiplicity) in ppm	δ_C in ppm
1	1.85 (s, 2H)	37.3	1.14 (m)	37.3
2	-	31.7	1.55 (m)	31.6
3	3.55 (m, 1H)	71.8	3.52 (td, *J* =11.2 Hz, 5.7 Hz)	71.8
4	-	42.3	2.30 (d, 5.0)	42.2
5	-	140.8	-	140.7
6	5.37 (d, *J* = 5.3 Hz, 1H)	121.7	5.35 (dd, *J* =5.4 Hz, 1.9 Hz)	121.7
7	2.01(m, 2H)	31.9	1.83 (m)	31.9
8	-	31.9	1.45 (m)	31.9

9	-	50.2	0.93 (m)	50.2
10	-	36.5	-	36.5
11	1.31(m, 2H)	21.2	1.30 (m)	22.7
12	1.31(m, 2H)	39.7	1.83 (m)	39.7
13	-	42.2	-	42.3
14	1.04 (d, *J* = 7.6 Hz, 1H)	56.9	1.00 (m)	56.9
15	-	24.4	1.55 (m)	24.4
16	1.31(m, 2H)	29.4	1.33 (m)	28.9
17	-	56.0	1.15 (m)	56.0
18	0.70 (s, 3H)	12.0	0.68 (s)	12.1
19	0.72 (s, 3H)	19.4	1.03 (s)	19.8
20	-	40.4	2.04 (m)	40.5
21	1.04 (d, *J* = 7.6 Hz, 3H)	21.1	1.04 (m)	21.1
22	5.10 (t, *J* = 5.1 Hz, 1H)	138.3	5.15 (m)	138.3
23	5.03 (m, 1H)	129.3	5.03 (dd, *J* =15.1 Hz, 8.8 Hz)	129.3
24	-	51.3	1.55 (m)	51.3
25	-	34.3	1.45 (m)	31.9
26	0.81 (d, *J* = 6.7 Hz, 3H)	18.9	0.94 (m)	11.0
27	0.85 (d, *J* = 7.3 Hz, 1H)	19.0	1.42 (m)	23.7
28	-	24.9	1.70 (m)	38.7
29	0.90 (t, *J* = 6.7 Hz, 3H)	12.1	4.22 (dd, *J* =11.4 Hz, 5.9 Hz)	68.2
1’	-	174.0	-	178.5
2’	2.36 (t, *J* = 8.1 Hz, 2H)	34.1	2.35 (t, *J* =7.5 Hz)	33.8
3’	1.65 (q, 2H)	25.4	1.65 (dt, *J* =34.2 Hz, 7.1 Hz)	24.7
4’	1.33 (bro. s, 2H)	29.1	1.86 (m)	31.9
5’		29.3	1.55 (m)	31.9
6’		29.7	1.30–1.45 (m)	29.7
7’		29.5	1.30–1.45 (m)	29.5
8’		29.3	1.30–1.45 (m)	29.3
9’	1.29 – 1.36 (m, 20H),	29.5	1.30–1.45 (m)	29.5
10’		29.7	1.30–1.45 (m)	29.6
11’		29.4	1.30–1.45 (m)	29.4
12’		29.7	1.30–1.45 (m)	29.7
13’		29.3	1.30–1.45 (m)	29.7
14’		31.9	1.27 (m)	30.4
15’	1.27 (brs, 2H)	22.7	1.33 (m)	23.0
16’	0.90 (t, *J* = 6.7 Hz, 3H)	14.1	0.91 (t, *J* =7.5 Hz)	14.1

Based on the number of hydrogens and carbons from the ^{1}H and ^{13}C-NMR spectrum in comparison with literature report, the proposed structure of compound **46** is given as depicted in Figure 5.

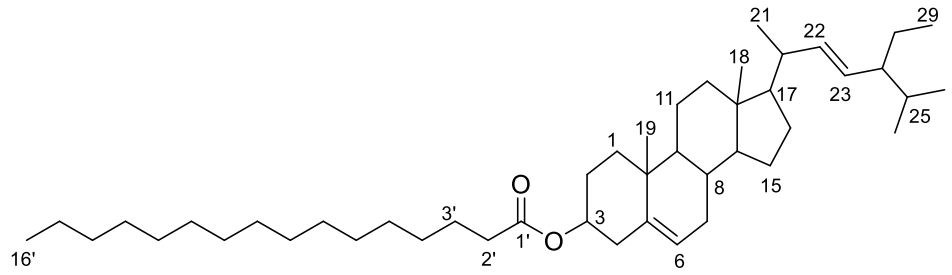

46

Figure 5: Proposed structure of compound **46**

Compound 47

Compound **47** (18 mg) was obtained as white crystals from dichloromethane extract of the stem bark of *D. angustifolia*. TLC showed a spot at R_f value of 0.42 with 10% EtOAc in *n*-hexane as mobile phase.

The ^{1}H-NMR (400 MHz, $CDCl_3$) spectrum (Table 6, Appendix 7) of compound **47** displayed an upfield proton signal at δ 0.89 (t, J = 6.7 Hz, 3H, H-18'), which is evident for the presence of terminal methyl proton in the compound. An intense signal at δ 1.27 (bro. s, 14H) is evident for the presence of many overlapping methylenes. This was supported by the appearance of an intense carbon signal at δ 29.7 in the ^{13}C-NMR spectrum. The spectrum also showed triplet signal at δ 2.36 (t, J = 7.6 Hz, 2H, H-2') and quintet signal at δ 1.63 (q, J = 7.3 Hz, 2H, H-3') each integrated for two protons, and suggesting of methylene protons at C-2' and C-3' in the chain relative to an alpha (-α) & beta (-β) to carbonyl group, respectively. Furthermore, the proton NMR spectrum of compound **47** suggests the presence of hydrogen on oxygenated carbon at δ 4.18 – 4.33, which is in agreement with the presence of oxygenated methylene at δ 65.1 and oxygenated methine at δ 68.4 in the ^{13}C-NMR spectrum.

The ^{13}C-NMR (101 MHz, $CDCl_3$) spectral data (Table 6, Appendix 8) with the aid of DEPT-135 (Appendix 9) revealed a total of 21 carbon signals for compound **47**. Seventeen of them being sp^3 hybridized methylenes with signals at δ 34.1, 33.9, 31.9, 29.7 (6-Cs), 29.68, 29.6, 29.5, 29.4, 29.3, 24.7, 22.7 and including one oxygenated methylene at δ 65.1. The signal at δ 65.1 (C-3) suggests the presence of methylene carbon linked through an oxygen bridge with the carbonyl carbon. The most downfield two signals appearing at δ 179.5 and δ 174.0 are attributed to carboxyl of acids and carbonyl of esters, respectively. Whereas, the upfield carbon signal at δ 14.1 accounts for the presence of terminal methyl group.

The above NMR data are in good agreement with data described in the literature for 2-hydroxy-3-(stearoyloxy) propanoic acid (salvastearolide) which was previously reported from the seeds of *Salvadora persica* (El-Desouky *et al*., 2018)**.** The difference is the signals for carboxyl of acids appeared at δ 179.5 in compound **47** and at δ 173.5 in the literature. To the best of our knowledge, there is no prior report in the literature for 2-hydroxy-3-(stearoyloxy) propanoic acid from the genus *Dodonaea*.

Table 6: ^{1}H and ^{13}C NMR spectral data of compound 47

Position	**NMR data of compound 47**			**Reported spectral data** (El-Desouky *et al*., 2018)	
	δ_H (multiplicity) in ppm	δ_C in ppm	DEPT-135	δ_H (multiplicity) in ppm	δ_C in ppm
1	–	179.5	Carboxyl	11.0 (*br*., OH)	173.50
2	4.33 (d, J = 3.6 Hz, 1H)	68.4	CH	5.25 (*m*, 1H), 1.57 (*br*., OH)	69.0
3	4.18 (dd, *J* = 10.5, 4.8 Hz, 1H) 4.12 (dd, *J* = 8.4, 2.6 Hz, 1H)	65.1	CH_2	4.26 (*dd*, 1H, 4.4, 16.4 Hz), 4.12 (*dd*, 1H, 6.0, 18.0 Hz)	62.30
1’	–	174.0	Carbonyl ester	–	173.0
2’	2.36 (t, *J* = 7.6 Hz, 2H)	34.1	CH_2	2.28 (*m*, 2H)	34.4
3’	1.63 (q, *J* = 7.3 Hz, 2H)	24.7	CH_2	1.55 (o, 2H)	25.0
4’	1.33 (d, *J* = 18.2 Hz, 2H)	29.3	CH_2		29.2
5’		29.4	CH_2		29.3
6’		29.5	CH_2		29.5
7’		29.6	CH_2		29.5
8’		29.7			29.7
9’		29.7			29.8
10’		29.7			29.9
11’	1.27 (bro, s, 26H)	33.9	CH_2	1.22 (m, 2H each)	32.1
12’		29.7			29.8
13’		29.7			29.6
14’		29.7			29.5
15’		29.7			29.4
16’		31.9	CH_2		34.2
17’		22.7	CH_2		22.9
18’	0.89 (t, *J* = 6.7 Hz, 3H)	14.1	CH_3	0.85 (t, 3H, 6.8 Hz)	14.3

Based on the above spectral data in comparison with literature report, compound **47** was identified as 2-hydroxy-3-(stearoyloxy) propanoic acid whose strcuture is depicted in Figure 6.

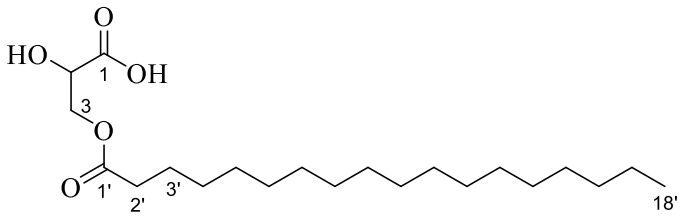

47

Figure 6: Proposed structure of compound **47**

Compound 48

Compound **48** (26 mg) was isolated as a solid from dichloromethane extract of the stem bark of *D. angustifolia*. TLC showed a spot at R_f 0.4 with 10% EtOAc in *n*-hexane as mobile phase. The spot was visualized after spraying with vanillin/H_2SO_4 followed by heating on hot plate.

The ^{1}H-NMR (400 MHz, $CDCl_3$) spectral data (Table 7, Appendix 10) showed a triplet signal integrated for three protons at δ 0.90 (t, J = 6.8 Hz, 3H, C-18), suggesting the presence of terminal methyl protons. The spectrum also displayed methylene signals at δ 2.33 (m, 2H, H-2) and 1.63 (d, J = 8.6 Hz, 2H), of which the former suggests methylene is connected to a carbonyl of ester group. The most intense singlet signal at δ 1.27 corresponds for many methylene protons. Furthermore, the proton signal at δ 5.36 (d, J = 4.2 Hz, 1H, H-2′) accounted for the presence of oxygenated methine proton, whereas signals at δ 4.31 (dd, J = 12.0, 4.3 Hz, 1H, H-1′) and δ 4.16 (dd, J = 11.9, 5.9 Hz, 1H, H-1′) attributed to oxygenated methylene protons.

The ^{13}C-NMR (101 MHz, $CDCl_3$) spectrum (Table 7, Appendix 11) together with DEPT-135 (Appendix 12) revealed the presence of one carbonyl of ester group, one oxygenated methines, eighteen methylenes, including two oxygenated ones, and one methyl group. The oxygenated methines were detected at δ 71.2 (C-2'), besides two oxygenated methylenes at δ 68.9 (C-1') and δ 62.1 (C-3'). The most downfield signals appearing at δ 173.3 is attributed to carbonyl of ester, whereas the up field signal at δ 14.2 suggests the presence of terminal methyl group.

The above spectral data of compound **48** was found in good agreement with pioneering literature data for salvastearolide, which was isolated from the seeds of *Salvadora persica* (El-Desouky *et al*., 2018). The difference is the absence of extra carboxyl of acids at C-3', in the case of 2,3-dihydroxypropyl stearate (**48)**. To the best of our knowledge, this is the first report of compound **48** from extract of *D. angustifolia* and it's new to the genus.

Table 7: ^{1}H and ^{13}C NMR spectral data of compound **48**

Position	NMR data of compound 48			Reported literature (El-Desouky *et al*., 2018)	
	δ_H (multiplicity) in ppm	δ_C in ppm	DEPT-135	δ_H (multiplicity) in ppm	δ_C in ppm
1	-	173.3	Carbonyl	-	173.0
2	2.33 (m, 2H)	34.1	CH_2	2.28 (m, 2H)	34.4
3	1.63 (d, *J* = 8.6 Hz, 2H)	24.9	CH_2	1.55 (2H)	25.0
4	1.35 (d, *J* = 12.2 Hz, 2H)	29.1	CH_2		29.2
5		29.31	CH_2		29.3
6		29.5	CH_2		29.5
7		29.7	CH_2		29.5
8		29.7	CH_2		29.7
9		27.22	CH_2		27.8
10	1.27 (bro. s, 24H, H-5 to H-16)	29.7	CH_2	1.22 (28H)	29.9
11		32.04	CH_2		32.1
12		29.7	CH_2		29.8
13		29.7	CH_2		29.6
14		29.7	CH_2		29.5
15		29.4	CH_2		29.4
16		31.9	CH_2		34.2
17	1.31 (bro. s, 2H)	22.7	CH_2		22.7
18	0.90 (t, *J* = 6.8 Hz, 3H)	14.2	CH_3	0.85 (t, 3H, 6.8 Hz)	14.1
1’	4.31 (dd, *J* = 12.0, 4.3 Hz, 1H), 4.16 (dd, *J* = 11.9, 5.9 Hz, 1H)	68.9	CH_2-O	4.26 (*dd*, 1H, 4.4, 16.4 Hz), 4.12 (*dd*, 1H, 6.0, 18.0 Hz)	62.3
2’	5.34 (m, 1H)	71.2	CH-OH	5.25 (*m*, 1H), 1.57 (*br*., OH)	69.0
3’	3.66 (m, 2H)	62.1	CH_2-OH	11.0 (*br*., OH)	173.5

The spectral data presented above led us to propose the structure of 2,3-dihydroxypropyl stearate (**48)** as depicted in Figure 7.

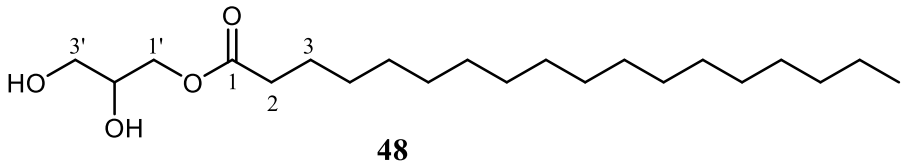

48

Figure 7: Proposed structure of compound **48**

Compound 49

Compound **49** (22 mg) was obtained as a white powder from dichloromethane extract of the stem bark of *D. angustifolia*. TLC showed a spot at R_f value of 0.54 with 20% EtOAc in *n*-hexane as

mobile phase, which was visualized after spraying with vanillin/H_2SO_4 followed by heating on hot plate.

The ^{1}H-NMR spectrum (Table 8, Appendix 13) displayed an up field signal at δ 0.90 (m, 3H, H-18) suggesting of the presence of terminal methyl protons. The most intense signal at δ 1.27 (bros, 28H) corresponds for many methylene protons.

The ^{13}C-NMR (101 MHz, $CDCl_3$) and DEPT spectral data (Table 8, Appendix 14Appendix 15) of compound **49** showed the presence of total of 18 carbon, of which sixteen methylene's with signals at δ 34.0, 33.2, 31.9, 29.7 (6-C), 29.6, 29.5, 29.4, 29.3, 29.1, 24.7 and 22.7. The most downfield signal at δ 179.7 (C-1) is attributed to carboxyl of acid, whereas the upfield carbon signal at δ 14.2 suggests the presence of terminal methyl group. The above spectral data is in good agreement with literature data for stearic acid (Di Pietro et al., 2020). This is the first report of compound **49** from extract of *D. angustifolia* and has not been reported before from the genus.

Table 8: ^{1}H and ^{13}C NMR spectral data of compound **49**

Position	**NMR data of compound 49**			**Literature reported for stearic acid** (Di Pietro et al., 2020)	
	δ_H (multiplicity) in ppm	δ_C in ppm	DEPT-135	δ_H (multiplicity) in ppm	δ_C in ppm
1	-	179.7	Carboxyl	–	182.78
2	2.38 (t, J = 8.0 Hz, 2H)	34.0	CH_2	2.35	36.7
3	1.65 (bro s., 2H)	26.1	CH_2	1.63	27.3
4		29.1	CH_2		
5		29.3	CH_2		
6		24.7	CH_2		
7		29.7	CH_2		
8		29.7	CH_2		
9		29.7	CH_2		
10	1.27 (bros., 28H, H-4 – H-17)	29.7	CH_2	1.25 (H-4 – H-17)	29-32 (C-4 – C-17)
11		29.7	CH_2		
12		29.6	CH_2		
13		29.5	CH_2		
14		29.4	CH_2		
15		33.2	CH_2		
16		31.9	CH_2		
17		22.7	CH_2		25.4
18	0.90 (m, 3H)	14.1	CH_3	–	16.8

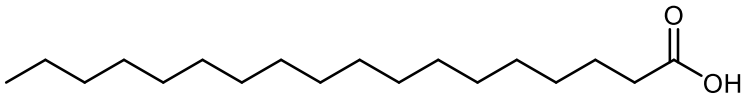

49

Figure 8: Proposed structure of compound **49**

Compound 50

Compound **50** (28 mg) was isolated as a pale yellow solid from dichloromethane extract of the stem bark of *D. angustifolia*. TLC showed a spot at R_f 0.6 with 10% EtOAc in *n*-hexane as mobile phase. The ^{1}H-NMR (400 MHz, $CDCl_3$) spectrum (Table 9, Appendix 16) demonstrated most intense signal around δ 1.30 to 1.27 (bro, s., 48H, H-2 – H-25), which were assigned for many methylene protons. This clearly indicates the presence of overlapping signals due to methylenes in the structure of the compound. An upfield triplet at δ 0.89 (t, J = 6.7 Hz, 6H, H–1 & H–26) is evident for the presence of terminal methyl group.

The ^{13}C NMR (101 MHz, $CDCl_3$) spectrum (Table 9, Appendix 17, & 18) with the aid of DEPT-135 displayed signals due to methylenes at δ 31.9, 29.7, 29.4 and 22.7. The carbon signal observed at δ 22.7 is due to methylene directly attached to terminal CH_3 group. Whereas signals at δ 29.4, 29.7 and 31.9 represents all the overlapping methylene carbons (CH_2) in the isolated compound, which agreed well with the ^{1}H-NMR. Furthermore, the carbon resonance which appears more upfield at δ 14.2 is characteristic signal for terminal methyl group.

The above NMR spectral data was in close agreement with literature for a long chain hydrocarbon named as hexacosane (Figure 11), which was previously isolated from ethyl acetate extract of *Sanseveria liberica (Gerome and Labroy)* (Rukaiyat *et al*., 2015), but has not been reported from genus *Dodonoea* and also from species of *D. angustifolia.*

Table 9: ^{1}H and ^{13}C NMR spectral data of compound 50

Position	**NMR data of compound 50**			**Data reported for Hexacosane** (Rukaiyat *et al*., 2015)	
	δ_H (multiplicity) in ppm	δ_C in ppm	DEPT-135	δ_H in ppm	δ_C in ppm
C_1 & C_{26}	0.9 (t, 6H)	14.2	14.1 CH_3	0.8	14
C_2 & C_{25}	1.3 (bro,s, 4H)	22.7	22.7 CH_2	1.2 to1.6	22

C_3 & C_{24}	1.3 (bro,s, 4H)	31.9	31.9 CH_2	30 -32
C_4 & C_{23}	1.3 (bro,s,4H)	29.4	29.4 CH_2	
C_5 & C_{22}	1.3 (bro,s,4H)	29.7	29.7 CH_2	
C_{6-13} & C_{14-21}	1.3 (brs, 32H)	29.7	29.7 CH_2	

50

Figure 9: Proposed structure of compound **50**

4.4 Compounds Isolated from the Leaves of *D. angustifolia*

Five compounds previously isolated by Yadessa Melaku and his coworkers at the Department of Applied Chemistry from ethyl acetate leaves extract of *D. angustifolia,* including 2-hydroxy-15,16-epoxyceloda-3,13(16),14-trien-18-oic acid (**6**), santin (**25**), pinocembrin (5,7-dihydroxyflavanone) (**26)**, 5,7,4′-Trihydroxy-3,6-dimethoxyflavone (**28**) and 5,6,5′-Trihydroxy-3,7,4’-trimethoxyflavone **(51**) were included herein for bioassay and *in-silico* computational studies. The structures of the compounds (**6**, **25**, **26**, **28** & **51**) were given in Figure 10.

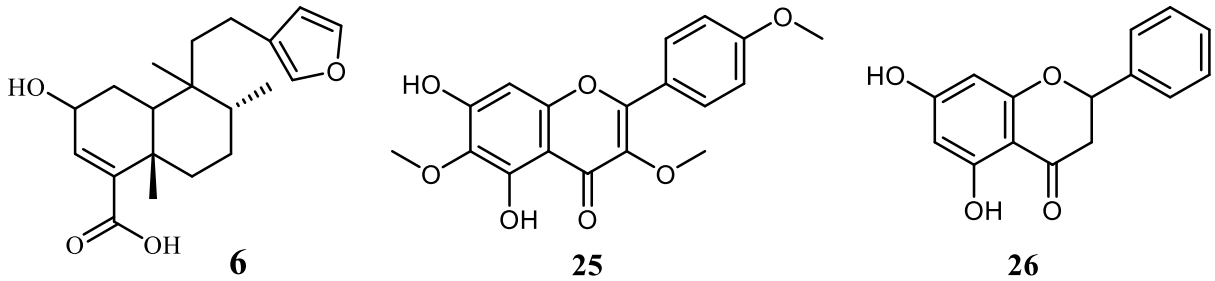

6 **25** **26**

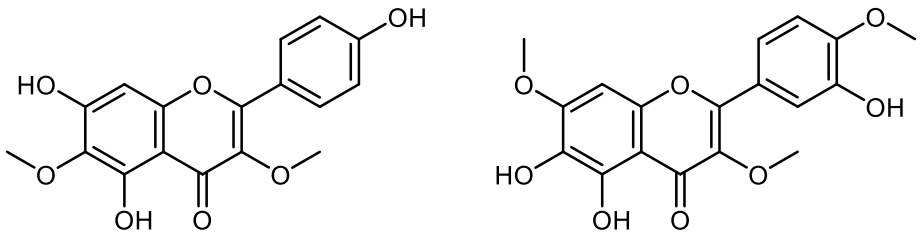

28 **51**

Figure 10: Structure of compounds isolated from the leaves of *D. angustifolia*

4.5 Biological activity of the extracts and compounds isolated from the stem bark and leaves of *D. angustifolia*

4.5.1 Anti-bacterial Activity

The stem bark extracts and compounds (**6**, **25**, **26**, **28** and **45-51**) were tested for their antibacterial activity against Gram-positive bacteria (*Staphylococcus aureus*, ATCC 25923 & *Staphylococcus pyogenes* ATCC 19615) and Gram-negative bacteria (*Escherichia coli* ATCC 25922 & *Pseudomonas aeruginosa* ATCC 27853) at different concentrations and compared with ciprofloxacin as positive control and DMSO as negative control.

Results from the *in vitro* antibacterial activity showed that all extracts exhibited growth inhibition against both Gram positive and Gram negative bacteria in dose-dependent manner, except the DCM:MeOH extract were showed no inhibition against *S. pyogenes*. The mean zone of inhibition for all samples on the four bacteria was varied from 6.00 to 13.00±2.52mm.

The aqueous methanol soluble portion of stem bark extract was in general the most active against all the test organisms with inhibition zone of 11.33±0.88, 10.00±0.58, 13.00±0.58 and 13.00±2.52 mm diameter at 100 mg/mL against *S. aureus*, *S. pyogenes*, *P. aeruginosa* and *E. coli*, respectively, in comparison to ciprofloxacin with 17.67±0.88 – 21.67±1.20 mm zone of inhibition at 30 µg/mL. DCM:MeOH extract was the second most active extract and possess reasonable activity against *S. pyogenes* with inhibition diameter of 13.00±0.58 mm at 100 mg/mL, but not active against *E. coli*. The DCM extract was demonstrated remarkable activity against *S. aureus*, *P. aeruginosa* and *E. coli* with inhibition zone of 10.00±0.58, 11.00±0.58, 10.00±0.58 mm respectively and weak activity against *S. pyogenes* (Table 10). This observation suggests that components of the extract which possess antibacterial activity might reside either in the medium or highly polar fractions of the plant extract.

Antibacterial activity of the methanol leaves extracts of *D. viscosa* species was determined in an earlier study in Ethiopia (Getie *et al*., 2003) and the highest zone of inhibition was shown against *S. pyogenes* (10 mm) and *S. aureus* (9 mm) at 100 mg/mL concentration and no activity was reported against the Gram negative bacteria (*P. aeruginosea* and *E. coli*). The results for the Gram positive bacteria postulated by Getie *et al.*, is consistent with the present study, but this was apparently not the case with *P. aeruginosea* and *E. coli*. The zone of inhibition obtained in this study was, however, higher (at 100 mg/mL concentration). This variation could be attributed

to the effect of using different plant species and plant part, which in turn may affect the phytochemical profiles.

Table 10: Antibacterial activity of the stem bark extracts of *D. angustifolia*

Sample/ Standard	Concentration (mg/mL)	Inhibition Diameter mm (mean ± SEM)			
		S. aureus	***S. pyogenes***	***P. aeruginosa***	***E. coli***
DCM	100	10.00±0.58	8.33±0.33	11.00±0.58	10.00±0.58
	50	8.00±0.58	7.33±0.33	9.33±0.33	7.67±0.33
	25	6.50±0.29	6.33±0.33	7.67±0.33	6.67±0.33
	12.5	6.00±0.00	6.00±0.00	6.67±0.33	6.17±0.17
DCM:MeOH	100	12.00±0.58	13.00±0.58	11.33±0.88	6.00±0.00
	50	9.00±0.58	9.00±0.58	9.67±0.88	6.00±0.00
	25	7.00±0.58	7.33±0.67	7.00±0.58	6.00±0.00
	12.5	6.83±0.17	6.67±0.33	6.50±0.29	6.00±0.00
Aqueous MeOH	100	11.33±0.88	10.00±0.58	13.00±0.58	13.00±2.52
	50	9.00±0.58	8.33±0.33	9.00±0.58	10.33±1.20
	25	7.66±0.33	6.33±0.33	7.00±0.58	7.00±0.58
	12.5	6.33±0.33	6.17±0.17	6.00±0.00	6.00±0.00
Ciprofloxacin (µg/mL)	30 µg/mL	17.67±0.88	18.33±0.88	19.33±0.67	21.67±1.20

S. aureaus = *Staphylococcus aureus*, ***S. Pyogenes*** = *Streptococcus pyogenes*, ***P. aeruginosa*** = *Pseudomonas aeruginosa*, ***E. coli*** = *Escherichia coli*

Another study done by Omosa *et al.*, (2014) reported the surface exudates extracts of *D. angustifolia* showed antibacterial activity against *E. coli, S. aureus* and *B. pumilus, with* minimum inhibition concentration (MIC) values less than 625µg/well or/and zone of inhibition of 8.97, 9.32, and 9.27 mm, respectively (L. K. Omosa *et al.*, 2014), which is in good agreement with the present study.

Among compounds isolated from the stem bark extract, compound **45** showed the best antibacterial activities (12.00±0.58, 10.00±0.58 and 13.33±0.88 mm, each at 2 mg/mL) against *S. aureaus*, *S. Pyogenes*, and *P. aeruginosa* respectively, compared to ciprofloxacin (19.17±1.05, 18.83±0.75 & 21.67±1.31 mm at 30 µg/mL) (Table 11). Compounds **47** and **48** were also displayed good activity (10.00±0.58 and 11.67±0.88 mm, each at 2mg/mL) against *E.coli*, whereas compounds **48** also showed activity (10.00±0.58 mm) against *S. aureus* as compared to

ciprofloxacin (20.33±0.61 mm against *E.coli*). The result also revealed that compound **46** and **49** exhibited the lowest zone of inhibitions against all the tested organisms, while compound **50** was found not active at the highest concentration tested. The isolated compound from bark extract displayed remarkable inhibitory effect at lower concentration when compared to the extract; where the antibacterial activity observed with the extract might be attributed to its bioactive compounds content.

Table 11: Anti-bacterial activity of compounds isolated from stem bark of *D. angustifolia*

Compound/ Standard	Concentration (mg/mL)	Inhibition Diameter mm (mean ± SEM)			
		S. aureus	***S. pyogenes***	***P. aeruginosa***	***E. coli***
45	2	12.00±0.58	10.00±0.58	13.33±0.88	9.00±0.00
	1	11.00±0.58	8.33±0.33	10.00±0.58	8.00±0.00
	0.5	8.00±0.58	6.68±0.33	8.67±0.33	6.67±0.33
	0.25	6.50±0.29	6.33±0.33	7.00±0.33	6.17±0.17
46	2	9.00±0.58	6.00±0.00	8.67±0.33	7.67±0.33
	1	7.33±0.33	6.00±0.00	7.00±0.00	6.67±0.33
	0.5	6.33±0.33	6.00±0.00	6.33±0.33	6.00±0.00
	0.25	6.00±0.00	6.00±0.00	6.00±0.00	6.00±0.00
47	2	9.67±0.33	6.00±0.00	7.33±0.33	10.00±0.58
	1	7.00±0.58	6.00±0.00	6.00±0.00	8.00±0.58
	0.5	6.00±0.00	6.00±0.00	6.00±0.00	6.67±0.33
	0.25	6.00±0.00	6.00±0.00	6.00±0.00	6.33±0.33
48	2	10.00±0.58	6.67±0.33	9.00±0.58	11.67±0.88
	1	8.00±0.58	6.00±0.00	6.67±0.67	8.33±0.88
	0.5	6.00±0.00	6.00±0.00	6.63±0.33	7.00±0.58
	0.25	6.00±0.00	6.00±0.00	6.00±0.00	6.33±0.33
49	2	6.00±0.00	9.00±0.58	8.00±0.58	8.33±0.33
	1	6.00±0.00	7.00±0.58	7.00±0.58	6.67±0.33
	0.5	6.00±0.00	6.00±0.00	6.00±0.00	6.00±0.00
	0.25	6.00±0.00	6.00±0.00	6.00±0.00	6.00±0.00
50	2	6.00±0.00	6.00±0.00	6.00±0.00	6.00±0.00
	1	6.00±0.00	6.00±0.00	6.00±0.00	6.00±0.00
	0.5	6.00±0.00	6.00±0.00	6.00±0.00	6.00±0.00
	0.25	6.00±0.00	6.00±0.00	6.00±0.00	6.00±0.00
Ciprofloxacin (μg/mL)	30 μg/mL	19.17±1.05	18.83±0.75	21.67±1.31	20.33±0.61

S. aureaus = *Staphylococcus aureus*, ***S. Pyogenes*** = *Streptococcus pyogenes*, ***P. aeruginosa*** = *Pseudomonas aeruginosa*, ***E. coli*** = *Escherichia coli*

Yusuf et al., (2018) reported the antibacterial effect of stigmasterol which was isolated from the stem bark extract of *N. macrophylla,* against test organisms (*S. aureus*, *E. coli*, MRSA, *Salmonella typhimurium*) with mean zone of inhibition range from 23 mm to 30 mm at 100 µg/mL concentration (Yusuf *et al*., 2018). Edilu *et al*., 2015 also reported antibacterial activity of stigmasterol from the roots of *Caylusea abyssinica* against *S. aureus*, *E. coli*, *P. aeruginosa* and *S. typhimurium* with zone of inhibition ranging from 11 mm to 18 mm at 50 mg/mL concentration (Edilu *et al*., 2015). In this study compound **45 & 46** were observed to have activities against the test organisms with 9.00±0.00 to 13.33±0.88 mm mean zone of inhibition at 2 mg/mL. This variability could be attributed to the difference in concentration of the compound used and to method of antimicrobial analysis employed. This study represents the first antibacterial evaluation of compounds **45-50** from the stem bark extract of *D. angustifolia*.

On the other hand, the antibacterial activity of compounds previously isolated from ethyl acetate leaves extract of *D. angustifolia* (clerodane diterpene **6**, and flavonoids **25**, **26**, **28** & **51**) were summarized in Table 12. The clerodane diterpene (**6**) was found the only compound with reasonable activity against *P. aeruginosa* with mean inhibition zone of 10.00±0.58 mm at 2 mg/mL, compared to ciprofloxacin (20.40±0.68 mm at 30 µg/mL), but had very low activity against *E.* coli and not active against the Gram positive bacteria. The flavanol santin (**25)** showed good activity against *S. pyogenes* with mean inhibition zone of 10.67±0.88 mm at 2 mg/mL, compared to ciprofloxacin (17.00±0.71 mm at 30 µg/mL).

The flavanone pinocembrin (**26**) was the most active compound against *E. coli* with mean inhibition zone of 12.67±0.88 mm, and also against *S. aureus* **(**10.33±0.88 mm) and *S. pyogenes* (11.00±0.58 mm) each at 2 mg/mL, compared with ciprofloxacin (19.80±0.53, 16.83±0.70, and 17.00±0.71 mm at 30 µg/mL, respectively). Compound **28** was exhibited antibacterial activity against *S. aureus* (12.00±1.00 mm) and *S. pyogenes* (10.00±0.58 mm) at 2 mg/mL concentration, and showed weak activity against the gram negative bacteria (*P. aeruginosea* and *E. coli*). Compound **51** was inhibited the growth of *P. aeruginosea* with 8.00±0.58 mm, at 2 mg/mL and not active against other tested organisms.

Table 12: Antibacterial activity of compounds isolated from ethyl acetate leaf extract of *D. angustifolia.*

Compound/ Standard	Concentration (mg/mL)	Inhibition Diameter mm (mean ± SEM)			
		S. aureus	***S. pyogenes***	***P. aeruginosa***	***E. coli***
6	2	6.00±0.00	6.00±0.00	10.00±0.58	7.00±0.58
	1	6.00±0.00	6.00±0.00	7.67±0.33	6.67±0.33
	0.5	6.00±0.00	6.00±0.00	6.00±0.00	6.00±0.00
	0.25	6.00±0.00	6.00±0.00	6.00±0.00	6.00±0.00
25	2	9.00±0.58	10.67±0.88	8.00±0.58	9.00±0.58
	1	7.33±0.33	8.00±0.58	6.33±0.33	8.00±0.58
	0.5	6.67±0.33	6.67±0.33	6.00±0.00	6.00±0.00
	0.25	6.00±0.00	6.00±0.00	6.00±0.00	6.00±0.00
26	2	10.33±0.88	11±0.58	6.00±0.00	12.67±0.88
	1	9.00±1.00	9.00±0.58	6.00±0.00	8.67±0.88
	0.5	8.00±0.58	7.00±0.58	6.00±0.00	7.00±0.58
	0.25	6.00±0.00	6.00±0.00	6.00±0.00	6.00±0.00
28	2	12.00±1.00	10.00±0.58	6.00±0.00	6.67±0.33
	1	9.00±0.58	8.33±0.33	6.00±0.00	6.00±0.00
	0.5	7.67±0.33	6.67±0.33	6.00±0.00	6.00±0.00
	0.25	6.00±0.00	6.63±0.33	6.00±0.00	6.00±0.00
51	2	6.00±0.00	6.00±0.00	8.00±0.58	6.00±0.00
	1	6.00±0.00	6.00±0.00	7.00±0.58	6.00±0.00
	0.5	6.00±0.00	6.00±0.00	6.00±0.00	6.00±0.00
	0.25	6.00±0.00	6.00±0.00	6.00±0.00	6.00±0.00
Ciprofloxacin (μg/mL)	30 μg/mL	16.83±0.70	17±0.71	20.40±0.68	19.80±0.53

S. aureaus *= Staphylococcus aureus,* ***S. Pyogenes*** *= Streptococcus pyogenes,* ***P. aeruginosa*** *= Pseudomonas aeruginosa,* ***E. coli*** *= Escherichia coli*

Earlier structure activity related study on the antimicrobial activity of flavonoids generally suggested that the hydroxyl group at position C-5 and C-7 is important for antibacterial activity. A hydroxyl was required at C-4' for activity against *P. aeruginosa* (T. Ngabaza *et al*., 2017; Teffo *et al*., 2010). The presence of two hydroxyl groups and a minimum of two methoxy groups was claimed necessary for good antimicrobial activity, while complete methylation, even if the C-5 hydroxy is free, negates activity (L. K. Omosa *et al*., 2014). This is evident from the observation that pinocembrin was showed good activities, than the tri-methoxy substituted compound **51 (**5,6,5′-Trihydroxy-3,7,4’-trimethoxyflavone).

Omosa *et al*., (2014) reported that pinocembrin (**26)** showed antibacterial activity with MIC 62.50 µg/ml (9.49 mm) against *S. aureus*, but no activity with *E. coli.* In contrast the current study was revealed that pinocembrin (**26**) has activity against *E. coli, S. aureus* and *S. Pyogenes*, the difference in activity could be linked to the difference in the concentrations used and method of antibacterial analysis employed.

Moreover, study by Teffo *et al*., (2010) also reported that Santin (**25**) have poor activity against *E. faecalis*, *S. aureus*, *E. coli*, and *P. aeruginosa* with MIC value between 63 and 125 µg/mL. This is consistent with results observed in present study by Santin, additionally it exhibited good activity against *S. pyogenes* (10.67±0.88 mm).

Furthermore, the reported data by Omosa *et al*., (2014) suggested that the activities of diterpenoids are dependent on the position of the hydroxyl group, with increasing order such as OH-6 > OH-2 > OH-19, even though they didn't tested activity for diterpenoids (L. K. Omosa *et al*., 2014). This is evident from the observation that compound **6**, having 2-hydroxy substituent, were more active against gram negative bacteria (*P. aeruginosa*, 10.00±0.58 mm at 2 mg/mL).

The overall antibacterial activity results of the plant extracts and isolated compounds may justify the traditional use of *D. angustifolia* for the treatment of several skin infections, sore throat, toothache, and wound healing. The antibacterial activity exhibited by the compounds on *S. aureus* and *P. aeruginosa* is worthy of mention as thus *S. aureus* and *P. aeruginosa* is a substantial public health problem worldwide causing morbidity and mortality. They are a leading cause of skin and soft tissue infections and *P. aeruginosa* has also been implicated in pneumonia, and surgical site infections.

4.5.2 Antioxidant Activity

The antioxidant activity was evaluated by DPPH method according to the descriptions by *Al Habsi & Hossain* with modification (Al Habsi & Hossain, 2018). This method is based on the reaction of DPPH that is characterized as stable free radical with a deep violet colour and any substance that can donate a hydrogen atom to DPPH reduces it to a stable diamagnetic molecule. It was reported that the effects of phenolic compounds on DPPH scavenging are thought to be due to their hydrogen donating ability. The decrease in the absorbance of the DPPH caused by phenolic compound is due to scavenging of the radical by hydrogen donation, which is visualized as a discoloration from purple to yellow, as depicted in Figure 11 (Riaz *et al*., 2012).

The radical scavenging activity of samples was followed through the decrease in absorbance at 517 nm using UV Visible spectrophotometer. The IC_{50} value is defined as the concentration of a substrate that causes 50 % loss of the DPPH activity. The lower the IC_{50} value, the higher is the scavenging potential (Riaz *et al*., 2012).

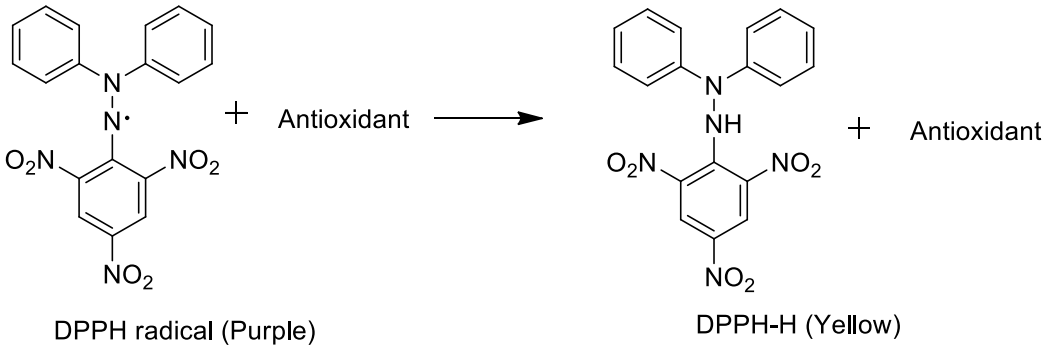

Figure 11: The structure of DPPH radical and its product (DPPH-H)

In this study, the DPPH radical scavenging activities of the extracts and compounds isolated from the stem bark and leaves of *D. angustifolia* were examined by comparison with ascorbic acid as a positive control. The IC_{50} values of all samples were calculated and the results are depicted in (Table 13-15, and Figure 12-14). The results generally revealed that activity increased with increasing concentration of the samples.

The aqueous MeOH soluble portion exhibited the highest percent inhibition of the DPPH radical as compared to the other extracts. It showed 92.02 % and 90.44% inhibition of the DPPH radical at a concentration of 1000 µg/mL and 31.25 µg/mL. The concentration of this extract leading to 50 % inhibition of the DPPH radical (IC_{50}) was found to be 13.15 µg/mL, compared to the positive control ascorbic acid, having an IC_{50} of 0.374 µg/mL. The lowest radical scavenging activity was found in DCM extract with inhibition value of 86.89% at 1000 µg/mL and IC_{50} value of 47.11 µg/mL. Whereas the IC_{50} value of the DCM: MeOH extract was found to be 23.71 µg/mL (Table 13, Figure 12).

Table 13: DPPH radical scavenging activities (%) of the stem bark extracts of *D. angustifolia*

Concentration (µg/mL)	Control	DPPH Assay Results of Extracts						Positive control	
		DCM		DCM:MeOH		Aqueous MeOH		Ascorbic Acid	
		A	%RSA	A	%RSA	A	%RSA	A	%RSA
1000	1.266	0.166	86.89	0.106	91.63	0.101	92.02	0.063	95.024
500	1.266	0.219	82.70	0.114	90.995	0.104	91.79	0.068	94.63
250	1.266	0.226	82.15	0.119	90.60	0.108	91.47	0.07	94.47
125	1.266	0.365	71.17	0.129	89.81	0.115	90.92	0.072	94.313
62.5	1.266	0.635	49.84	0.177	86.02	0.116	90.84	0.077	93.92
31.25	1.266	0.817	35.47	0.323	74.49	0.121	90.44	0.079	93.76
IC_{50} (µg/mL)		47.11		23.71		13.15		0.374	

Each value is a mean of three biological replicates.

A- Absorbance, RSA-Radical Scavenging Activity

The DPPH assay also revealed varying degrees of antioxidant activity for the compounds with IC_{50} values ranging from 0.089 to 34.47 µg/mL. Among the compounds (**45-50)** isolated from dichloromethane stem bark extract, compound **45** was the most active, found to have an IC_{50} of 0.58 µg/mL. Compounds **46** and **49** were showed very close IC_{50} values of 2.06 and 2.81 µg/mL, respectively. Compound **47** and **48** exhibited IC_{50} value of 7.69 and 5.23 µg/mL. Compound **50** showed the lowest scavenging potential (IC_{50}: 34.47 µg/mL), because this compound had open chain structure. The results are expressed relative to the ascorbic acid, a reference standard having an IC_{50} = 0.11 µg/mL (Table 14, Figure 13).

On the other hand, the antioxidant activity of compounds **6**, **25**, **26**, **28** and **51** were depicted in Table 15 & Figure 14. Compound **26** (5, 7-dihydroxyflavanone) exhibited the highest DPPH radical scavenging activity (IC_{50}: 0.089 µg/mL), followed by compound **6 (**clerodane diterpene), (IC_{50}: 4.45 µg/mL), compound **28** (IC_{50}: 5.63 µg/mL), and Santin (**25)** (IC_{50}: 7.07 µg/mL). However, compound **51** showed weak percent DPPH radical scavenging activity (40.84%) at 400 µg/mL concentrations, having an IC_{50} = 20.42 µg/mL. The antioxidant activity of the compounds was investigated compared to the positive control ascorbic acid, having IC_{50} = 0.11 µg/mL.

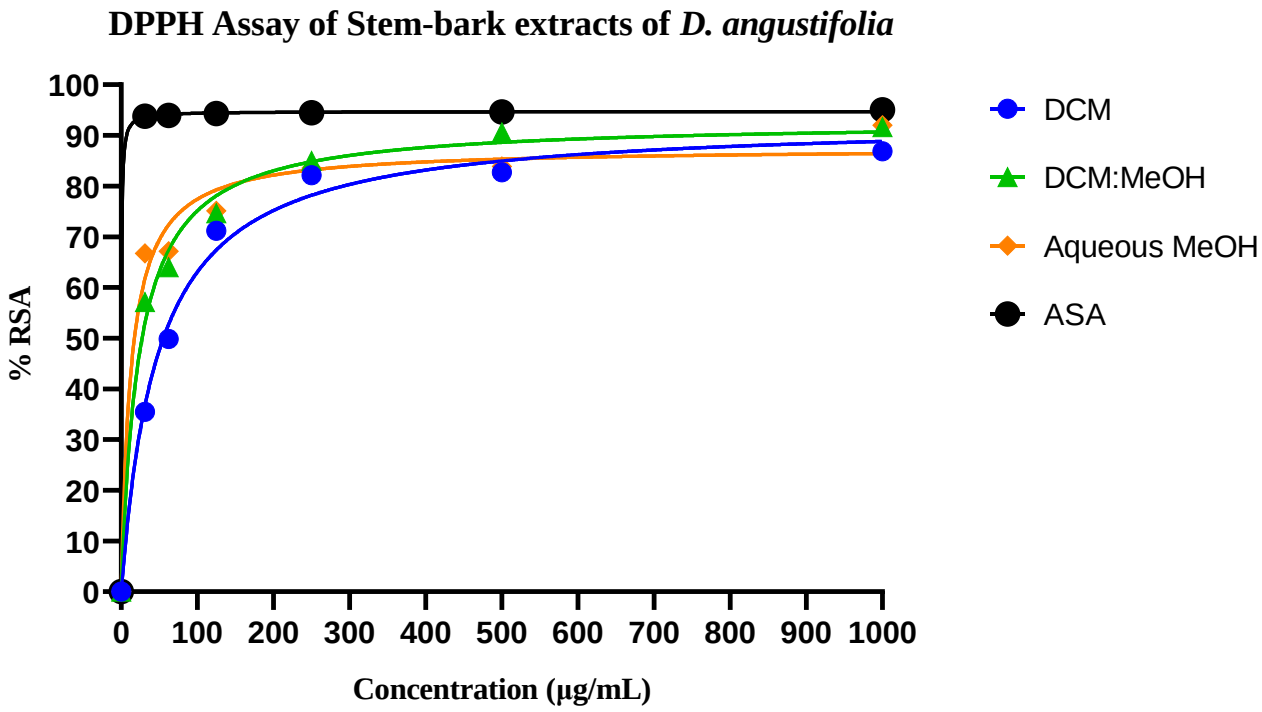

Figure 12: DPPH radical scavenging activities (%) of the stem-bark extracts of *D. angustifolia*

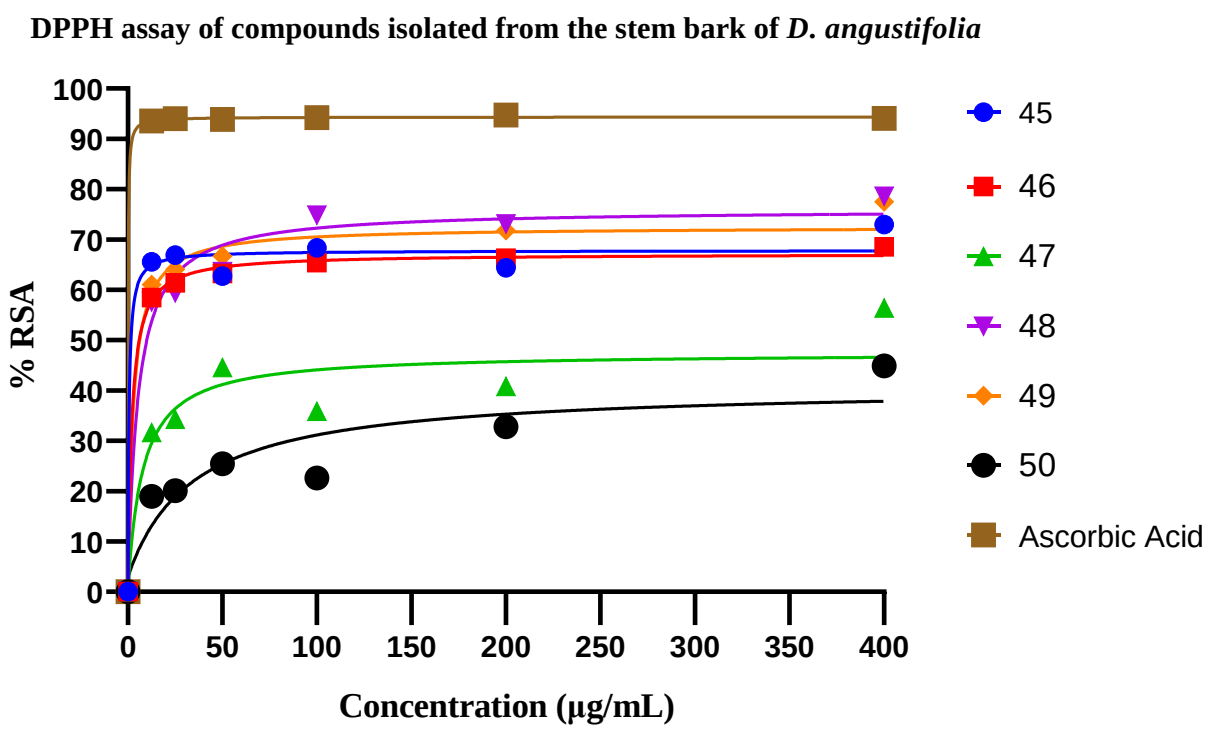

Figure 13: DPPH radical scavenging activities (%) of compounds isolated from stem bark extract of *D. angustifolia*.

Table 14: DPPH radical scavenging activities (%) of compounds isolated from stem bark extract of *D. angustifolia*

Concentration (µg/mL)	Control	DPPH Assay of Compounds Isolated from the Stem-bark of *D. angustifolia*							
		45		46		47		48	
		A	%RSA	A	%RSA	A	%RSA	A	%RSA
400	1.266	0.342	72.99	0.398	68.56	0.552	56.398	0.271	78.59
200	1.266	0.451	64.38	0.427	66.27	0.749	40.84	0.341	73.06
100	1.266	0.401	68.33	0.438	65.403	0.812	35.86	0.319	74.803
50	1.266	0.472	62.72	0.465	63.27	0.702	44.55	0.461	63.59
25	1.266	0.419	66.90	0.489	61.37	0.832	34.28	0.514	59.40
12.5	1.266	0.436	65.56	0.526	58.452	0.865	31.675	0.537	57.58
IC50 (µg/mL)		0.58		2.06		7.69		5.23	

Concentration (µg/mL)		49		50		Ascorbic Acid	
		A	%RSA	A	%RSA	A	%RSA
400	1.266	0.285	77.49	0.698	44.87	0.07	94.08
200	1.266	0.357	71.801	0.851	32.78	0.078	94.71
100	1.266	0.431	65.96	0.98	22.591	0.074	94.234
50	1.266	0.422	66.67	0.944	25.43	0.081	93.84
25	1.266	0.455	64.06	1.012	20.06	0.089	93.997
12.5	1.266	0.493	61.06	1.026	18.96	0.127	93.523
IC50 (µg/mL)		2.81		34.47		0.11	

Each value is a mean of three biological replicates.

A- Absorbance, RSA-Radical Scavenging Activity

Earlier structure activity relationships studies showed that the position and number of hydroxyl groups (–OH) plays significant role in the antioxidant activity. Particularly, the flavonoids moiety having hydroxyl groups at ortho or para position, exhibit higher antioxidant activity than at meta position. The effect of the functional group is responsible for antioxidant activity in the following order: –OH > –OAc > –C=O (oxo) (Muhammad et al., 2016). In consistent to this because of the free 5, 7-dihydroxy groups, compound **26** exhibited better antioxidant activities compared to compound **25** & **28**, as C-3 and C-6 position of compound **25** & **28** has -OCH_3. Notably, that compound **26** (5, 7-dihydroxyflavanone), is significantly effective at lower doses and showed highest IC_{50} value (0.089 µg/mL), than the reference standard ascorbic acid (IC_{50}: 0.11 µg/mL).

Table 15: DPPH radical scavenging activities (%) of compounds isolated from ethyl acetate leaves extract of *D. angustifolia*

Concentration (µg/mL)	**Control**	**DPPH Assay of Compounds from the Leaves of *D. angustifolia***					
		6		**25**		**26**	
		A	**%RSA**	**A**	**%RSA**	**A**	**%RSA**
400	1.266	0.465	63.27	0.858	32.23	0.081	93.602
200	1.266	0.65	48.66	0.899	28.99	0.087	93.13
100	1.266	0.668	47.24	0.938	25.91	0.076	93.997
50	1.266	0.73	42.34	0.973	23.144	0.082	93.523
25	1.266	0.685	45.893	0.988	21.96	0.087	93.13
12.5	1.266	0.734	42.02	0.996	21.33	0.089	92.97
IC50 (µg/mL)		4.45		7.07		0.089	

Concentration (µg/mL)	**Control**	**Compounds**				**Positive control**	
		28		**51**		**Ascorbic Acid**	
		A	**%RSA**	**A**	**%RSA**	**A**	**%RSA**
400	1.266	0.487	61.53	0.749	40.84	0.075	94.08
200	1.266	0.694	45.182	0.89	29.70	0.067	94.71
100	1.266	0.677	46.52	0.895	29.305	0.073	94.234
50	1.266	0.699	44.79	0.98	22.591	0.078	93.84
25	1.266	0.751	40.68	1.008	20.38	0.076	93.997

12.5	1.266	0.769	39.26	1.019	19.51	0.082	93.523
IC50 (µg/mL)		5.63		20.42		**0.11**	

Each value is a mean of three biological replicates.

A- Absorbance, RSA-Radical Scavenging Activity

However, earlier study done on compounds isolated from *D. viscosa* by Muhammad *et al*., (2015) have been reported that flavonoid that have OCH_3 group at C-6 that lies between two OH located at C-5 and C-7 has increased antioxidant activity (Muhammad *et al*., 2015). This report was in contrary to the earlier structural activity study claimed by Cao *et al*. (1997) that the O-methylation of OH diminishes the antioxidant activity of flavonoids (Cao *et al*., 1997). This fact is supported by relatively lowest radical scavenging activity of compound **25, 28** and **52**, were compounds with more OCH_3 showed less activity. The variation could be attributed to the difference in concentration of the compound used and to method of antioxidant analysis employed (*i.e.* DPPH and ABTS).

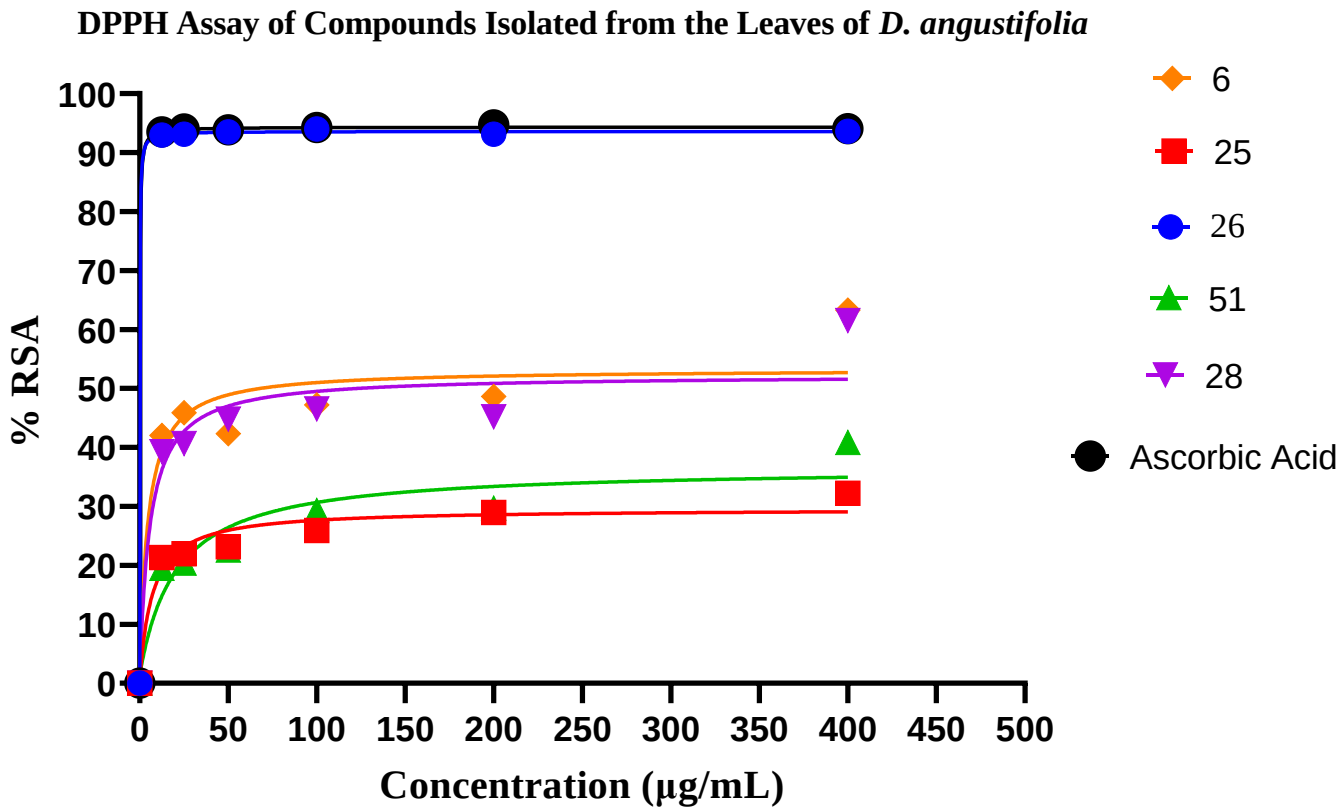

Figure 14: DPPH radical scavenging activities (%) of compounds isolated from ethyl acetate leaves extract of *D. angustifolia*

4.6 *In silico* ADMET and Drug Likeness Prediction

Physicochemical properties, drug-likeness, boiled-egg model, and pharmacokinetic (ADME) properties of compounds (**6**, **25**, **26**, **28**, **45**, **47**, **48**, **49** & **51**) isolated from the extracts of *D. angustifolia*, were determined using the SwissADME (Daina *et al*., 2017) and PreADMET (Lee *et al*., 2003) and toxicity profile using ProTox-II (Banerjee *et al*., 2018) online tools. Lipinski's rule of five (Lipinski *et al*., 1997) is one of the most effective tools for predicting new chemical entities (NCE) drug-likeness. Veber's rule is a commonly acknowledged technique for predicting the oral bioavailability of NCE (Veber *et al*., 2002). The drug-likeness of the isolated compounds was predicted according to Lipinski and Veber's rule.

The results revealed that the control ciprofloxacin (CPFX) and isolated compounds met Lipinski's criteria, with the exception of compound **45**, and **49**, which had one violation because of their high lipophilic character (cLogP > 5). According to Veber's rule, compounds **47, 48** and **49** had one violation because of more number of rotatable bonds (>10) as these compounds had open chain structure. Except compound **47-49** all the compounds and reference drug, CPFX appeared to be good oral drug candidates based on these findings as presented in Table 16.

Table 16: Drug-likeness predictions of compounds and standard, computed by SwissADME

Compounds	Formula	MW (g/mol)	NHD	NHA	LogP (cLogP)	Lipinski's ROF violation	NRB	TPSA ($Å^2$)	Veber's rule violation
45	$C_{29}H_{48}O$	412.69	1	1	6.97	1	5	20.23	0
47	$C_{21}H_{40}O_5$	372.54	2	5	5.32	0	20	83.83	1
48	$C_{21}H_{42}O_4$	358.56	2	4	5.41	0	20	66.76	1
49	$C_{18}H_{36}O_2$	284.48	1	2	5.93	1	16	37.3	1
6	$C_{20}H_{28}O_4$	332.43	2	4	3.46	0	4	70.67	0
25	$C_{18}H_{16}O_7$	344.32	2	7	2.52	0	4	98.36	0
26	$C_{15}H_{12}O_4$	256.25	2	4	2.26	0	1	66.76	0
28	$C_{17}H_{14}O_7$	330.29	3	7	2.1	0	3	109.36	0
51	$C_{18}H_{16}O_8$	360.31	3	8	2.15	0	4	118.59	0
CPFX	$C_{17}H_{18}FN_3O_3$	331.34	2	6	1.1	0	3	74.57	0

CPFX = Ciprofloxacin, NHD = Number of Hydrogen donor, NHA = Number of Hydrogen acceptor, NRB = Number of rotatable bonds, and TPSA = total polar surface area

ADME and Toxicity Prediction

The reference drug, CPFX, and the isolated compounds exhibited high GI absorption, except with compound **45,** probably due to the low TPSA (23.23 $Å^2$) (Table 16) that leads to poor aqueous solubility, which is a rate limiting step for dissolution (Tambosi et al., 2018). BBB permeability is one of the important parameter that molecules exhibit their action at CNS (Kadry *et al*., 2020). Among all the isolated compounds and reference drug, only compound **6** and **26** showed BBB permeability (Table 17), which is an indication that these compounds (**6**, **26**) act on the CNS.

The rate at which a substance penetrates the stratum corneum is measured by skin permeability (Kp). This value is commonly used to quantify the transport of molecules in the epidermal skin's outermost layer and to highlight the importance of skin absorption. The more negative the log Kp, the lower the cutaneous permeability of the molecule, with permissible range of LogKp - 8.0 to - 1.0 **cm/s** (Chen *et al*., 2018; Zeng *et al*., 2021). In this study, compared to CPFX, the isolated compounds showed lesser LogKp value ranging from -2.19 to -6.52 (Table 17), so these compounds might have better skin permeation than CPFX. This might supports the promising results observed from *in vitro* antibacterial test of the constituents against photogenic bacteria, implied in skin and soft tissue infections.

Increased P-glycoprotein (P-gp) expression in the intestine can limit the absorption of medicines that are P-gp substrates. As a result, bioavailability is diminished, and therapeutic plasma concentrations are not achieved (Elmeliegy *et al*., 2020). The results revealed that compounds **6, 47** and reference CPFX showed substrate for P-gp, whereas the other compounds are not. Therefore, compound **25, 26, 28, 45, 48, 49, 51** may have better bioavailability than other compounds and standard.

Moreover, about 60% of prescribed drugs are metabolized by CYP enzymes, with CYP3A4 accounting for about half of this metabolism, followed by CYP2D6, CYP2C9, and CYP2C19 (Esteves *et al*., 2021). As observed from SwissADME computed study the CYP3A4 and CYP2D6 enzymes were inhibited by compounds **25, 28, 51**, suggesting that these enzymes may not metabolize these compounds. Similarly, CYP2C9 inhibited by compounds **25**, **28, 45**, **47**, and **51**, whereas, CYP2C19 inhibited only by compounds **26** and **47**. CYP1A2 inhibited by all compounds except with compounds **6, 45** and reference CPFX (Table 17).

Table 17: ADME predictions of the compounds and standard, computed by SwissADME and PreADMET

Compounds	GI ABS	BBB Permeability	log Kp (cm/s)	P-gp substrate	Inhibitor Interaction (SwissADME/PreADMET)				
					CYP3A4 inhibitor	CYP2D6 inhibitor	CYP2C9 inhibitor	CYP2C19 inhibitor	CYP1A2 inhibitor
45	Low	No	-2.74	No	No	No	Yes	No	No
47	High	No	-3.27	Yes	No	No	Yes	Yes	Yes
48	High	No	-3.23	No	No	No	No	No	Yes
49	High	No	-2.19	No	No	No	No	No	Yes
6	High	Yes	-5.25	Yes	No	No	No	No	No
25	High	No	-6.17	No	Yes	Yes	Yes	No	Yes
26	High	Yes	-5.82	No	No	No	No	Yes	Yes
28	High	No	-6.31	No	Yes	Yes	Yes	No	Yes
51	High	No	-6.52	No	Yes	Yes	Yes	No	Yes
CPFX	High	No	-9.09	Yes	No	No	No	No	No

GI = Gastro-Intestinal, ABS = Absorption, BBB = Blood Brain Barrier, P-gp = P-glycoprotein, CYP = Cytochrome-P

Furthermore, the cLogP and TPSA values of the compounds were plotted to predict human intestinal absorption (HIA) and blood brain barrier (BBB) access using **BOILED-Egg model** (Daina & Zoete, 2016) (Figure 15). The egg-shaped plot is divided into 3 parts including a white area (human intestinal absorption, HIA), a yellow area (BBB access) and a grey area (no HIA or BBB access). In this prediction, compound **25, 28, 47**, **48**, **49** and **51** are in white area, so these compounds may be absorbed through intestine, whereas compound **6** and **26** are in yellow area, suggesting that these two compounds may passed through the BBB, as presented in Figure 15. However, only compound **45** shown in grey area, which indicates no HIA or BBB access.

This model also predicted whether those compounds are substrates of P-gp (PGP). Blue dots (PGP+) represent compounds that are substrates of PGP CNS efflux transporter and could effluated from the CNS, while, red dots (PGP-) represent compounds that are not substrates of the PGP could pass through and acting on CNS (Daina & Zoete, 2016). In this study only compounds **6** and **47** had blue dots, suggesting that these compounds are PGP substrate and eventually not acting on the CNS.

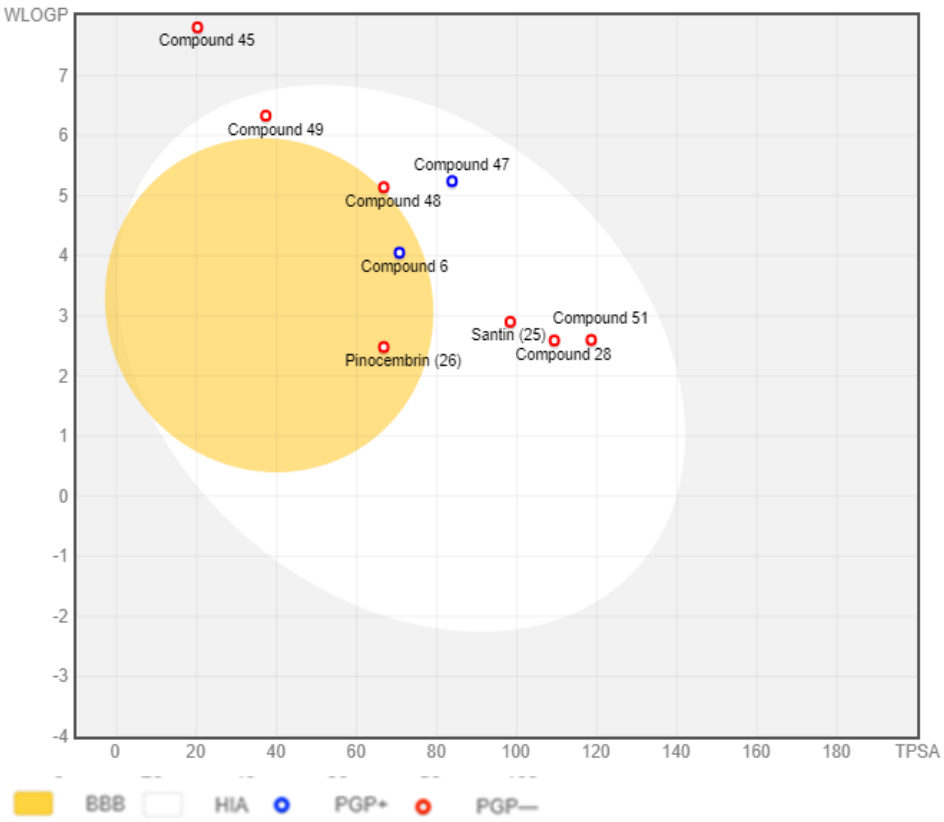

Figure 15: BOILED-Egg model for predicting gastrointestinal absorption and brain access

Toxicity studies

The level of toxicity is expressed on a scale from 1 to 6, with a greater number indicating a lower level of toxicity. It is determined based on the LD_{50} (mg/kg) value, which denotes a dose that will kill 50% of the test animal (Drwal *et al*., 2014). Among all the studied compounds **47** was predicted to be less or no toxic since it falls under Class 6. Compounds **6**, **26**, **45** and **49** showed toxic class 4, like CPFX, whereas compound **25**, **28**, **48** and **51** were showed toxic class 5. None of the isolated compounds revealed hepatotoxicity, carcinogenicity or mutagenicity. CPFX only exhibited mutagenicity, whereas **6, 25**, **28**, **45** and **51** showed immunotoxicity. Likewise compound **26** exhibited cytotoxicity (Table 18).

Table 18: Toxicity prediction of isolated compounds and standard, computed by Pro-Tox II

Compound	LD_{50} (mg/kg)	Toxicity Class	Organ Toxicity				
			Hepatotoxicity	Carcinogenicity	Immunotoxicity	Mutagenicity	Cytotoxicity
45	890	4	No	No	Yes	No	No
47	10000	6	No	No	No	No	No
48	5000	5	No	No	No	No	No
49	900	4	No	No	No	No	No
6	370	4	No	No	yes	No	No
25	5000	5	No	No	Yes	No	No
26	2000	4	No	No	No	No	Yes
28	5000	5	No	No	Yes	No	No
51	5000	5	No	No	Yes	No	No
CPFX	2000	4	No	No	No	Yes	No

4.7 *In silico* Molecular Docking study of isolated compounds

4.7.1 Molecular Docking with *E. coli* DNA gyrase

DNA gyrase is a topoisomerase-type enzyme that is required during bacterial DNA replication and transcription to maintain topology and integrity. It consists of four subunits (two A subunits and two B subunits) attached together to form a tetrameric holoenzyme (Janupally *et al*., 2015). Currently, DNA gyrase is considered one of the primary targets and has been clinically validated in most pathogenic bacteria (Narramore *et al*., 2019). Fluoroquinolones are well-known DNA gyrase inhibitors that target the enzyme's A subunit specifically.

In this study *E. coli* DNA gyrase B (PDB ID: 6F86) was used as a target and a fluroquinolone class of antibacterial CPFX, was used as a reference control for docking with the target. Binding affinity and interactions with different amino acids are presented in the Table 19, and 3D and 2D binding interactions is depicted in Figure 16. Compound **26** showed highest binding affinity (-8.1 kcal/mol) among all compounds and standard drug (-7.3 kcal/mol) followed by compound **45** (-7.4 kcal/mol). Since, compound **26** had highest *in vitro* activity against *E. coli* this prediction also confirms the considerable potential of the compound against pathogenic bacteria like *E. coli*. CPFX formed hydrogen bonding interactions with Asn-46 and Asp-73. Similarly compound **26** showed interactions with these two amino acids along with Gly-77 and Arg-76. Other test compounds showed H-bonding interactions with either Asn-46 or Asp-73 along with other amino

acids. Most of the compounds showed residual interactions with Pro-79, Ile-78, Glu-50, Gly-77, Ala-47. Since compounds **47** – **49** showed less binding affinity (< 5.5 kcal/mol), their interactions were not recorded.

Table 19: Molecular docking binding affinity and interactions of isolated compounds and standard with the target *E. coli* DNA gyrase B (PDB ID: 6F86)

Compounds	Affinity (kcal/mol)	H-bond	Residual Amino acid Interactions	
			Hydrophobic/Pi-Cation/Pi-Anion/ Pi-Alkyl interactions	Van-der Walls interactions
45	-7.4	Asp-73	Ile-78	Gly-77, Ile-94, Pro-79, Thr-165
47	-5.3	-	-	-
48	-5.1	-	-	-
49	-4.8	-	-	-
6	-6.7	Arg-136, Asn-46, Asp-49	Pro-79, Arg-76	Gly-77, Glu-50, Asp-73, Ile-94,
25	-7.2	Asn-46, Thr-165	Pro-79, Ile-78, Glu-50, Arg-76	Gly-77, Ala-47, Arg-136, Ala-73, Asp-73, Asp49
26	-8.1	Asn-46, Asp-73, Gly-77, Arg-76	Ile-78, Glu-50, Ile-94	Ala-47, Pro-79, Thr-165
28	-7.2	Arg-136, Asp-73	Ile-78, Glu-50, Arg-76	Gly-77, Ala-47, Pro-79, Thr-165, Asn-46
51	-7.0	Asn-46, Arg-136	Pro-79, Ile-78, Glu-50, Arg-76	Gly-77, Ala-47, Asp-73, Asp49
CPFX	-7.3	Asn-46, Asp-73, Asp-49*	Pro-79, Asn-46, Asp-49	Gly-77, Ala-47, Glu-50, Arg-76, Ile-78

*Carbon Hydrogen bond

Figure 16: Molecular docking binding interactions (3D & 2D) of isolated compounds and standard with the target *E. coli* DNA gyrase B (PDB ID: 6F86)

No.	3D	2D
45	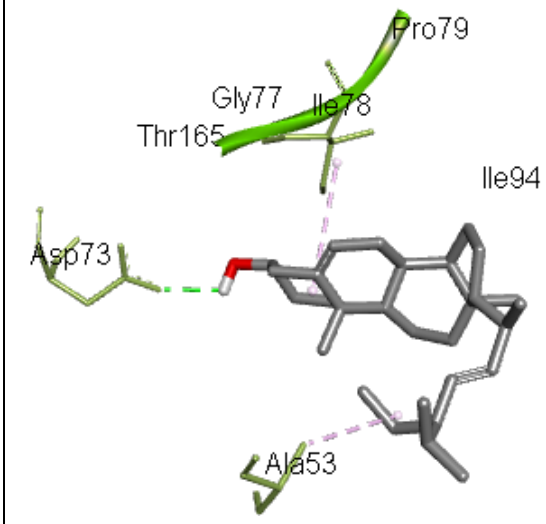	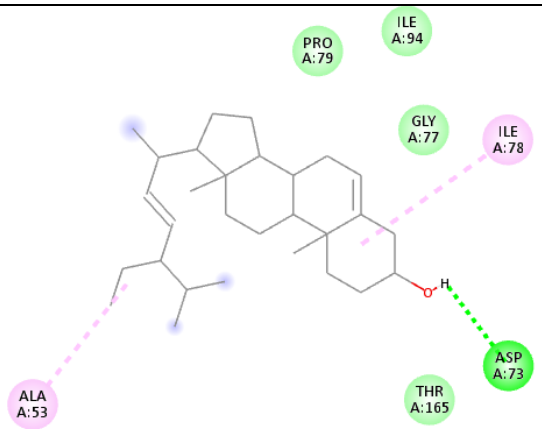
6	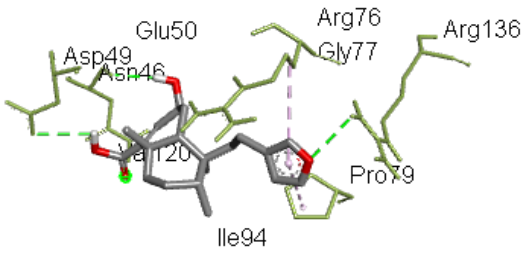	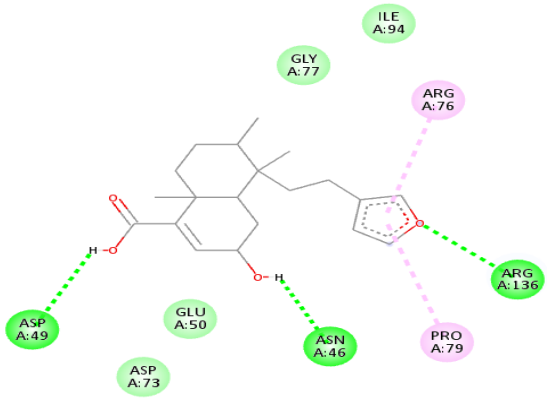
25	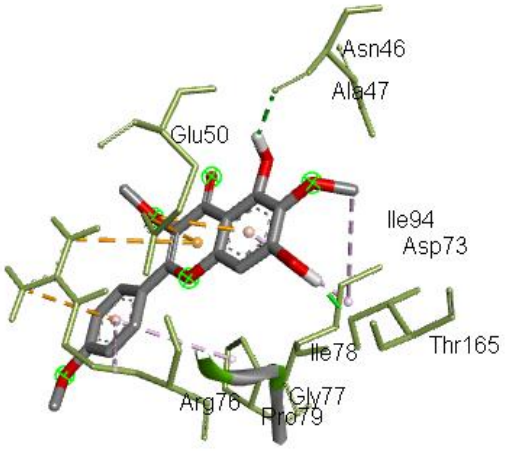	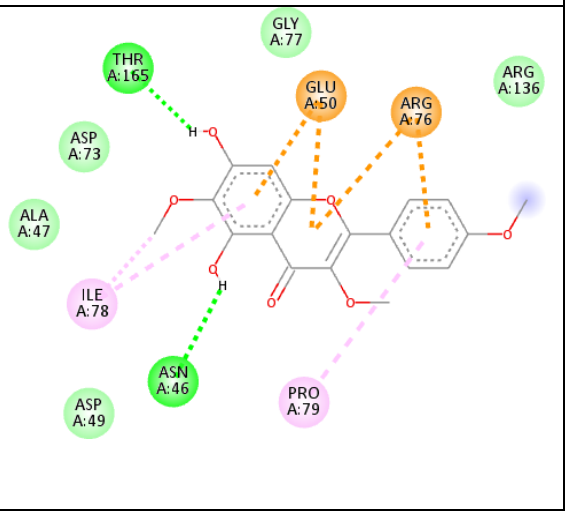

26	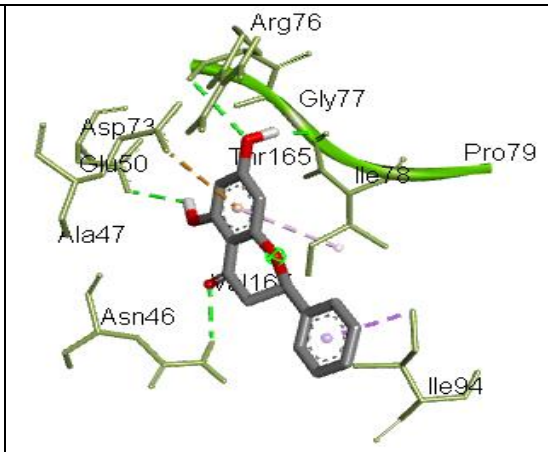 Arg76 Gly77 Asp73 Glu50 Thr165 Pro79 Ile78 Ala47 Asn46 Ile94	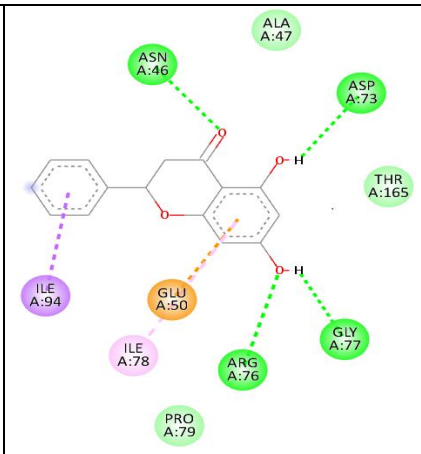 ALA A:47 ASN A:46 ASP A:73 THR A:165 ILE A:94 GLU A:50 GLY A:77 ILE A:78 ARG A:76 PRO A:79
28	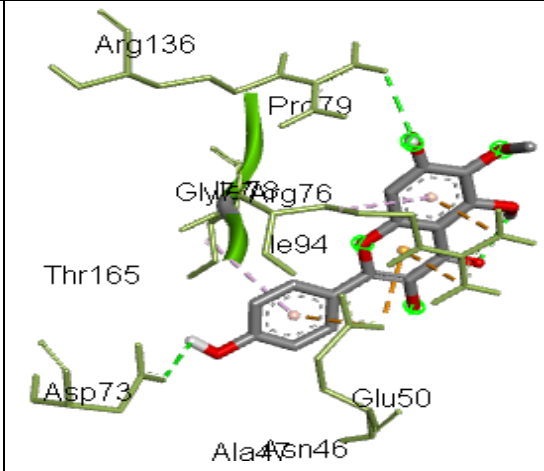 Arg136 Pro79 Arg76 Ile94 Thr165 Asp73 Glu50 Asn46	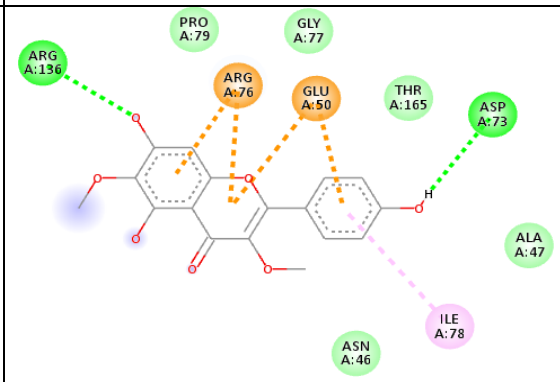 PRO A:79 GLY A:77 ARG A:136 ARG A:76 GLU A:50 THR A:165 ASP A:73 ALA A:47 ILE A:78 ASN A:46
51	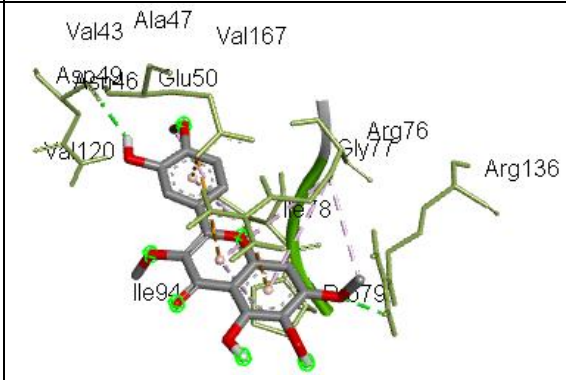 Val43 Ala47 Val167 Asp49 Asn46 Glu50 Val120 Arg76 Gly77 Arg136 Ile78 Ile94	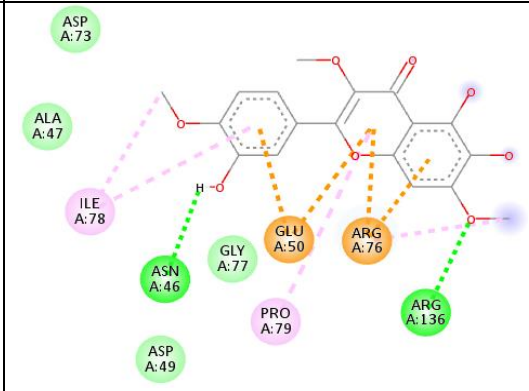 ASP A:73 ALA A:47 ILE A:78 GLU A:50 ARG A:76 GLY A:77 ASN A:46 PRO A:79 ARG A:136 ASP A:49
CPFX	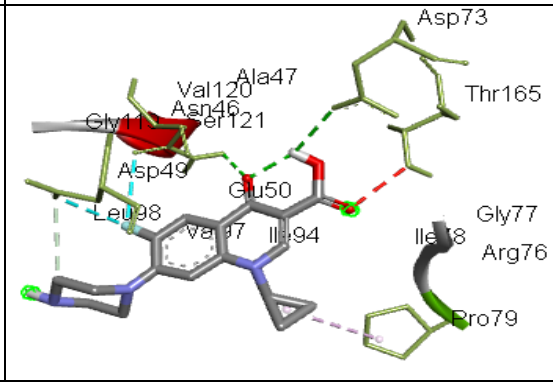 Asp73 Ala47 Val120 Thr165 Asn46 Asp49 Glu50 Gly77 Arg76 Pro79	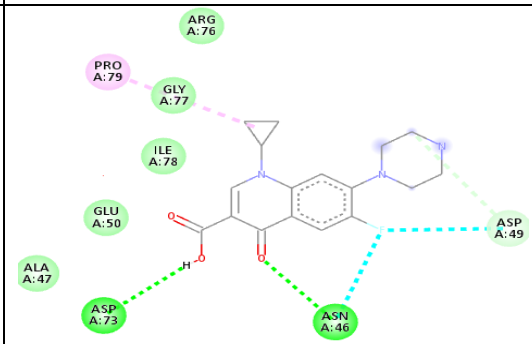 ARG A:76 PRO A:79 GLY A:77 ILE A:78 GLU A:50 ASP A:49 ALA A:47 ASP A:73 ASN A:46

4.7.2 Molecular Docking with *S. aureus* Pyruvate kinase

Pyruvate kinase (PK) has been identified as a crucial enzyme in staphylococci, and regulates their growth, antibiotic resistance, and biofilm formation (Vasu *et al*., 2015). Furthermore, it was found to be structurally distinct from human homologs, and hence it provides a promising target for novel antimicrobial agents (Akunuri *et al*., 2022). For the docking studies, *S. aureus* PK (PDB ID: 3T07) was used as a target and CPFX was used as reference control. Binding affinity and interactions with different amino acids are presented in the Table 20, and 3D and 2D binding interactions is depicted in Figure 17.

Santin (**25)** had highest binding affinity (-5.1 kcal/mole), followed by compound **28** (-5.0 kcal/mole) and **51** (-4.9 kcal/mole), the latter is similar to that of CPFX. Whereas, scoring poses of compounds **45** and pinocembrin (**26**) was -4.8 kcal/mole. Santin (**25**) showed similar H-bonding interaction like CPFX with Ser-362, Thr-366 and Asn-369. Other compounds (**6**, **26**, **28**, **51**) showed H-bonding interaction either one or two of these amino acids. Most of the compounds showed residual amino acids interactions with Ile-361 and His-365. Since compounds **47** – **49** showed less binding affinity (< 3.5 kcal/mol), their interactions were not recorded.

Table 20: Molecular docking binding affinity and interactions of isolated compounds and standard with the target *S. aureus* PK (PDB ID: 3T07)

Compounds	Affinity (kcal/mol)	H-bond	Residual Amino acid Interactions	
			Hydrophobic/Pi-Cation/Pi-Anion/ Pi-Alkyl interactions	Van-der Walls interactions
45	-4.8	Asn-369	Ile-361, His-365	-
47	-3.4	-	-	-
48	-3.7	-	-	-
49	-3.2	-	-	-
6	-4.3	Ser-362, Thr-366, Asn369*	-	-
25	-5.1	Ser-362, Thr-366, Asn-369	His-365	-
26	-4.8	Ser-362	Ile-361, His-365, Ala-358	-
28	-5.0	Ser-362, Thr-366	Ile-361, His-365	-
51	-4.9	Ser-362, Asn-369	His-365	Thr-366
CPFX	-4.9	Ser-362, Thr-366, Asn-369	Ile-361	His-365

*Carbon Hydrogen bond

Figure 17: Binding interactions (3D & 2D) of isolated compounds and standard with the target *S. aureus* PK (PDB ID: 3T07)

No.	3D	2D
45	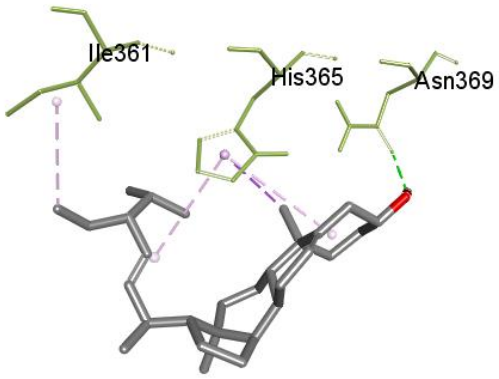	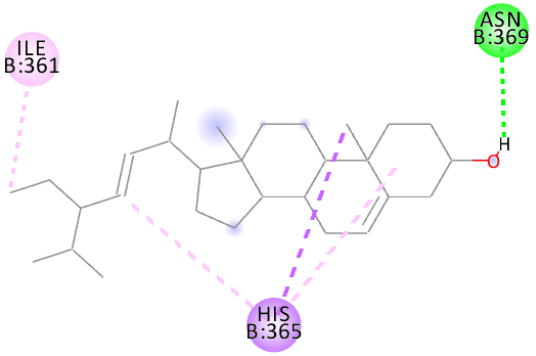
6	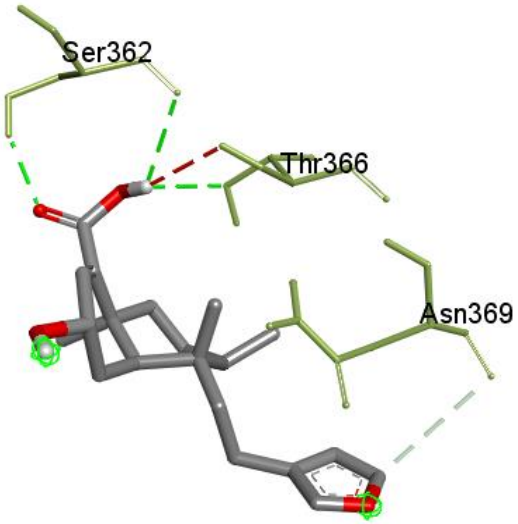	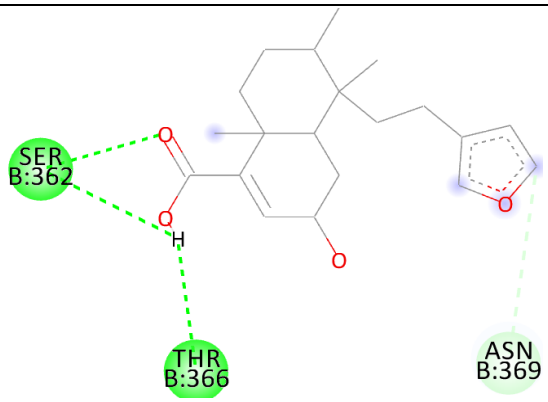
25	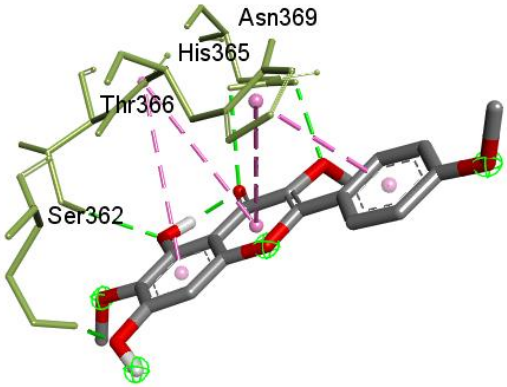	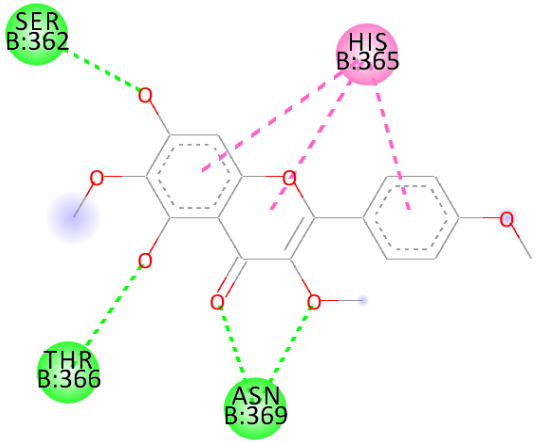

26	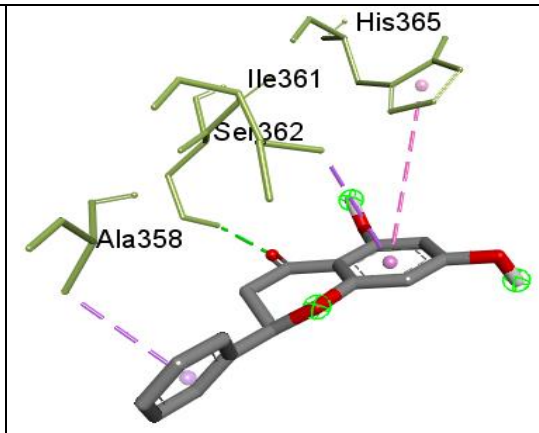 His365 Ile361 Ser362 Ala358	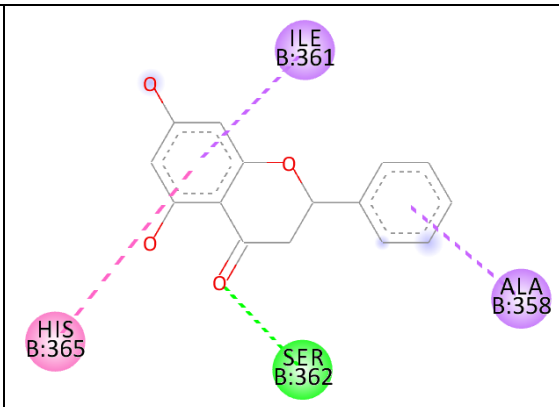 ILE B:361 ALA B:358 HIS B:365 SER B:362
28	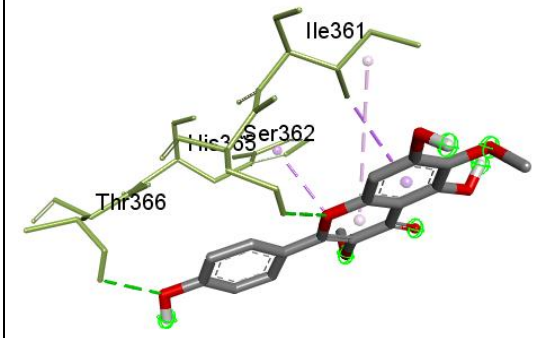 Ile361 Ser362 Thr366	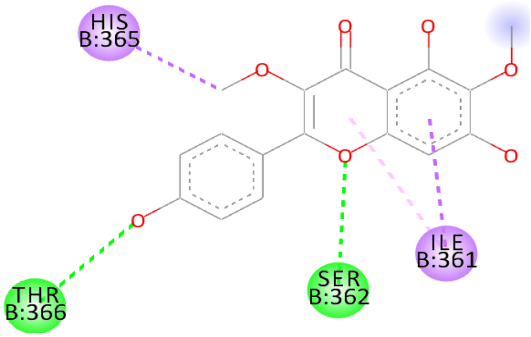 HIS B:365 ILE B:361 SER B:362 THR B:366
51	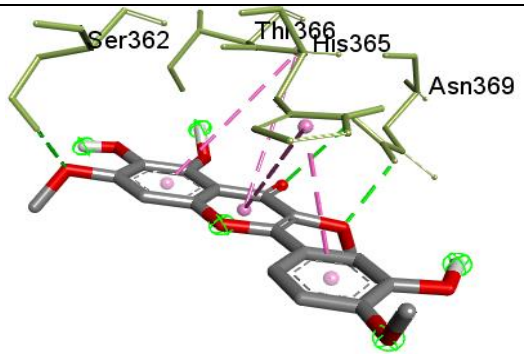 Ser362 His365 Asn369	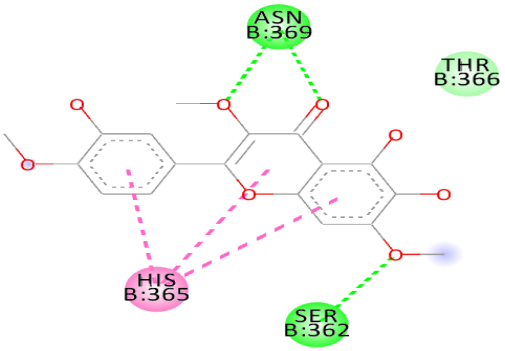 ASN B:369 THR B:366 HIS B:365 SER B:362
CPFX	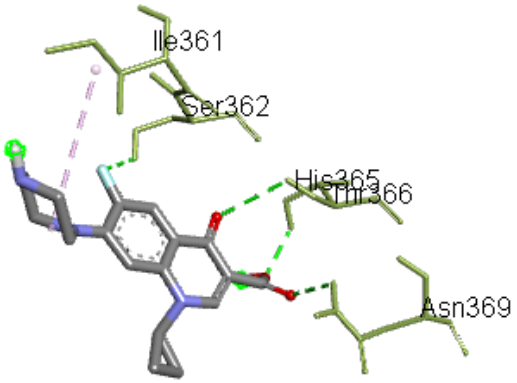 Ile361 Ser362 Asn369	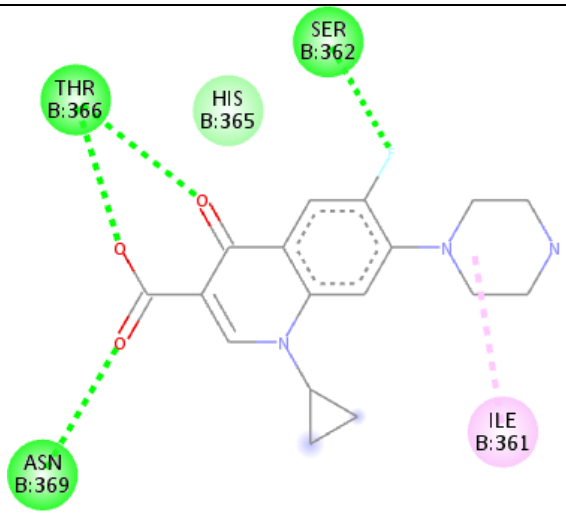 SER B:362 THR B:366 HIS B:365 ILE B:361 ASN B:369

4.7.3 Molecular docking with Human Topoisomerase II*β*

Topoisomerase II (TOP2) enzyme is a nuclear enzyme that plays crucial functions during DNA processes such as, replication, transcription, and repair *via* catalysis of the relaxation and unwinding of double-stranded DNA (Delgado *et al*., 2018). Recent studies showed that TOP2*β* is an important target for many anticancer agents including etoposide (EVP) (Farouk *et al*., 2023). In the present study human TOP2*β* (PDB ID: 3QX3) is used as a target and EVP is used as a reference control. Binding affinity and interactions with different amino acids are presented in the Table 21, and 3D and 2D binding interactions is depicted in Figure 18.

Among the isolated compounds, **51** showed highest binding affinity (-6.0 kcal/mol), whereas standard EVP exhibited -7.5 kcal/mol. EVP showed H-bonding interactions with His-775, Lys-505, Asp-561, Arg-503, and pinocembrin (**6)** showed similar interaction with these amino acids except Arg-503. Other test compounds exhibited H-bonding interactions with one or two of these amino acids. Most of the compounds showed residual amino acid interactions with Glu-477 and Gly-504. Compounds **47-49** showed lesser binding affinities (< 3.8 kcal/mol) compared to other compounds and standard, their interactions were not recorded.

Table 21: Molecular docking binding affinity and amino acid interactions of isolated compounds and standard with the target human topoisomerase II*β* (PDB ID: 3QX3)

Compounds	Affinity (kcal/mol)	H-bond	Residual Amino acid Interactions	
			Hydrophobic/Pi-Cation/Pi-Anion/ Pi-Alkyl interactions	Van-der Walls interactions
45	-5.9	His-775, Asp-561, Arg-503	-	Arg-503
47	-3.7	-	-	-
48	-3.7	-	-	-
49	-3.5	-	-	
6	-5.7	His-775, Asp-561, Asp-557	-	Gly-504, Gly-776, Ala-779, Arg-729, Lys-505, Glu-477, Arg-503
25	-5.8	Arg-503, Glu-477*, Asp-557*	Glu-477, His-775	Gly-504, Asp-561, Asp-479, Gly-478, Ser-480
26	-5.6	His-775, Lys-505, Asp-561	Glu-477, Asp-561	-
28	-5.9	His-775, Glu-477, Asp-557, Asp-559*, His-774*	His-475	Arg-503, Asp-561
51	-6.0	His-775, Asp-561, Arg-729, Glu-477, Asp-557*, Gly-478*	Glu-477, Arg-503	Gly-504, Asp-479, Ser-480, Lys-505

EVP	-7.5	His-775, Lys-505, Asp-561, Arg-503	Arg-503, His-775, Glu-522	Gly-504, Gly-776, Ala-779, Arg-729, Asp-559, His-774, Glu-477,

*Carbon Hydrogen bond

Figure 18: Binding interactions (3D & 2D) of isolated compounds and standard with Human TOP-IIβ (PDB ID: 3QX3)

No.	3D	2D
45	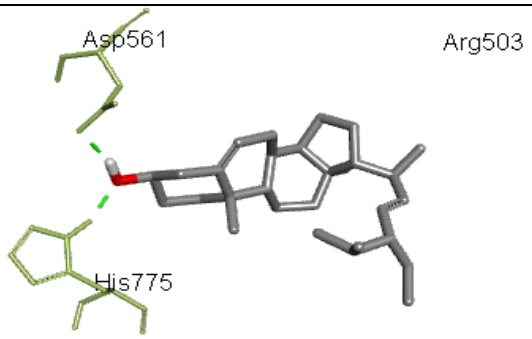	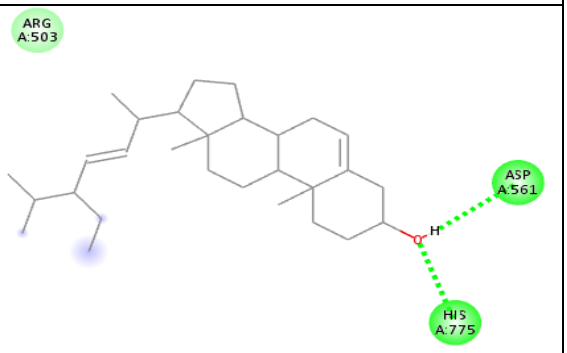
6	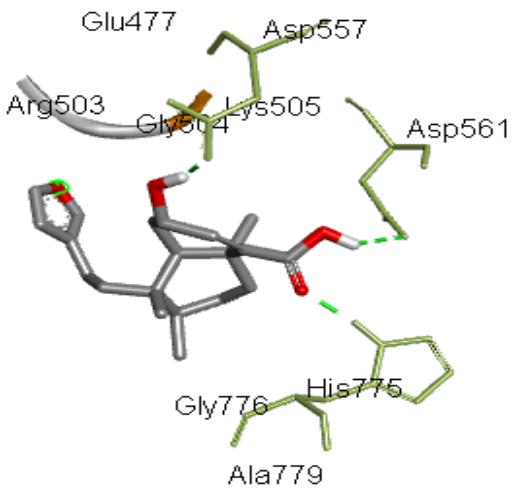	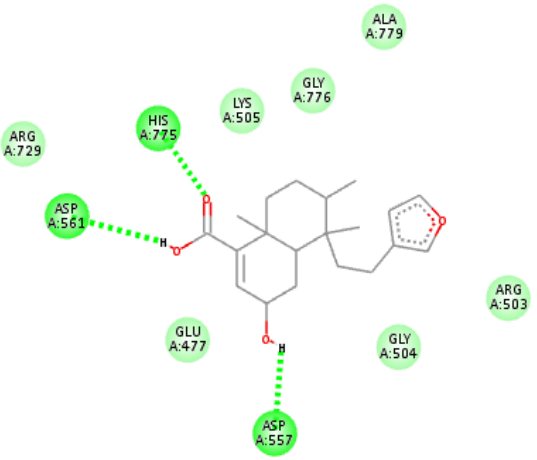
25	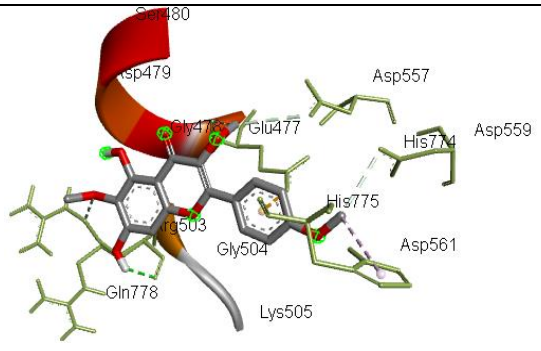	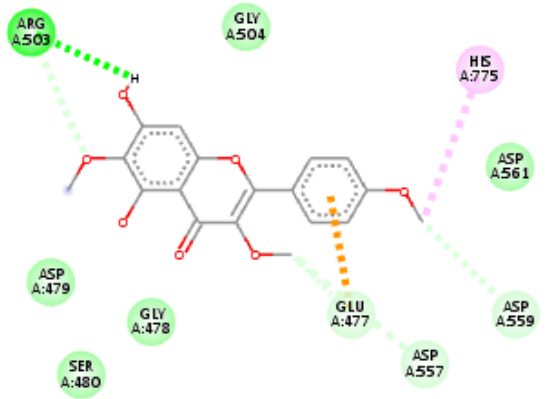

26	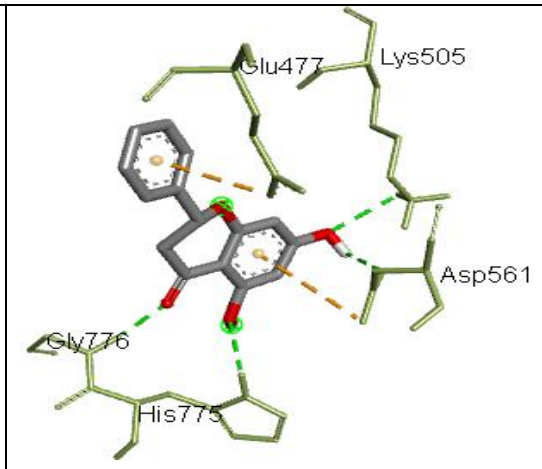 Glu477 Lys505 Asp561 Gly776 His775	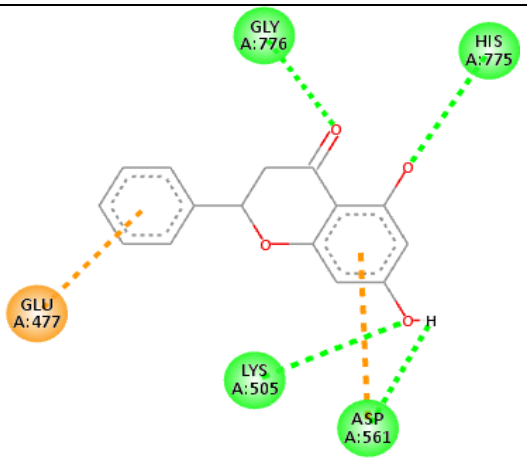 GLY A:776 HIS A:775 GLU A:477 LYS A:505 ASP A:561
28	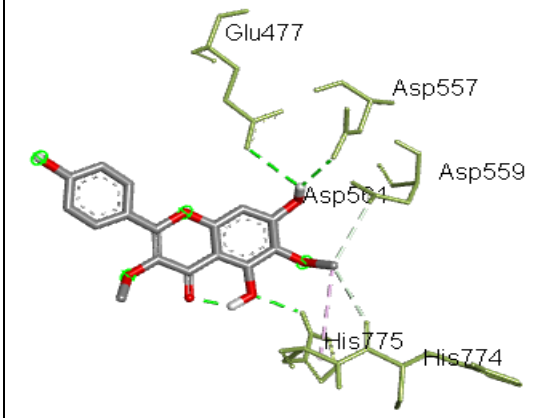 Glu477 Asp557 Asp559 Asp561 His775 His774	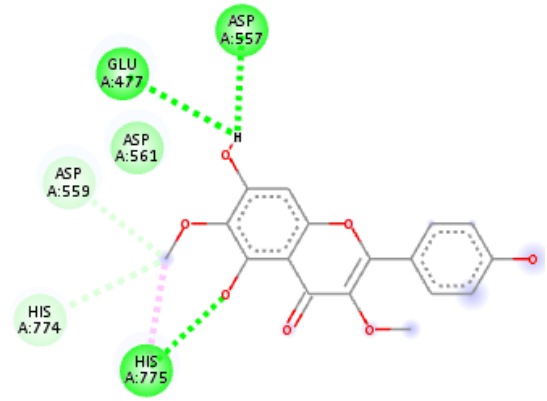 ASP A:557 GLU A:477 ASP A:561 ASP A:559 HIS A:774 HIS A:775
51	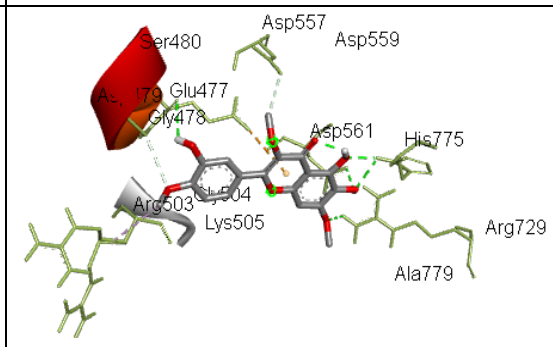 Ser480 Asp557 Asp559 Glu477 Gly478 Asp561 His775 Arg503 Lys505 Arg729 Ala779	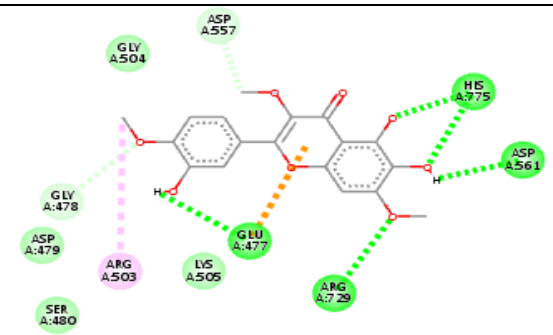 ASP A:557 GLY A:504 HIS A:775 ASP A:561 GLY A:478 ASP A:479 GLU A:477 ARG A:503 LYS A:505 ARG A:729 SER A:480
EVP	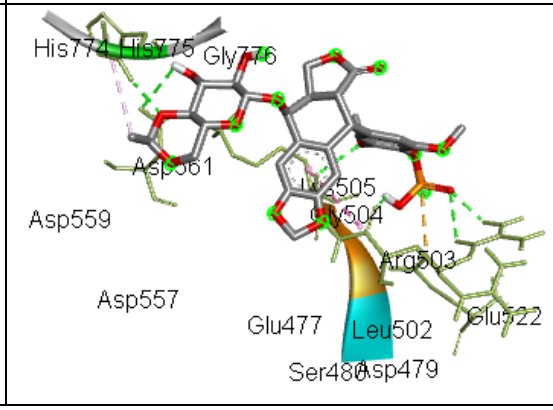 His774 His775 Gly776 Asp561 Asp559 Asp557 Glu477 Leu502 Glu522 Ser480 Asp479	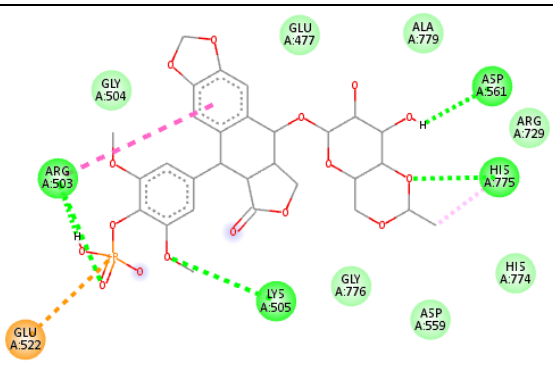 GLU A:477 ALA A:779 GLY A:504 ASP A:561 ARG A:729 ARG A:503 HIS A:775 HIS A:774 LYS A:505 GLY A:776 ASP A:559 GLU A:522

4.7.4 Molecular docking with Human Peroxiredoxins

Human peroxiredoxin 5 (PRDX5) is a member of the peroxireoxin family of antioxidant enzymes, which reduce hydrogen peroxide and alkyl hydroperoxides. The encoded protein interacts with peroxisome receptor 1 and plays an antioxidant protective role in different tissues under normal conditions and during inflammatory processes (Declercq *et al*., 2001). In this present study *human peroxiredoxins 5* (PDB ID: 1HD2) enzyme is used as a target. Ascorbic acid (AA) was utilized as a reference control for docking with PRDX5. Binding affinity and interactions with different amino acids are presented in the Table 22, and 3D and 2D binding interactions is depicted in Figure 19.

All the compounds except **47**, **48**, **49** and **50** showed higher binding affinity compared to the standard, AA. Among all, compound **45** showed the highest binding affinity (-5.9 kcal/mol) followed by **6** (-5.8 kcal/mol) and **26** (-5.5 kcal/mol). AA had H-bonding interactions with Cys-47, Arg-127, Thr-44, and Gly-46. All the isolated compounds had one or two of these amino acids except compound **45** and **49**. Since compound **50** did not show any H-bonding interactions, it showed least binding affinity (-3.5 kcal/mole). Most of the test compounds showed residual interactions with Pro-45, Ile-119, Phe-120 and Pro-40, whereas, the standard drug, AA did not show any residual interactions.

Table 22: Molecular docking binding affinity and interactions of isolated compounds and standard with the target human peroxiredoxins *5* (PDB ID: 1HD2)

Compounds	Affinity (kcal/mol)	H-bond	Residual Amino acid Interactions	
			Hydrophobic/Pi-Cation/Pi-Anion/ Pi-Alkyl interactions	Van-der Walls interactions
45	-5.9	Asp-145	Pro-45	Phe-120, Ile-119, Thr-147, Leu-116
47	-4.0	Thr-44, Pro-45*	Pro-45, Ile-119, Phe-120	Thr-147, Arg-127, Pro-40
48	-4.0	Arg-127, Gly-46*, Gly-148*	Pro-45, Ile-119, Phe-120, Pro-40, Leu-116	-
49	-3.9	Thr-147, Gly-148*	Pro-45, Ile-119, Phe-120, Pro-40, Leu-116, Leu-149	Gly-46, Thr-44
50	-3.5	-	Pro-45, Ile-119, Phe-120, Pro-40, Cys-47	Leu-116, Leu-149
6	-5.8	Cys-47, Thr-44, Thr-147	Thr-44	Phe-120, Pro-45, Gly-46, Ile-116, Ile-119
25	-5.3	Arg-127, Thr-147	Pro-45, Pro-40, Phe-	Ile-119, Gly-46, Leu-

			120, Leu-116	149, Thr-44
26	-5.5	Cys-47, Arg-127, Thr44*	Pro-45, Ile-119	Phe-120, Thr-147, Gly-46, Pro-40
28	-5.2	Cys-47, Thr-44, Asp-145	Pro-40, Thr-147, Arg-127, Cys-47	Phe-120, Pro-45, Leu-149, Gly-148
51	-5.0	Thr-44, Gly-46, Thr-147	Pro-45, Phe-120, Asp-145	Cys-47, Leu-149, Arg-127, Gly-148
AA	-4.2	Cys-47, Arg-127 Thr-44, Gly-46	-	-

*Carbon Hydrogen bond

Figure 19: Binding interactions (3D & 2D) of isolated compounds and standard compounds with human peroxiredoxins 5 (PDB ID: 1HD2)

No.	3D	2D
45	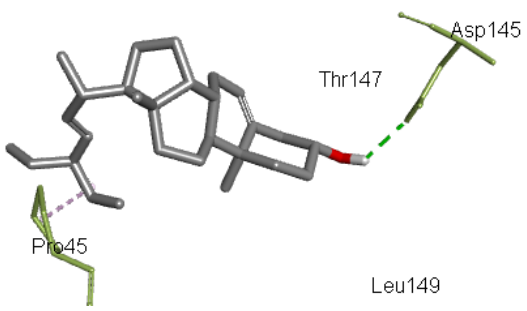	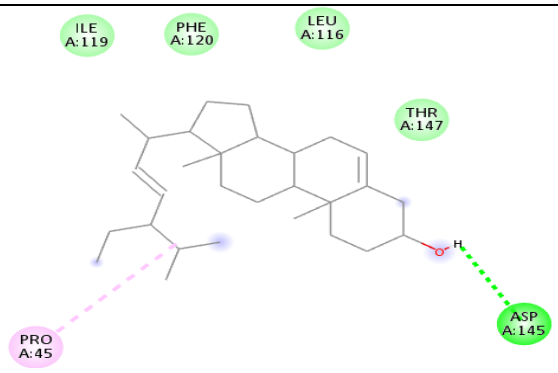
47	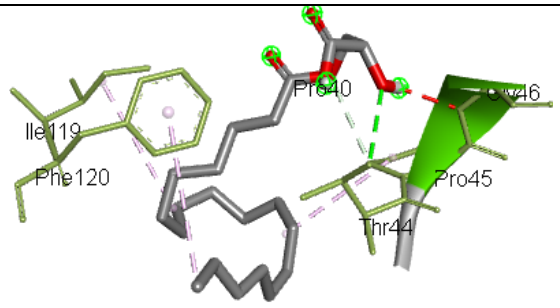	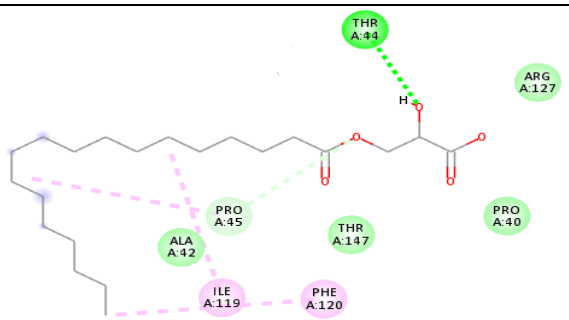
48	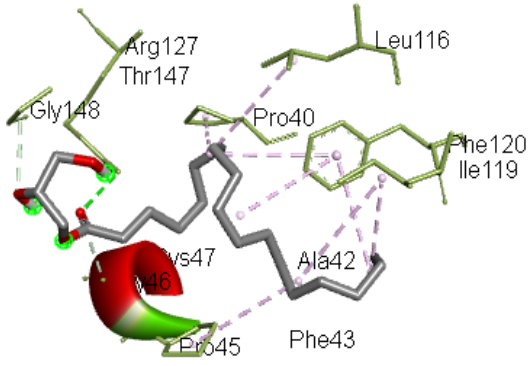	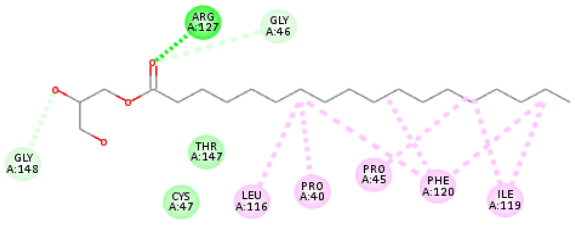

49	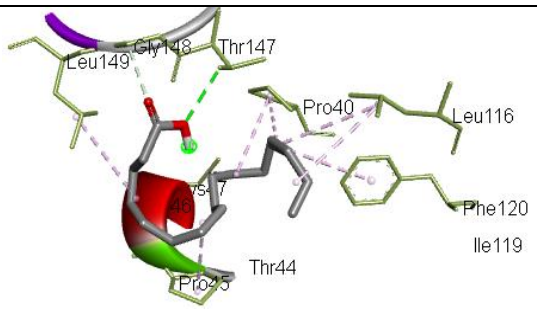 Leu149 Gly148 Thr147 Pro40 Leu116 Phe120 Ile119 Thr44 Pro45	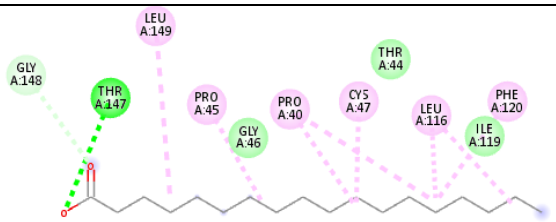 LEU A:149 GLY A:148 THR A:147 PRO A:45 PRO A:40 GLY A:46 THR A:44 CYS A:47 LEU A:116 PHE A:120 ILE A:119
50	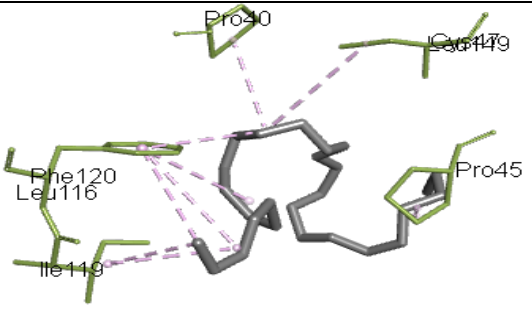 Pro40 Leu149 Phe120 Leu116 Pro45 Ile119	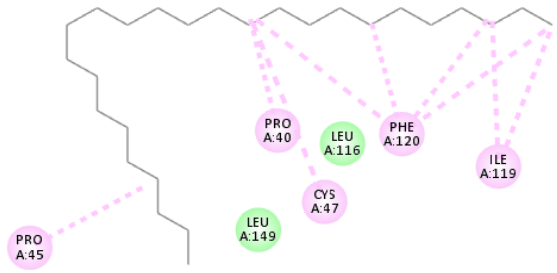 PRO A:40 LEU A:116 PHE A:120 ILE A:119 CYS A:47 LEU A:149 PRO A:45
6	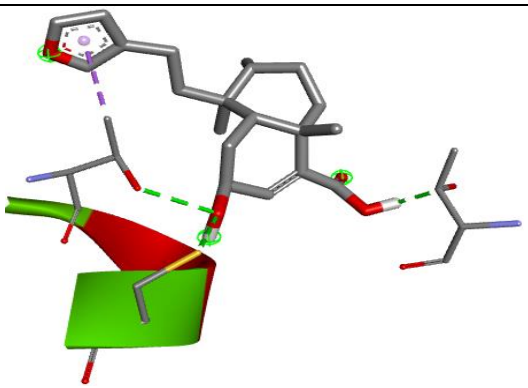	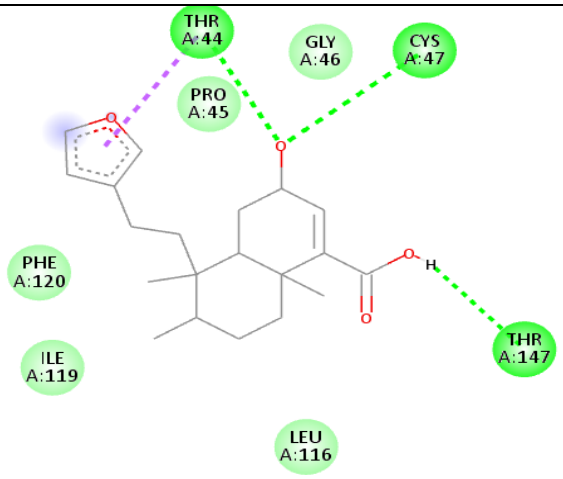 THR A:44 GLY A:46 CYS A:47 PRO A:45 PHE A:120 ILE A:119 THR A:147 LEU A:116
25	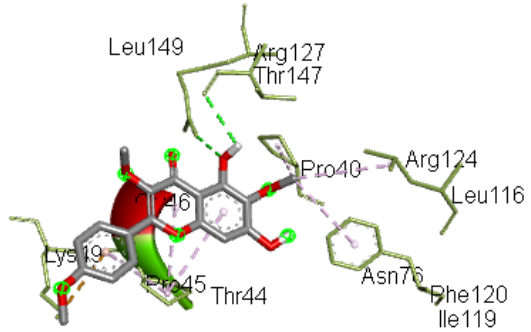 Leu149 Arg127 Thr147 Pro40 Arg124 Leu116 Lys19 Pro45 Thr44 Asn76 Phe120 Ile119	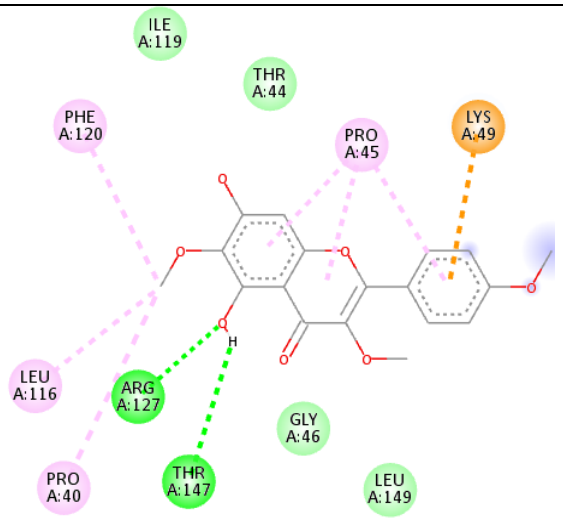 ILE A:119 THR A:44 PHE A:120 PRO A:45 LYS A:49 LEU A:116 ARG A:127 GLY A:46 PRO A:40 THR A:147 LEU A:149

26	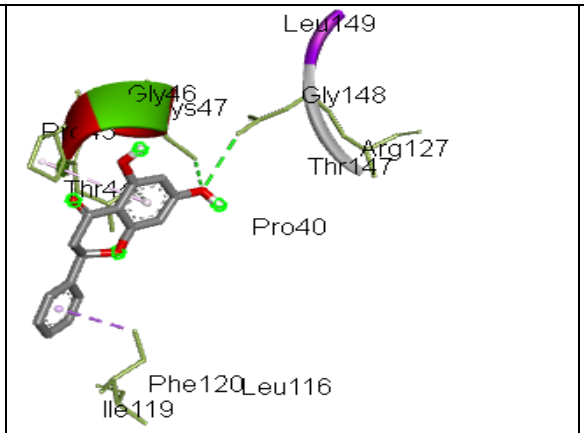 Leu149 Gly148 Arg127 Thr147 Pro40 Phe120 Leu116 Ile119	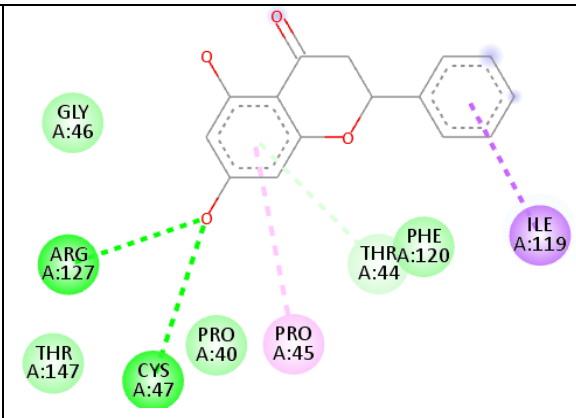 GLY A:46 ARG A:127 THR A:44 PHE A:120 ILE A:119 THR A:147 CYS A:47 PRO A:40 PRO A:45
28	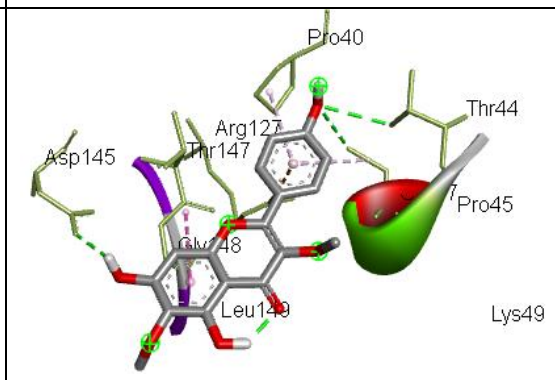 Pro40 Thr44 Arg127 Thr147 Asp145 Pro45 Leu149 Lys49	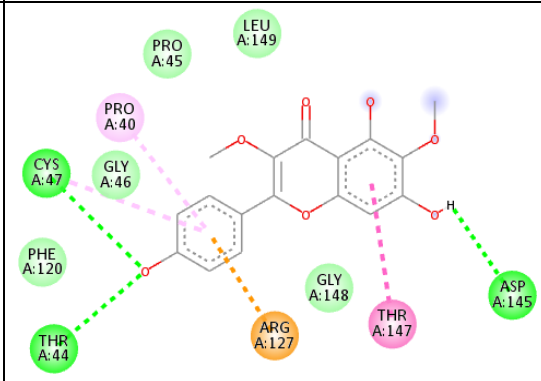 PRO A:45 LEU A:149 PRO A:40 CYS A:47 GLY A:46 PHE A:120 GLY A:148 ASP A:145 THR A:147 THR A:44 ARG A:127
51	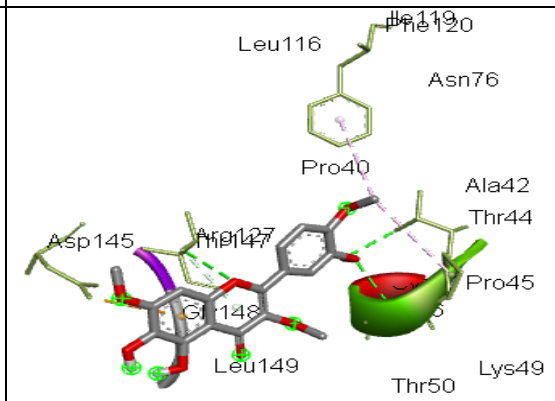 Phe120 Leu116 Asn76 Pro40 Ala42 Thr44 Asp145 Arg127 Thr147 Pro45 Leu149 Thr50 Lys49	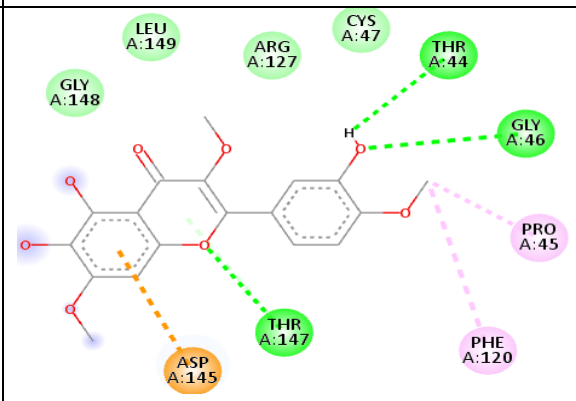 LEU A:149 ARG A:127 CYS A:47 THR A:44 GLY A:148 GLY A:46 PRO A:45 THR A:147 PHE A:120 ASP A:145
AA	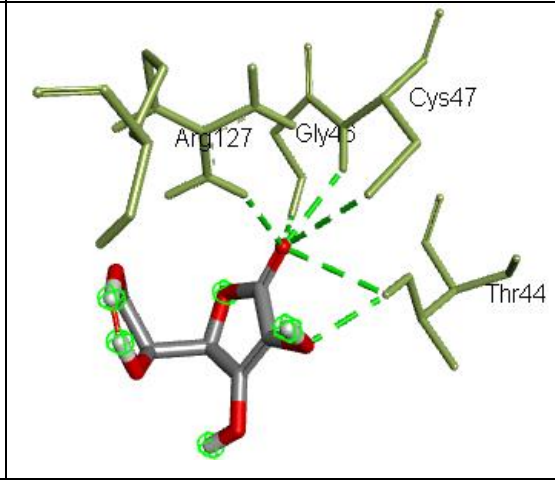 Cys47 Arg127 Thr44	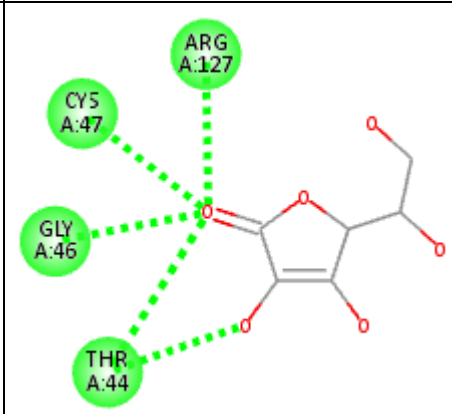 ARG A:127 CYS A:47 GLY A:46 THR A:44

5. CONCLUSION AND RECOMMENDATION

5.1 Conclusion

In conclusion, phytochemical screening analysis conducted on stem bark extracts of *D. angustifolia* revealed the presence of flavonoids, terpenoids, glycosides, steroids, coumarins, phenolics and saponins, suggesting the plant has a valuable reservoir of secondary metabolites. Column chromatographic fractionation of the dichloromethane extract afforded six compounds namely, stigmasterol (**45**), stigmasterol derivatives (**46),** 2-hydroxy-3-(stearoyloxy) propanoic acid (**47**), 2,3-dihydroxypropyl stearate (**48)**, stearic acid (**49**) and hexacosane (**50)**.

The antibacterial activity revealed that the aqueous methanol soluble portion was identified to be the most active. Among compounds isolated from the extracts of *D. angustifolia*, compound **45** possess antibacterial activity against *S. aureaus*, *S. pyogenes* and *P. aeruginosa*, whereas compound **47** & **48** exhibited promising activity against *E. coli* and the later against *S. aureus*. The study also demonstrated pronounced antibacterial activities of clerodane diterpene (**6**) against *P. aeruginosa*, santin (**25**) against *S. pyogenes*. Likewise, pinocembrin (**26**) and compound **28** possess antibacterial activity against *S. aureaus* and *S. pyogenes*, with pinocembrin (**26**) identified as the most active compound against *E. coli*. The overall antibacterial activity suggests the potential of the plant to treat bacterial infections.

The highest percent inhibition of DPPH radical was observed with aqueous MeOH soluble portion, and compound **45.** Compounds isolated from the leaves of *D. angustifolia* exhibited pronounced radical scavenging activities with 5, 7-dihydroxyflavanone (**26**) identified to be the most potent compound effective at lower doses.

The *in silico* drug-likeness prediction revealed that compounds **6, 25, 26, 28, 45 and 51** met Lipinski's rule of five and appeared to be good oral drug candidates. The ADMET prediction suggested that majority of the isolated compounds possess high GI absorption, only compound **6** and **26** showed BBB permeability, all compounds showed lesser LogKp value suggestive of better skin permeation than CPFX. The LD_{50} and toxicity profile prediction suggested none of the isolated compounds showed hepatotoxicity, carcinogenicity or mutagenicity, whereas **6, 25**, **28**, **45** and **51** exhibited immunotoxicity and only compound **26** found to be cytotoxic.

The molecular docking studies suggests that compound **25, 26, 28, 45** and **51** exhibited promising docking efficiency with the target DNA gyrase B and *S. aureus* PK, where compound **26 & 45** displayed the highest binding affinity with DNA gyrase B. Whereas, compound **25** and

28 showed the highest scoring pose with the target *S. aureus* PK. Pinocembrin (**26)** and santin (**25**) were also found to possess similar hydrogen bonding interactions like that of the known antibacterial drug ciprofloxacin. Additionally, compound **51** showed highest binding affinity with the target human TOP-II β and compounds **6**, **25, 26, 28, 45** and **51** showed higher binding affinity than the standard ascorbic acid with the target human peroxiredoxins 5.

Based on the *in vitro* studies and *in silico* molecular docking analysis it can be concluded that the plant are promising source of antimicrobial and antioxidant compounds which supports the traditional use of the leaves and stem bark of *D. angustifolia.* Further studies are also needed to investigate the pharmacokinetic profile of the promising compounds in animal model.

5.2 Recommendation

In this study only 1D NMR spectrum and literature data was used for structural elucidation of isolated compounds, so this paper recommend 2D NMR spectroscopic techniques (HMBC, HSQC, COSY, and NOESY) and mass spectrophotometry for further confirmation of the structure of compounds isolated from stem bark extracts.

This work recommends further antimicrobial activity test of compounds and extracts based on methods used to determine Minimum Inhibitory Concentration (MIC)/ Minimum bactericidal concentration (MBC) that may address the problem of antimicrobial resistance.

The results presented in these study supports the traditional use of the plant *D. angustifolia* for disease caused by pathogenic bacteria, but further *in vitro* and *in vivo* antimicrobial studies are recommended on other resistant clinical isolate pathogenic bacteria such as methicillin-resistant *S. aureus*, vancomycin-resistant Enterococcus and multidrug-resistant *Mycobacterium tuberculosis* and fungal test organisms.

Owing to the remarkable *in vitro* antioxidant activities of promising compounds (**25**, **26, 28, 45),** this work recommend further activity test to be held by researchers by targeting diseases caused by oxidative stress (cytotoxicity, anti-proliferative, antidiabetic, Anticholinesterase activity).

This study recommends conducting further extraction, isolation and bioassay on the stem-bark of *D. angustifolia* using methanol as extractive solvent.

Further phytochemical study is recommended on other parts of the plant, such as the seed and root.

This study recommends further research works to be done on the under-investigated class of compounds (e.g. alkaloids, anthraquinones and essential oils).

6. REFERENCES

Abate, L., Tadesse, M. G., Bachheti, A., & Bachheti, R. K. (2022). Traditional and Phytochemical Bases of Herbs, Shrubs, Climbers, and Trees from Ethiopia for Their Anticancer Response. *BioMed Research International*, *2022*, 1–27. https://doi.org/10.1155/2022/1589877

Akhalwaya, S., van Vuuren, S., & Patel, M. (2018). An in vitro investigation of indigenous South African medicinal plants used to treat oral infections. *Journal of Ethnopharmacology*, *210*, 359–371. https://doi.org/10.1016/j.jep.2017.09.002

Akunuri, R., Unnissa, T., Vadakattu, M., Bujji, S., Mahammad Ghouse, S., Madhavi Yaddanapudi, V., Chopra, S., & Nanduri, S. (2022). Bacterial Pyruvate Kinase: A New Potential Target to Combat Drug-Resistant Staphylococcus aureus Infections. *ChemistrySelect*, *7*(29). https://doi.org/10.1002/slct.202201403

Al-Aamri, K. K., & Hossain, M. A. (2016). New prenylated flavonoids from the leaves of Dodonea viscosa native to the Sultanate of Oman. *Pacific Science Review A: Natural Science and Engineering*, *18*(1), 53–61. https://doi.org/10.1016/j.psra.2016.08.001

Al-Snafi, P. D. A. E. (2017). A review on Dodonaea viscosa: A potential medicinal plant. *IOSR Journal of Pharmacy (IOSRPHR)*, *07*(02), 10–21. https://doi.org/10.9790/3013-0702011021

Al Habsi, A. A. S., & Hossain, M. A. (2018). Isolation, structure characterization and prediction of antioxidant activity of two new compounds from the leaves of Dodonaea viscosa native to the Sultanate of Oman . *Egyptian Journal of Basic and Applied Sciences*, *5*(2), 157–164. https://doi.org/10.1016/j.ejbas.2018.04.004

Anode, S. O., Abraha, T., & Araya, S. (2018). Phytochemical analysis of Dodonaea angustifolia plant extracts. *International Journal of Herbal Medicine*, *6*(5), 37–42.

Ates, H., & Yalcin, E. (2022). Therapeutic Source: Plants. *Black Sea Journal of Agriculture*, *5*(3), 336–343. https://doi.org/10.47115/bsagriculture.1078368

Ayele, T. T. (2018). A Review on Traditionally Used Medicinal Plants/Herbs for Cancer Therapy in Ethiopia: Current Status, Challenge and Future Perspectives. *Organic Chemistry: Current Research*, *07*(02), 192. https://doi.org/10.4172/2161-0401.1000192

Ayele, T. T., Gurmessa, G. T., Abdissa, Z., Kenasa, G., & Abdissa, N. (2022). Oleanane and Stigmasterol-Type Triterpenoid Derivatives from the Stem Bark of Albizia gummifera and Their Antibacterial Activities. *Journal of Chemistry*, *2022*, 1–7.

https://doi.org/10.1155/2022/9003143

B.Anilreddy. (2009). Preparation, Characterization and Biological Evaluation of Some Overview of Dodonaea Viscosa Linn. *Journal of Pharmaceutical Science and Technology*, *1*(1), 1–9.

Banchiamlak, N. T., & Young-dongKim. (2019). Ethnobotanical study of medicinal plants in the Hawassa Zuria District , Sidama zone , Southern Ethiopia. *Journal of Ethnobiology and Ethnomedicine*, *7*, 1–21.

Banerjee, P., Eckert, A. O., Schrey, A. K., & Preissner, R. (2018). ProTox-II: A webserver for the prediction of toxicity of chemicals. *Nucleic Acids Research*, *46*(1), 257–263. https://doi.org/10.1093/nar/gky318

Bargah, & Rohit. (2015). Preliminary test of phytochemical screening of crude ethanolic and aqueous extract of Moringa pterygosperma Gaertn. *Journal of Pharmacognosy and Phytochemistry*, *4*(1), 7–9.

Bauer, A. W., Kirby, W. M. M., Sherris, J. C., & Turck, M. (1966). Antibiotic Susceptibility Testing by a Standardized Single Disk Method. *American Journal of Clinical Pathology*, *45*(4_ts), 493–496. https://doi.org/10.1093/ajcp/45.4_ts.493

Berhan, A., Asfaw, Z., & Kelbessa, E. (2006). Ethnobotany of plants used as insecticides, repellents and antimalarial agents in Jabitehnan district, West Gojjam. *SINET: Ethiopian Journal of Science*, *29*(1), 87–92. https://doi.org/10.4314/sinet.v29i1.18263

Beshah, F., Hunde, Y., Getachew, M., Bachheti, R. K., Husen, A., & Bachheti, A. (2020). Ethnopharmacological, phytochemistry and other potential applications of Dodonaea genus: A comprehensive review. *Current Research in Biotechnology*, *2*, 103–119. https://doi.org/10.1016/j.crbiot.2020.09.002

Bultum, L. E., Woyessa, A. M., & Lee, D. (2019). ETM-DB: Integrated Ethiopian traditional herbal medicine and phytochemicals database. *BMC Complementary and Alternative Medicine*, *19*(1), 1–11. https://doi.org/10.1186/s12906-019-2634-1

Cao, G., Sofic, E., & Prior, R. L. (1997). Antioxidant and prooxidant behavior of flavonoids: Structure-activity relationships. *Free Radical Biology and Medicine*, *22*(5), 749–760. https://doi.org/10.1016/S0891-5849(96)00351-6

Chen, C. P., Chen, C. C., Huang, C. W., & Chang, Y. C. (2018). Evaluating molecular properties involved in transport of small molecules in stratum corneum: A quantitative structure-activity relationship for skin permeability. *Molecules*, *23*(4), 1–17.

https://doi.org/10.3390/molecules23040911

CLSI, C. and L. S. I. (2012). *Performance standards for antimicrobial disk susceptibility tests: Approved standard - Eleventh edition* (Vol. 32, Issue 1). https://doi.org/M02-A11

Cunningham, P. L., Joubert, D. F., & Adank, W. (2004). Dodonaea angustifolia – an alien invasive to the Auas Mountains in Namibia ? *Dinteria*, *29*, 11–18.

Daina, A., Michielin, O., & Zoete, V. (2017). SwissADME: A free web tool to evaluate pharmacokinetics, drug-likeness and medicinal chemistry friendliness of small molecules. *Scientific Reports*, *7*(October 2016), 1–13. https://doi.org/10.1038/srep42717

Daina, A., & Zoete, V. (2016). A BOILED-Egg To Predict Gastrointestinal Absorption and Brain Penetration of Small Molecules. *ChemMedChem*, *11*(11), 1117–1121. https://doi.org/10.1002/cmdc.201600182

Deans, B. J., Olivier, W. J., Girbino, D., Bissember, A. C., & Smith, J. A. (2018). Extraction of carboxylic acid-containing diterpenoids from Dodonaea viscosa via pressurised hot water extraction. *Fitoterapia*, *126*(October 2017), 65–68. https://doi.org/10.1016/j.fitote.2017.10.008

Declercq, J. P., Evrard, C., Clippe, A., Stricht, D. Vander, Bernard, A., & Knoops, B. (2001). Crystal structure of human peroxiredoxin 5, a novel type of mammalian peroxiredoxin at 1.5 Å resolution. *Journal of Molecular Biology*, *311*(4), 751–759. https://doi.org/10.1006/jmbi.2001.4853

Dekebo, A. (2019). Introductory Chapter: Plant Extracts. In *Plant Extracts* (pp. 1–10). IntechOpen. https://doi.org/10.5772/intechopen.85493

Delgado, J. L., Hsieh, C., Chan, N., & Hiasa, H. (2018). Topoisomerases as anticancer targets. *Biochemical Journal*, *475*(2), 373–398. https://doi.org/10.1042/BCJ20160583

Desai, N. C., Patel, B. Y., & Dave, B. P. (2017). Synthesis and antimicrobial activity of novel quinoline derivatives bearing pyrazoline and pyridine analogues. *Medicinal Chemistry Research*, *26*(1), 109–119. https://doi.org/10.1007/s00044-016-1732-6

Di Pietro, M. E., Mannu, A., & Mele, A. (2020). NMR Determination of Free Fatty Acids in Vegetable Oils. *Processes*, *8*(4), 410. https://doi.org/10.3390/pr8040410

Digafie, Z., Melaku, Y., Belay, Z., & Eswaramoorthy, R. (2021). Synthesis, Molecular Docking Analysis, and Evaluation of Antibacterial and Antioxidant Properties of Stilbenes and Pinacol of Quinolines. *Advances in Pharmacological and Pharmaceutical Sciences*, *2021*.

https://doi.org/10.1155/2021/6635270

Drwal, M. N., Banerjee, P., Dunkel, M., Wettig, M. R., & Preissner, R. (2014). ProTox: A web server for the in silico prediction of rodent oral toxicity. *Nucleic Acids Research*, *42*(W1), 3–8. https://doi.org/10.1093/nar/gku401

Edilu, A., Adane, L., & Woyessa, D. (2015). In vitro antibacterial activities of compounds isolated from roots of Caylusea abyssinica. *Annals of Clinical Microbiology and Antimicrobials*, *14*(1), 1–8. https://doi.org/10.1186/s12941-015-0072-6

El-Desouky, S. K., Hawas, U. W., Khemira, H., & Kim, Y. K. (2018). Salvastearolide, a new acyl-glyceride, and other constituents from the seeds of Salvadora persica. *Revista Brasileira de Farmacognosia*, *28*(5), 564–567. https://doi.org/10.1016/j.bjp.2018.05.013

Ellington, M. J., Ekelund, O., & Aarestrup, F. M. et al. (2017). The role of whole genome sequencing in antimicrobial susceptibility testing of bacteria: report from the EUCAST Subcommittee. *Clinical Microbiology and Infection*, *23*(1), 2–22. https://doi.org/10.1016/j.cmi.2016.11.012

Elmeliegy, M., Vourvahis, M., Guo, C., & Wang, D. D. (2020). Effect of P-glycoprotein (P-gp) Inducers on Exposure of P-gp Substrates: Review of Clinical Drug–Drug Interaction Studies. *Clinical Pharmacokinetics*, *59*(6), 699–714. https://doi.org/10.1007/s40262-020-00867-1

Erwin, Pusparohmana, W. R., Safitry, R. D., Marliana, E., Usman, & Kusuma, I. W. (2020). Isolation and characterization of stigmasterol and β-sitosterol from wood bark extract of baccaurea macrocarpa miq. Mull. arg. *Rasayan Journal of Chemistry*, *13*(4), 2552–2558. https://doi.org/10.31788/RJC.2020.1345652

Esteves, F., Rueff, J., & Kranendonk, M. (2021). The Central Role of Cytochrome P450 in Xenobiotic Metabolism—A Brief Review on a Fascinating Enzyme Family. *Journal of Xenobiotics*, *11*(3), 94–114. https://doi.org/10.3390/jox11030007

Farouk, F., Elmaaty, A. A., Elkamhawy, A., Tawfik, H. O., Alnajjar, R., Abourehab, M. A. S., Saleh, M. A., Eldehna, W. M., & Al-Karmalawy, A. A. (2023). Investigating the potential anticancer activities of antibiotics as topoisomerase II inhibitors and DNA intercalators: in vitro , molecular docking, molecular dynamics, and SAR studies. *Journal of Enzyme Inhibition and Medicinal Chemistry*, *38*(1). https://doi.org/10.1080/14756366.2023.2171029

Getie, M., Gebre-Mariam, T., Rietz, R., Höhne, C., Huschka, C., Schmidtke, M., Abate, A., &

Neubert, R. H. H. (2003). Evaluation of the anti-microbial and anti-inflammatory activities of the medicinal plants Dodonaea viscosa, Rumex nervosus and Rumex abyssinicus. *Fitoterapia*, *74*(1–2), 139–143. https://doi.org/10.1016/S0367-326X(02)00315-5

Hailemariam, M., Alemayehu, T., Tadesse, B., Nigussie, N., Agegnehu, A., Habtemariam, T., Ali, M., Mitiku, E., & Azerefegne, E. (2021). Major bacterial isolate and antibiotic resistance from routine clinical samples in Southern Ethiopia. *Scientific Reports*, *11*(1), 19710. https://doi.org/10.1038/s41598-021-99272-2

Hajhashemi, V., Ghannadi, A., & Sharif, B. (2003). Anti-inflammatory and analgesic properties of the leaf extracts and essential oil of Lavandula angustifolia Mill. *Journal of Ethnopharmacology*, *89*(1), 67–71. https://doi.org/10.1016/S0378-8741(03)00234-4

Harrington, M. G., & Gadek, P. A. (2009). A species well travelled - The Dodonaea viscosa (Sapindaceae) complex based on phylogenetic analyses of nuclear ribosomal ITS and ETSf sequences. *Journal of Biogeography*, *36*(12), 2313–2323. https://doi.org/10.1111/j.1365-2699.2009.02176.x

Hedgerg, I., & Edwards, S. (1989). Flora of Ethiopia. Vol. 3, Pittosporaceae to Araliaceae. *National Herbarium, Addis Ababa University*, *3*, 490–503.

Huang, Z., Jiang, M. Y., Zhou, Z. Y., & Xua, D. (2010). Two new clerodane diterpenes from dodonaea viscosa. *Zeitschrift Fur Naturforschung - Section B Journal of Chemical Sciences*, *65*(1), 83–86. https://doi.org/10.1515/znb-2010-0114

Hudzicki, J. (2012). Kirby-Bauer Disk Diffusion Susceptibility Test Protocol Author Information. *American Society For Microbiology*, *December 2009*, 1–13. https://www.asm.org/Protocols/Kirby-Bauer-Disk-Diffusion-Susceptibility-Test-Pro

Janupally, R., Medepi, B., Brindha Devi, P., Suryadevara, P., Jeankumar, V. U., Kulkarni, P., Yogeeswari, P., & Sriram, D. (2015). Design and Biological Evaluation of Furan/Pyrrole/Thiophene-2-carboxamide Derivatives as Efficient DNA GyraseB Inhibitors of Staphylococcus aureus. *Chemical Biology and Drug Design*, *86*(4), 918–925. https://doi.org/10.1111/cbdd.12529

Kadry, H., Noorani, B., & Cucullo, L. (2020). A blood–brain barrier overview on structure, function, impairment, and biomarkers of integrity. *Fluids and Barriers of the CNS*, *17*(1), 1–24. https://doi.org/10.1186/s12987-020-00230-3

Khurram, M., Hameed, A., Amin, M. U., Gul, A., Ullah, N., Hassan, M., Qayum, A., Chishti, K.

A., & Manzoor, W. (2011). Phytochemical screening and in vitro evaluation of anticandidal activity of Dodonaea viscosa (L.) Jaeq. (sapindaceae). *African Journal of Pharmacy and Pharmacology*, *5*(11), 1422–1426. https://doi.org/10.5897/AJPP11.404

Kundu, R., & De, S. (2021). Characterization and analysis of the triglyceride transesterification process. *Biomass Conversion and Biorefinery*, *0123456789*, 1–16. https://doi.org/10.1007/s13399-021-01785-3

Lee, S. K., Lee, I. H., Kim, H. J., Chang, G. S., & Chung, J. E., & No, K. T. (2003). The PreADME Approach: Web-based program for rapid prediction of physico-chemical, drug absorption and drug-like properties. *EuroQSAR 2002 Designing Drugs and Crop Protectants: Processes, Problems and Solutions*, 418–420.

Li, J. W., & Vederas, J. C. (2009). Drug Discovery and Natural Products : *Science*, *325*(5935), 161–165.

Lipinski, C. A., Lombardo, F., Dominy, B. W., & Feeney, P. J. (1997). Experimental and computational approaches to estimate solubility and permeability in drug discovery and development settings. *Advanced Drug Delivery Reviews*, *23*(1–3), 3–25. https://doi.org/10.1016/S0169-409X(96)00423-1

Makhaeva, G. F., Lushchekina, S. V., Boltneva, N. P., Serebryakova, O. G., Rudakova, E. V., Ustyugov, A. A., Bachurin, S. O., Shchepochkin, A. V., Chupakhin, O. N., Charushin, V. N., & Richardson, R. J. (2017). 9-Substituted acridine derivatives as acetylcholinesterase and butyrylcholinesterase inhibitors possessing antioxidant activity for Alzheimer's disease treatment. *Bioorganic and Medicinal Chemistry*, *25*(21), 5981–5994. https://doi.org/10.1016/j.bmc.2017.09.028

Melaku, Y. (2015). *Bioassay Directed Chemical Study of Antimalarial Substances from Clerodendrum myricoides and Dodonaea angustifolia and Comparative Chemical Studies ofMoringa stenopetala andMoringa oleifera*. 33–36.

Melaku, Y., Worku, T., Tadesse, Y., Mekonnen, Y., Schmidt, J., Arnold, N., & Dagne, E. (2017). Antiplasmodial Compounds from Leaves of Dodonaea angustifolia. *Current Bioactive Compounds*, *13*(3), 268–273. https://doi.org/10.2174/1573407213666170403121222

Mostafa, A. E., El-Hela, A. A., Mohammad, A. E. I., Jacob, M., Cutler, S. J., & Ross, S. A. (2014). New secondary metabolites from Dodonaea viscosa. *Phytochemistry Letters*, *8*(1),

10–15. https://doi.org/10.1016/j.phytol.2013.12.008

Muhammad, A., Anis, I., Ali, Z., Awadelkarim, S., Khan, A., Khalid, A., Shah, M. R., Galal, M., Khan, I. A., & Iqbal Choudhary, M. (2012). Methylenebissantin: A rare methylene-bridged bisflavonoid from Dodonaea viscosa which inhibits Plasmodium falciparum enoyl-ACP reductase. *Bioorganic and Medicinal Chemistry Letters*, *22*(1), 610–612. https://doi.org/10.1016/j.bmcl.2011.10.072

Muhammad, A., Tel-Çayan, G., Öztürk, M., Duru, M. E., Nadeem, S., Anis, I., Ng, S. W., & Shah, M. R. (2016). Phytochemicals from Dodonaea viscosa and their antioxidant and anticholinesterase activities with structure–activity relationships. *Pharmaceutical Biology*, *54*(9), 1649–1655. https://doi.org/10.3109/13880209.2015.1113992

Muhammad, A., Tel-Cayan, G., Öztürk, M., Nadeem, S., Duru, M. E., Anis, I., Ng, S. W., & Shah, M. R. (2015). Biologically active flavonoids from Dodonaea viscosa and their structure-activity relationships. *Industrial Crops and Products*, *78*, 66–72. https://doi.org/10.1016/j.indcrop.2015.10.011

Naidoo, R., Patel, M., Gulube, Z., & Fenyvesi, I. (2012). Inhibitory activity of Dodonaea viscosa var. angustifolia extract against Streptococcus mutans and its biofilm. *Journal of Ethnopharmacology*, *144*(1), 171–174. https://doi.org/10.1016/j.jep.2012.08.045

Narramore, S., Stevenson, C. E. M., Maxwell, A., Lawson, D. M., & Fishwick, C. W. G. (2019). New insights into the binding mode of pyridine-3-carboxamide inhibitors of E. coli DNA gyrase. *Bioorganic and Medicinal Chemistry*, *27*(16), 3546–3550. https://doi.org/10.1016/j.bmc.2019.06.015

Ngabaza, T., Johnson, M. M., Moeno, S., & Patel, M. (2017). Identification of 5,6,8-Trihydroxy-7-methoxy-2-(4-methoxyphenyl)-4H-chromen-4-one with antimicrobial activity from Dodonaea viscosa var. angustifolia. *South African Journal of Botany*, *112*(2017), 48–53. https://doi.org/10.1016/j.sajb.2017.05.024

Ngabaza, Thamsanqa. (2016). *Phytochemical analysis of Dodonaea viscosa var . angustifolia and their beneficial effects against Streptococcus mutans Thamsanqa Ngabaza Degree of Master of Science in Medicine by research only*.

Nguyen, N. T., Nguyen, T. H., Pham, T. N. H., Huy, N. T., Bay, M. Van, Pham, M. Q., Nam, P. C., Vu, V. V., & Ngo, S. T. (2020). Autodock Vina Adopts More Accurate Binding Poses but Autodock4 Forms Better Binding Affinity. *Journal of Chemical Information and*

Modeling, *60*(1), 204–211. https://doi.org/10.1021/acs.jcim.9b00778

Nn, A. (2015). A Review on the Extraction Methods Use in Medicinal Plants, Principle, Strength and Limitation. *Medicinal & Aromatic Plants*, *04*(03), 3–8. https://doi.org/10.4172/2167-0412.1000196

Nwodo, O., & Nkwocha, P. (2015). Qualitative and Quantitative Phytochemical Screening of the Aqueous Leaf Extract of Senna mimosoides : Its Effect in in vivo Leukocyte mobilization induced by inflammatory stimulus. *International Journal of Current Microbiology and Appliied Science*, *4*(5), 1176–1188.

Olivier, W. J., Kilah, N. L., Horne, J., Bissember, A. C., & Smith, J. A. (2016). ent-Labdane Diterpenoids from Dodonaea viscosa. *Journal of Natural Products*, *79*(12), 3117–3126. https://doi.org/10.1021/acs.jnatprod.6b00858

Omosa, L., Akala, H., Kenanda, E. O., & Ndunda, B. (2016). Variability of Surface Exudates of Dodonaea angustifolia L . f , Antioxidant and Antiplasmodial activities of the compounds. *Journal of Natural Sciences Research ISSN*, *6*(10), 78–85.

Omosa, L. K., Amugune, B., Ndunda, B., Milugo, T. K., Heydenreich, M., Yenesew, A., & Midiwo, J. O. (2014). Antimicrobial flavonoids and diterpenoids from Dodonaea angustifolia. *South African Journal of Botany*, *91*, 58–62. https://doi.org/10.1016/j.sajb.2013.11.012

Omosa, L. K., Midiwo, J. O., Derese, S., Yenesew, A., Peter, M. G., & Heydenreich, M. (2010). Neo-Clerodane diterpenoids from the leaf exudate of Dodonaea angustifolia. *Phytochemistry Letters*, *3*(4), 217–220. https://doi.org/10.1016/j.phytol.2010.08.001

Ortega, A., García, P. E., Cárdenas, J., Mancera, C., Marquina, S., Del Carmen Garduño, M. L., & Maldonado, E. (2001). Methyl dodonates, a new type of diterpenes with a modified clerodane skeleton from Dodonaea viscosa. *Tetrahedron*, *57*(15), 2981–2989. https://doi.org/10.1016/S0040-4020(01)00161-2

Orwa, C., Mutua, A., Kindt, R., Jamnadass, R., Anthony, S. (2009). *Dodonaea angustifolia L. f. Agroforestree Database: A Tree Reference and Selection Guide Version 4.0*. 1–5.

Pawar, S. S., & Rohane, S. H. (2021). Review on Discovery Studio: An important Tool for Molecular Docking. *Asian Journal Of Research in Chemistry*, *14*(1), 1–3. https://doi.org/10.5958/0974-4150.2021.00014.6

Praiwala, B., Priyanka, S., Raghu, N., Gopenath, N., Gnanasekaran, A., Karthikeyan, M.,

Indumathi, R., Ebrahim, N. K., Pugazhandhi, B., Pradeep, P., Ranjith, M. S., Balasubramanian, S., & Basalingappa, K. M. (2019). In vitro anti-bacterial activity of Tinospora cordifolia leaf extract and its phytochemical screening. *Journal of Biomedical Sciences*, *5*(2), 10–17. https://doi.org/10.3126/jbs.v5i2.23633

Raghu, P. S. (2019). Synthesis, Characterization and Antioxidant Activity of Novel 3-(2,5-dioxo-imidazolidin-1-yl)-1,1-diethylurea Derivatives. *Chemical Science Transactions*, *8*(4), 1739–1749. https://doi.org/10.7598/cst2019.20190008

Rani, M. S., K. M. & P. R. S. (2009). Dodonaea Viscosa Linn.-an Overview. *Jprhc*, *1*(1), 97–112.

Riaz, T., Abbasi, M. A., Aziz-Ur-Rehman, Shahzadi, T., Ajaib, M., & Khan, K. M. (2012). Phytochemical screening, free radical scavenging, antioxidant activity and phenolic content of Dodonaea viscosa Jacq. *Journal of the Serbian Chemical Society*, *77*(4), 423–435. https://doi.org/10.2298/JSC110621183R

Rukaiyat, M., Garba, S., & Labaran, S. (2015). Antimicrobial activities of hexacosane isolated from Sanseveria liberica (Gerome and Labroy) plant. *Advancement in Medicinal Plant Research*, *3*(3), 120–125.

S.Veliyil., G. (2019). Phenology, floral sexuality and breeding system in rambutan (Nephelium lappaceum). *Acta Horticulturae*, *1241*, 239–245. https://doi.org/10.17660/ActaHortic.2019.1241.33

Saeidnejad, A. H. (2021). Seed Dormancy and Germination in Medicinal Plants. *Handbook of Plant and Crop Physiology*, 57–67. https://doi.org/10.1201/9781003093640-7

Sahu, R. K., Kar, M., & Routray, R. (2013). Journal of Medicinal Plants Studies DPPH Free Radical Scavenging Activity of Some Leafy Vegetables used by Tribals of Odisha , India. *Journal of Medicinal Plants Studies*, *1*, 21–27.

Santhi, K., & Sengottuvel, R. (2016). Qualitative and Quantitative Phytochemical analysis of Moringa concanensis Nimmo. *International Journal of Current Microbiology and Applied Sciences*, *5*(1), 633–640. https://doi.org/10.20546/ijcmas.2016.501.064

Saranya, K., & Divyabharathi, U. (2019). Phytochemical and histochemical screening of Dodonaea viscosa leaves. *Pramana Res. J.*, *9*(9), 53–59.

Shwe, H. H., Thein, W. W., Win, S. S., Pe, N. N., & Win, T. (2019). Structural characterization of stigmasterol and β-sitosterol from the roots of Premna herbacea Roxb. *International*

European Extended Enablement in Science, Engineering & Management, *7*(8), 195–201.

Sies, H., Berndt, C., & Jones, D. P. (2017). Oxidative Stress. *Annual Review of Biochemistry*, *86*(1), 715–748. https://doi.org/10.1146/annurev-biochem-061516-045037

Simpson, B. S., Claudie, D. J., Smith, N. M., Gerber, J. P., McKinnon, R. A., & Semple, S. J. (2011). Flavonoids from the leaves and stems of Dodonaea polyandra: A Northern Kaanju medicinal plant. *Phytochemistry*, *72*(14–15), 1883–1888. https://doi.org/10.1016/j.phytochem.2011.05.006

Simpson, B. S., Claudie, D. J., Smith, N. M., McKinnon, R. A., & Semple, S. J. (2012). Rare, seven-membered cyclic ether labdane diterpenoid from Dodonaea polyandra. *Phytochemistry*, *84*, 141–146. https://doi.org/10.1016/j.phytochem.2012.07.016

Singh, S., Charani, E., Devi, S., Sharma, A., Edathadathil, F., Kumar, A., Warrier, A., Shareek, P. S., Jaykrishnan, A. V., & Ellangovan, K. (2021). A road-map for addressing antimicrobial resistance in low- and middle-income countries: lessons learnt from the public private participation and co-designed antimicrobial stewardship programme in the State of Kerala, India. *Antimicrobial Resistance and Infection Control*, *10*(1), 1–9. https://doi.org/10.1186/s13756-020-00873-9

Stéphane, F. F. Y., Jules, B. K. J., Batiha, G. E.-S., &, & Bruno, I. A. and L. N. (2012). Extraction of Bioactive Compounds from Medicinal Plants and Herbs Fongang. In *In Intech* (p. 13).

Tambosi, G., Coelho, P. F., Soares, L., Lenschow, I. C. S., Zétola, M., Stulzer, H. K., & Pezzini, B. R. (2018). Challenges to improve the biopharmaceutical properties of poorly water-soluble drugs and the application of the solid dispersion technology. *Revista Materia*, *23*(4). https://doi.org/10.1590/s1517-707620180004.0558

Tauchen, J., Doskocil, I., Caffi, C., Lulekal, E., Marsik, P., Havlik, J., Damme, P. Van, & Kokoska, L. (2015). In vitro antioxidant and anti-proliferative activity of Ethiopian medicinal plant extracts. *Industrial Crops and Products*, *74*, 671–679. https://doi.org/10.1016/j.indcrop.2015.05.068

Teffo, L. S., Aderogba, M. A., & Eloff, J. N. (2010). Antibacterial and antioxidant activities of four kaempferol methyl ethers isolated from Dodonaea viscosa Jacq. var. angustifolia leaf extracts. *South African Journal of Botany*, *76*(1), 25–29. https://doi.org/10.1016/j.sajb.2009.06.010

Tegen, D., Dessie, K., & Damtie, D. (2021). Candidate Anti-COVID-19 Medicinal Plants from Ethiopia: A Review of Plants Traditionally Used to Treat Viral Diseases. *Evidence-Based Complementary and Alternative Medicine, 2021*. https://doi.org/10.1155/2021/6622410

Teklay, A., Abera, B., & Giday, M. (2013). An ethnobotanical study of medicinal plants used in Kilte Awulaelo District, Tigray Region of Ethiopia. *Journal of Ethnobiology and Ethnomedicine*, *9*(1), 65. https://doi.org/10.1186/1746-4269-9-65

Temitope, O. A., & Ogundipe, O. T. (2012). Biodiversity of Sapindaceae in West Africa: A checklist. *International Journal of Biodiversity and Conservation*, *4*(10), 326–331. https://doi.org/10.5897/ijbc12.032

Trott, O., & Olson, A. J. (2009). AutoDock Vina: Improving the speed and accuracy of docking with a new scoring function, efficient optimization, and multithreading. *Journal of Computational Chemistry*, *31*, 455–461. https://doi.org/10.1002/jcc.21334

Uddin, Z., Li, Z., Song, Y. H., Kim, J. Y., & Park, K. H. (2017). Visconata: A rare flavonol having long chain fatty acid from Dodonaea viscosa which inhibits Human neutrophil elastase (HNE). *Tetrahedron Letters*, *58*(25), 2507–2511. https://doi.org/10.1016/j.tetlet.2017.05.059

Van Wyk, B. E., Heerden, F. V., & Oudtshoorn, B. V. (2002). Medicinal Plants of South Africa. *Briza Publications*, 108–109.

Vasu, D., Sunitha, M. M., Srikanth, L., Swarupa, V., Prasad, U. V., Sireesha, K., Yeswanth, S., Kumar, P. S., Venkatesh, K., Chaudhary, A., & Sarma, P. V. G. K. (2015). In Staphylococcus aureus the regulation of pyruvate kinase activity by serine/threonine protein kinase favors biofilm formation. *3 Biotech*, *5*(4), 505–512. https://doi.org/10.1007/s13205-014-0248-3

Veber, D. F., Johnson, S. R., Cheng, H. Y., Smith, B. R., Ward, K. W., & Kopple, K. D. (2002). Molecular properties that influence the oral bioavailability of drug candidates. *Journal of Medicinal Chemistry*, *45*(12), 2615–2623. https://doi.org/10.1021/jm020017n

Wink, M. (2015). Modes of Action of Herbal Medicines and Plant Secondary Metabolites. *Medicines*, *2*(3), 251–286. https://doi.org/10.3390/medicines2030251

Wolde-mariam, M., Limenih, Y., & Umer, S. (2015). Ethnobotanical study on traditional medicinal plants in Dega Damot woreda, Amhara region, North Ethiopia. *International Journal of Research in Pharmacy and Chemistry*, *5*(2), 258–273.

World Health Organization (WHO). (2013). WHO Traditional Medicine Strategy 2014-2023. *World Health Organization (WHO)*, 1–76. https://doi.org/2013

Yusuf, A. J., Abdullahi, M. I., Aleku, G. A., Ibrahim, I. A. A., Alebiosu, C. O., Yahaya, M., Adamu, H. W., Sanusi, A., Mailafiya, M. M., & Abubakar, H. (2018). Antimicrobial activity of stigmasterol from the stem bark of *Neocarya macrophylla*. *Journal of Medicinal Plants for Economic Development*, *2*(1), 1–5. https://doi.org/10.4102/jomped.v2i1.38

Zeng, R., Deng, J., Dang, L., & Yu, X. (2021). Correlation between the structure and skin permeability of compounds. *Scientific Reports*, *11*(1), 1–8. https://doi.org/10.1038/s41598-021-89587-5

Zhang, X., Wang, J., Zhu, L., Wang, X., Meng, F., Xia, L., & Zhang, H. (2022). Advances in Stigmasterol on its anti-tumor effect and mechanism of action. *Frontiers in Oncology*, *12*(December), 1–13. https://doi.org/10.3389/fonc.2022.1101289

Zonyane, S., Van Vuuren, S. F., & Makunga, N. P. (2013). Antimicrobial interactions of Khoi-San poly-herbal remedies with emphasis on the combination; Agathosma crenulata, Dodonaea viscosa and Eucalyptus globulus. *Journal of Ethnopharmacology*, *148*(1), 144–151. https://doi.org/10.1016/j.jep.2013.04.003

APPENDIX

Appendix 1: ^{1}H-NMR spectrum (400 MHz, $CDCl_3$) of compound **45**

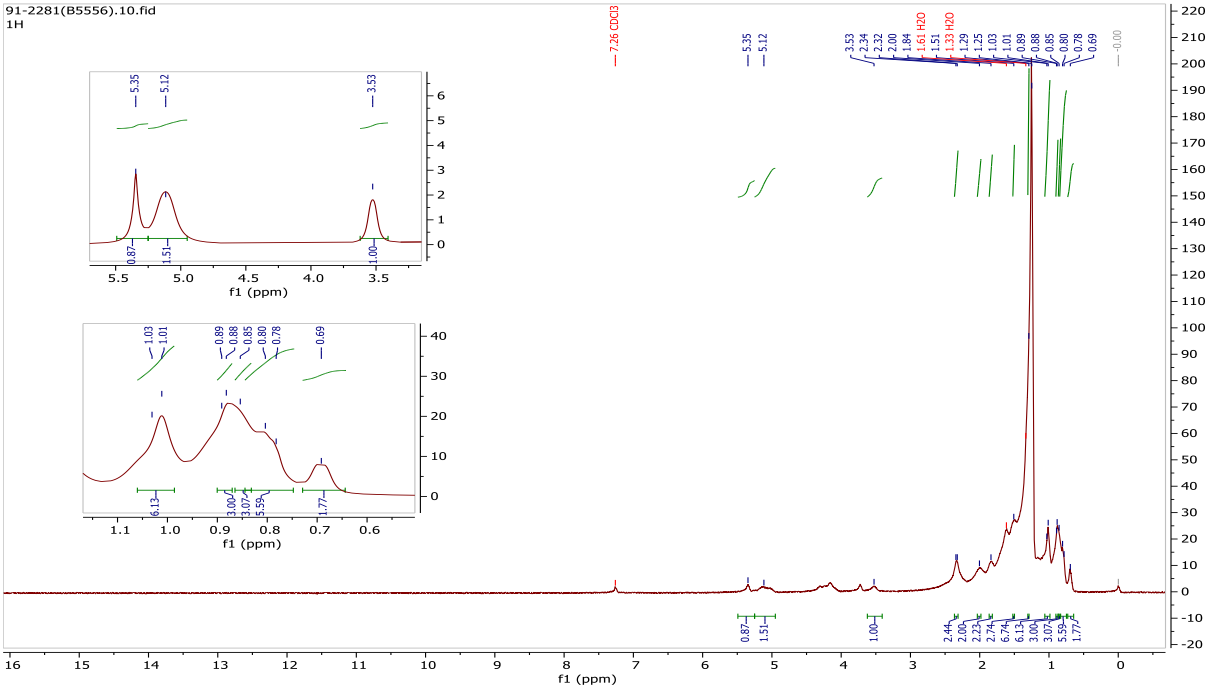

Appendix 2: ^{13}C NMR spectrum (101 MHz, $CDCl_3$) of compound **45**

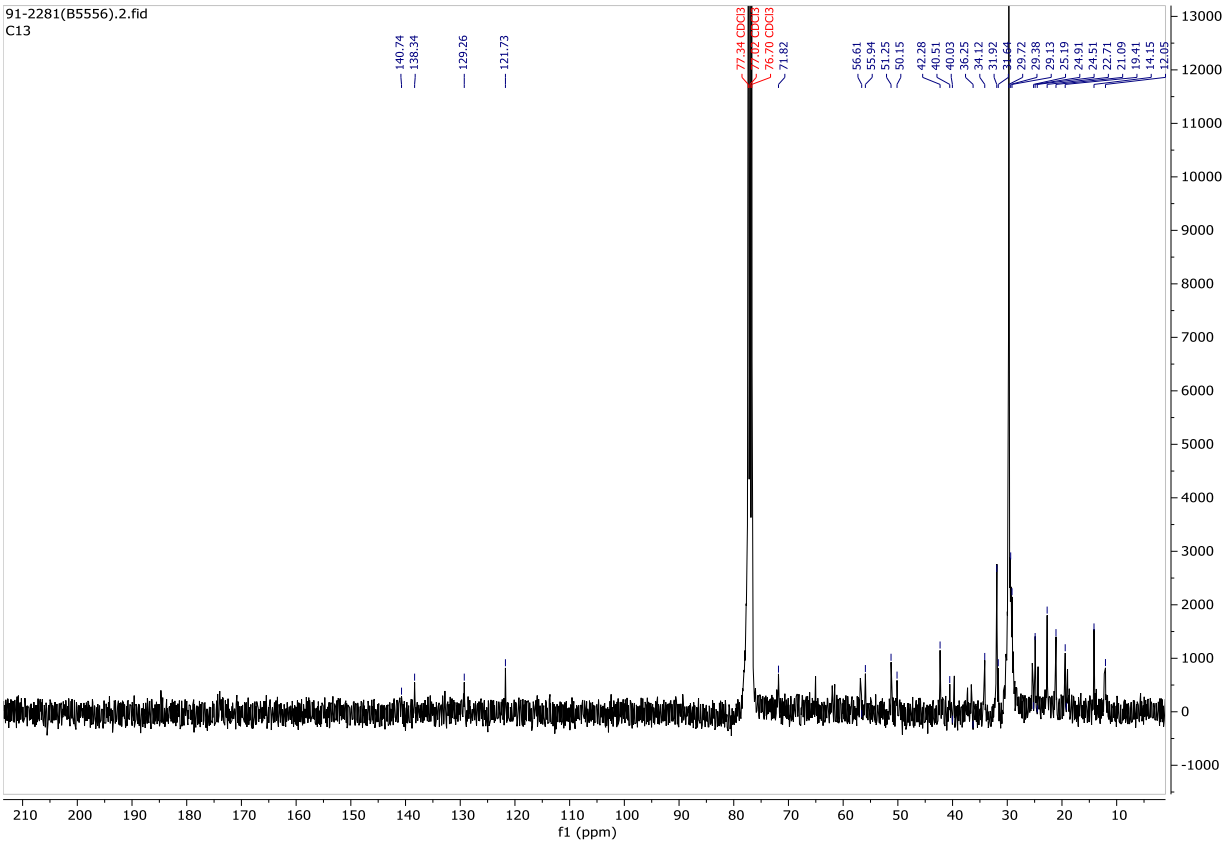

Appendix 3: DEPT-135 spectrum (101 MHz, $CDCl_3$) of compound **45**

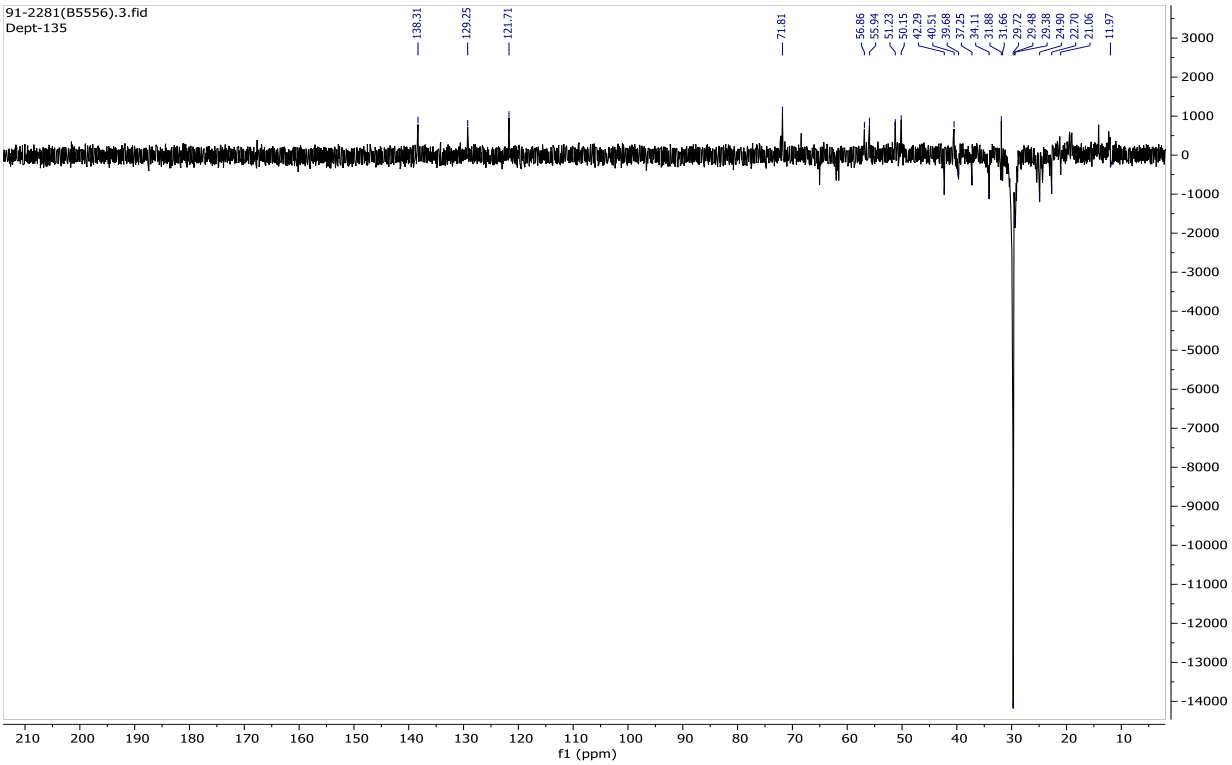

Appendix 4: ^{1}H-NMR spectrum (400 MHz, $CDCl_3$) of compound **46**

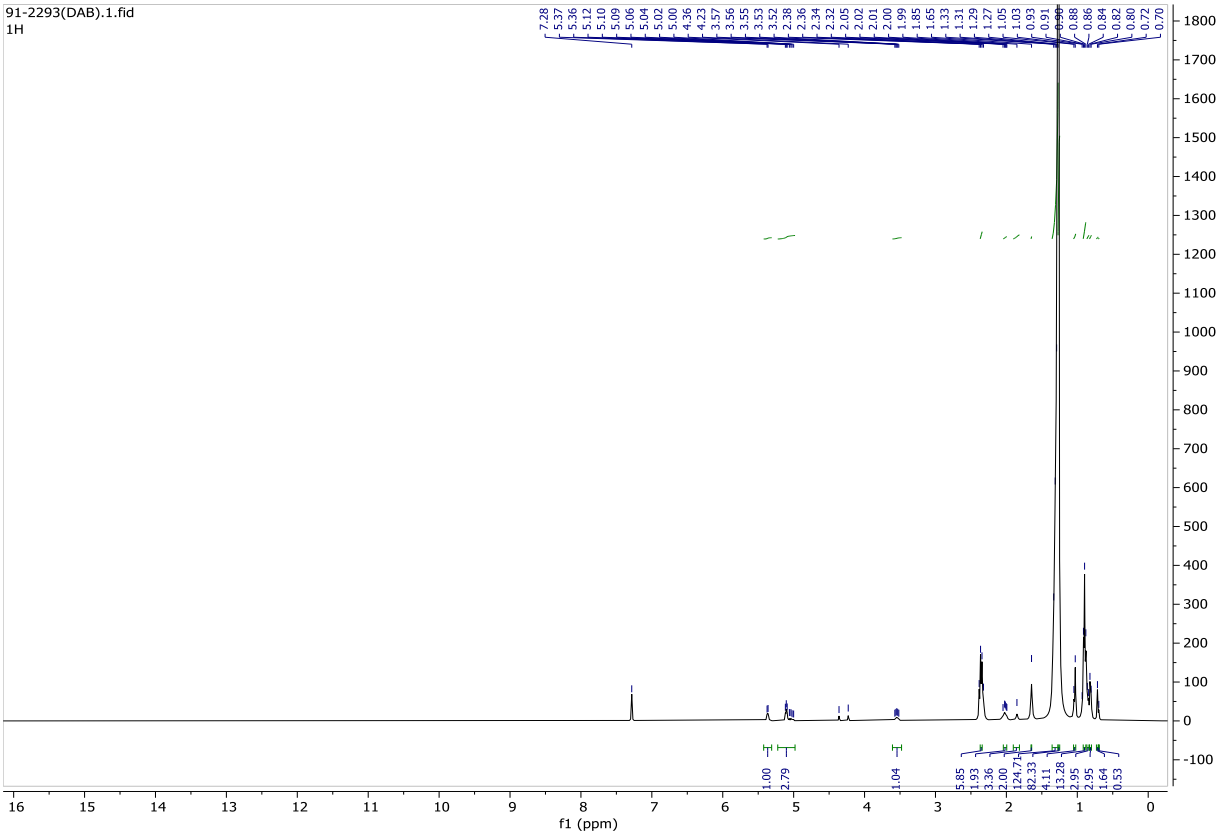

Appendix 5: ^{13}C NMR spectrum (101 MHz, $CDCl_3$) of compound **46**

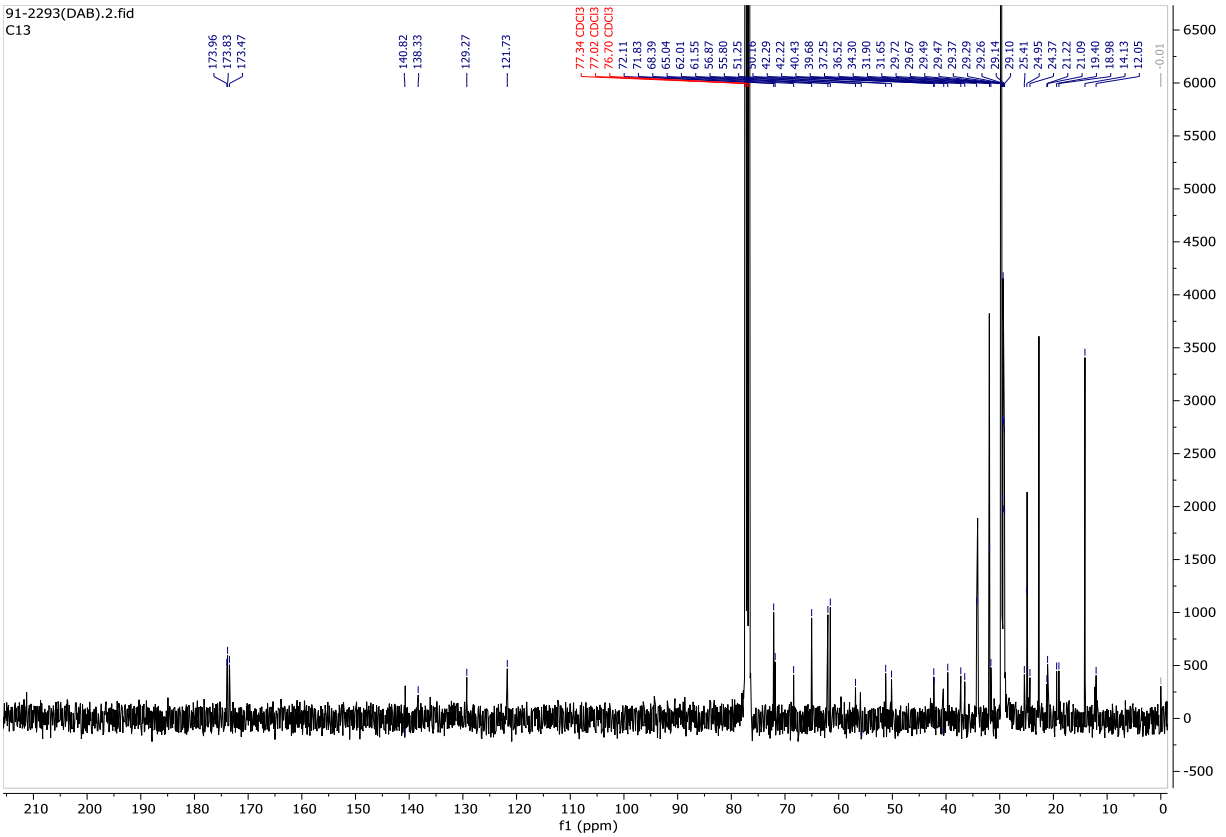

Appendix 6: DEPT-135 spectrum (101 MHz, CDCl3) of compound **46**

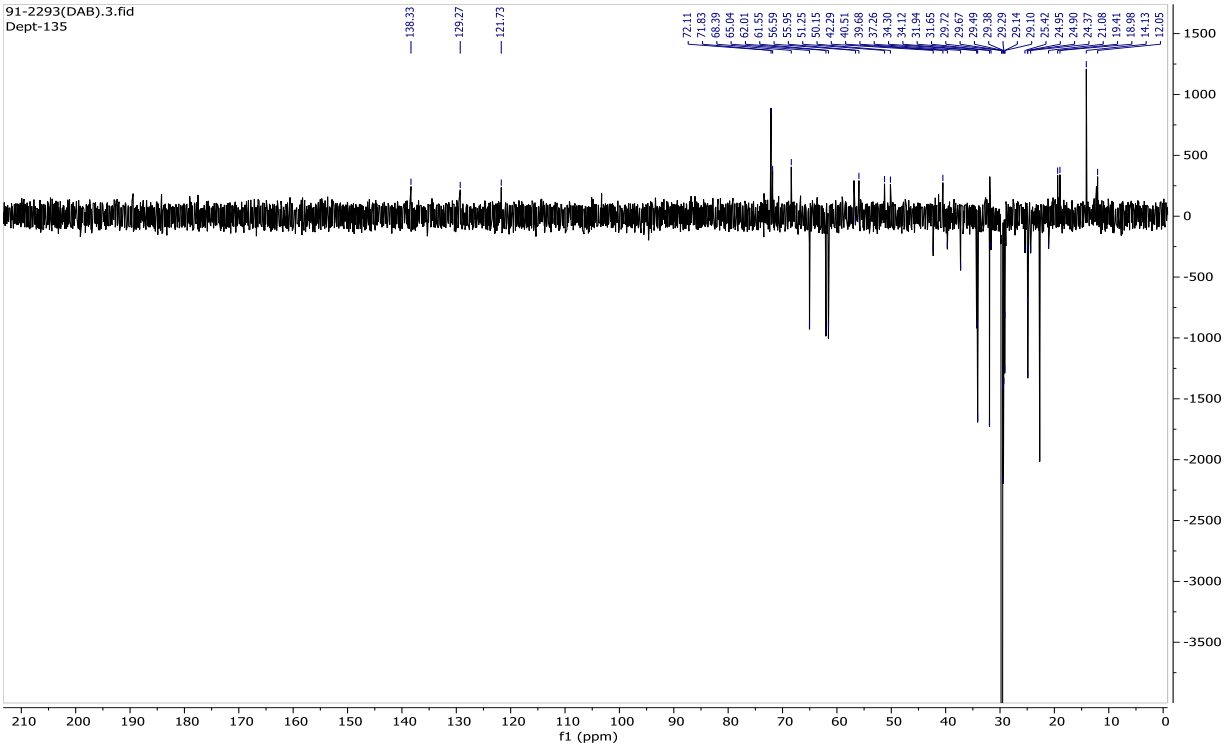

Appendix 7: ^{1}H-NMR spectrum (400 MHz, $CDCl_3$) of compound **47**

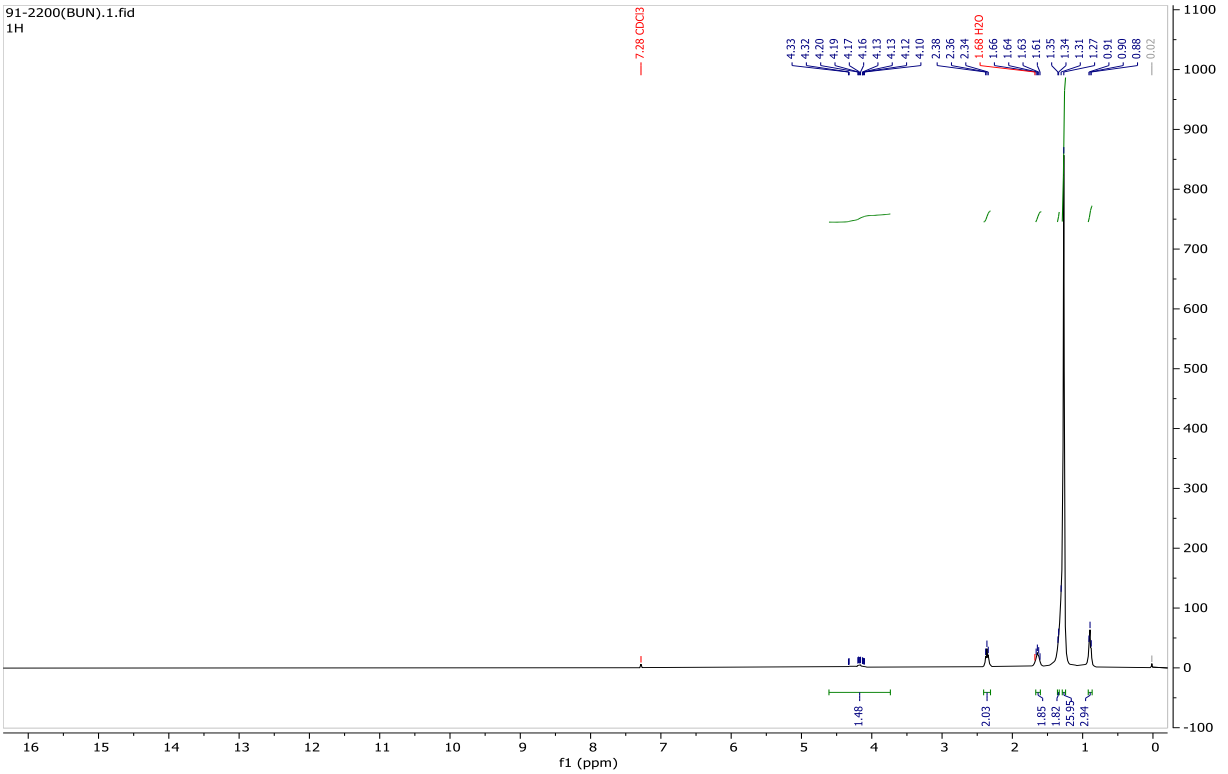

Appendix 8: ^{13}C NMR spectrum (101 MHz, $CDCl_3$) of compound **47**

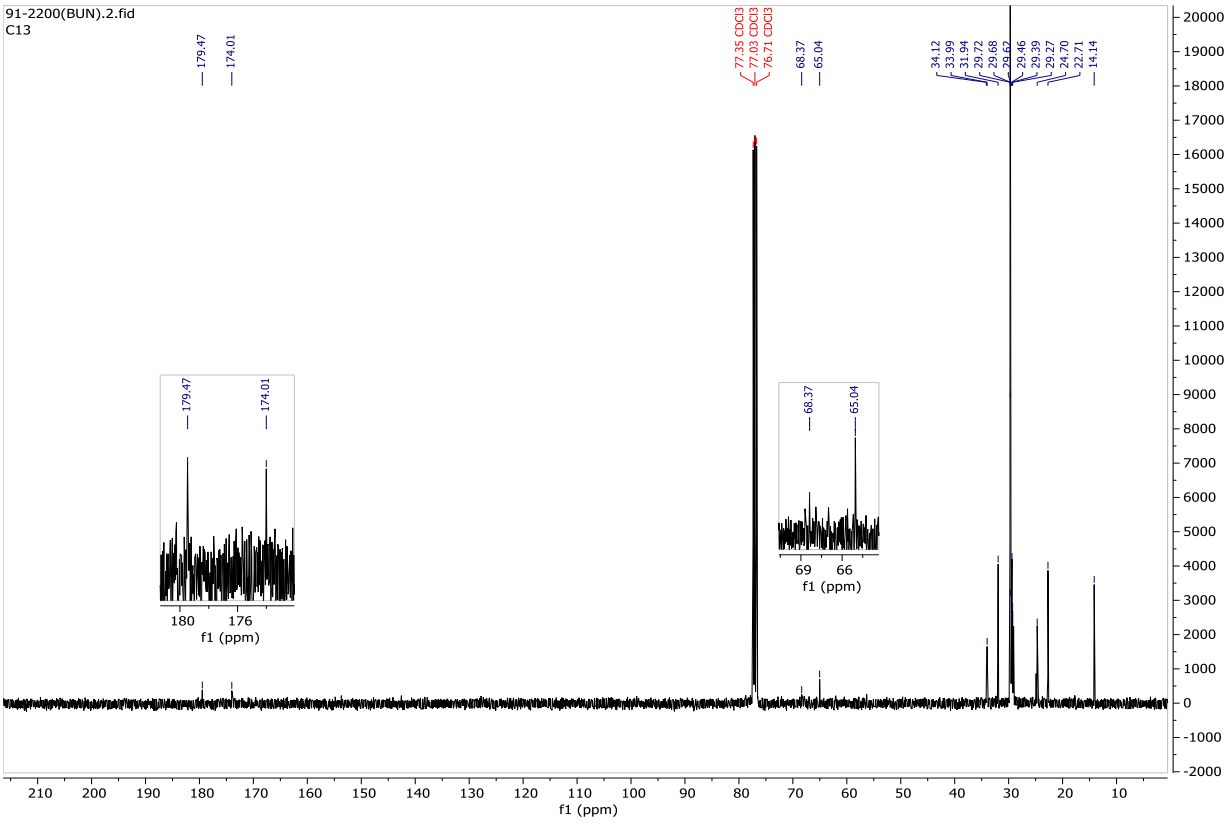

Appendix 9: DEPT-135 spectrum (101 MHz, $CDCl_3$) of compound **47**

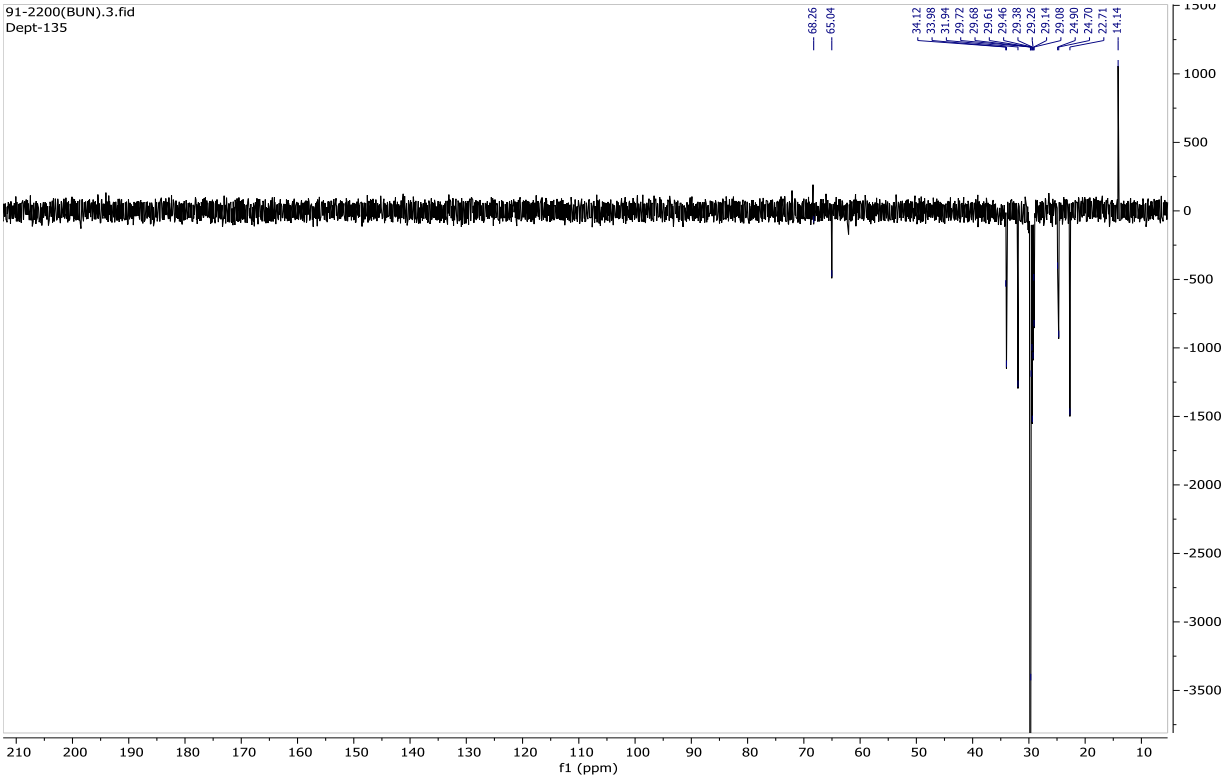

Appendix 10: ^{1}H-NMR spectrum (400 MHz, $CDCl_3$) of compound **48**

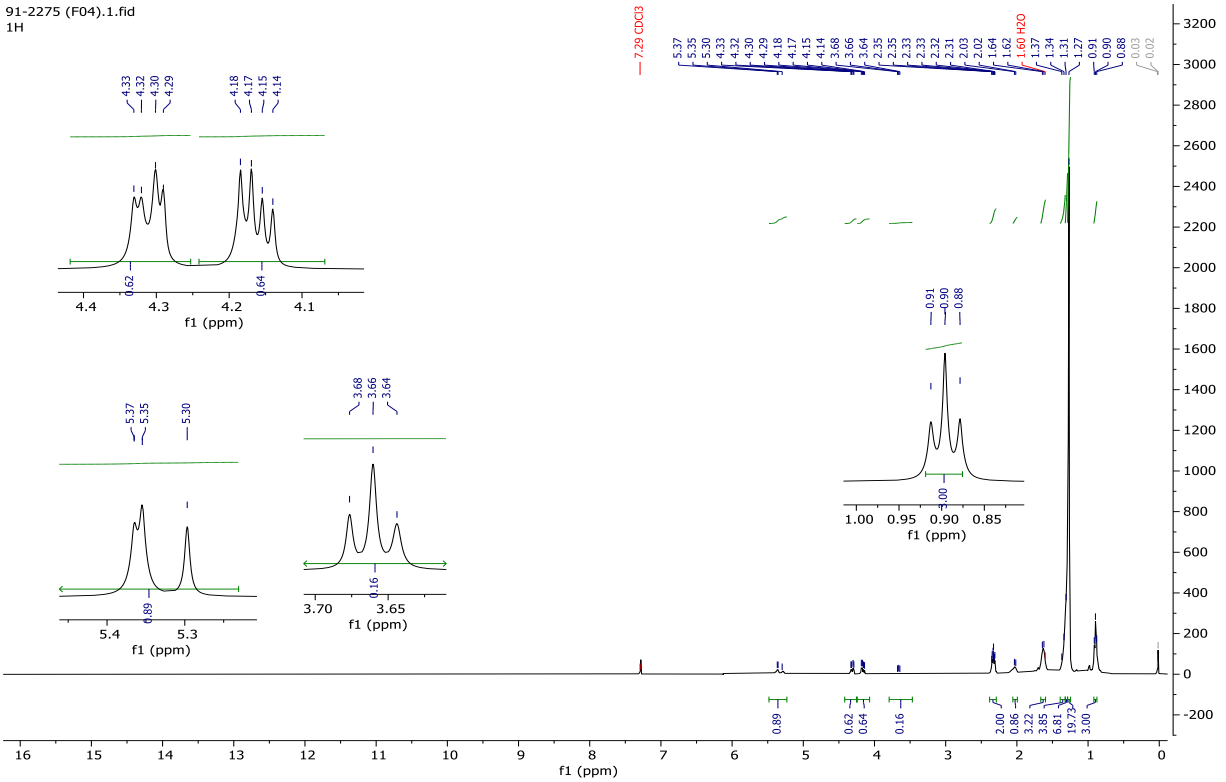

Appendix 11: ^{13}C NMR spectrum (101 MHz, $CDCl_3$) of compound **48**

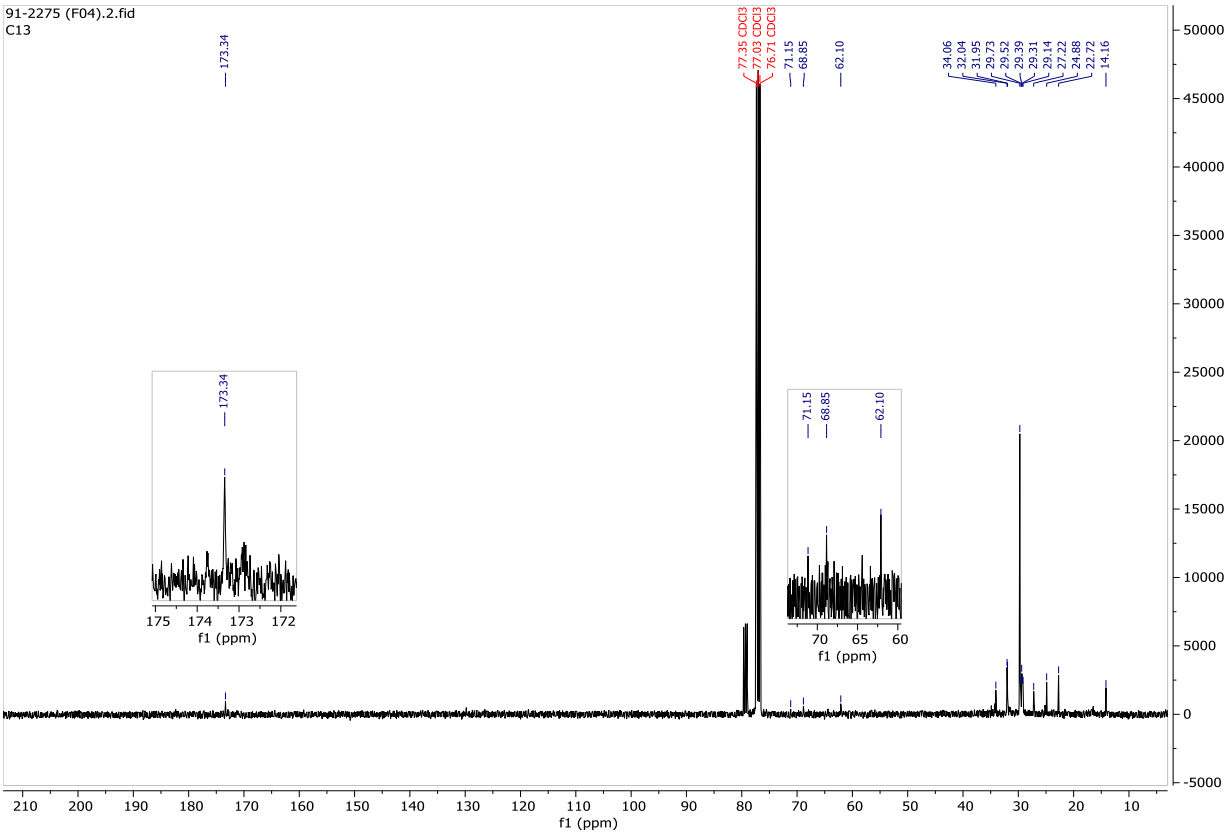

Appendix 12: DEPT-135 spectrum (101 MHz, $CDCl_3$) of compound **48**

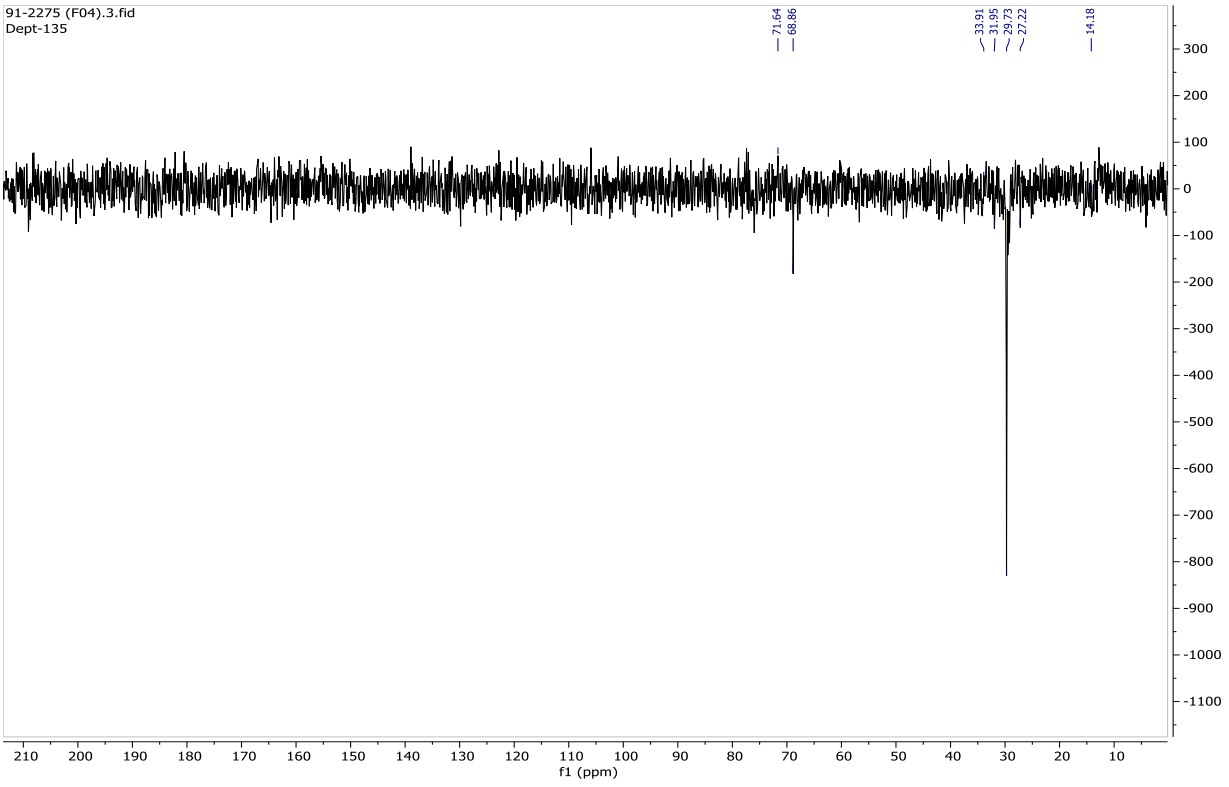

Appendix 13: ^{1}H-NMR spectrum (400 MHz, $CDCl_3$) of compound **49**

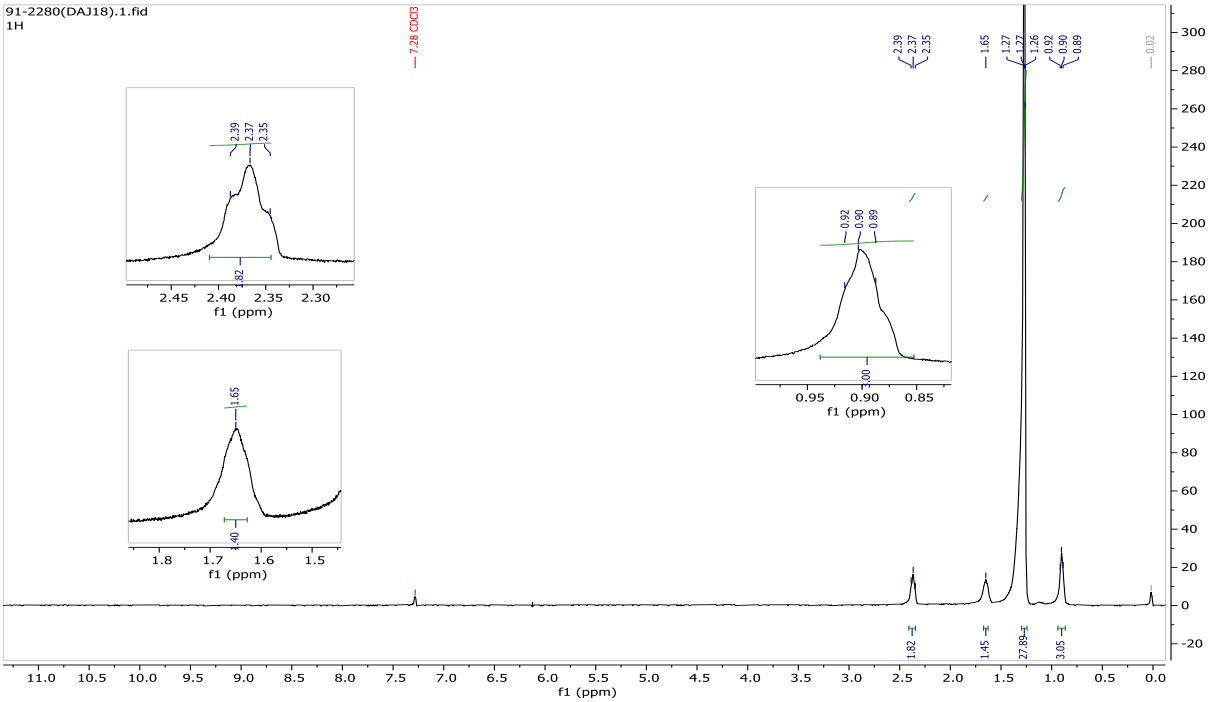

Appendix 14: ^{13}C NMR spectrum (101 MHz, $CDCl_3$) of compound **49**

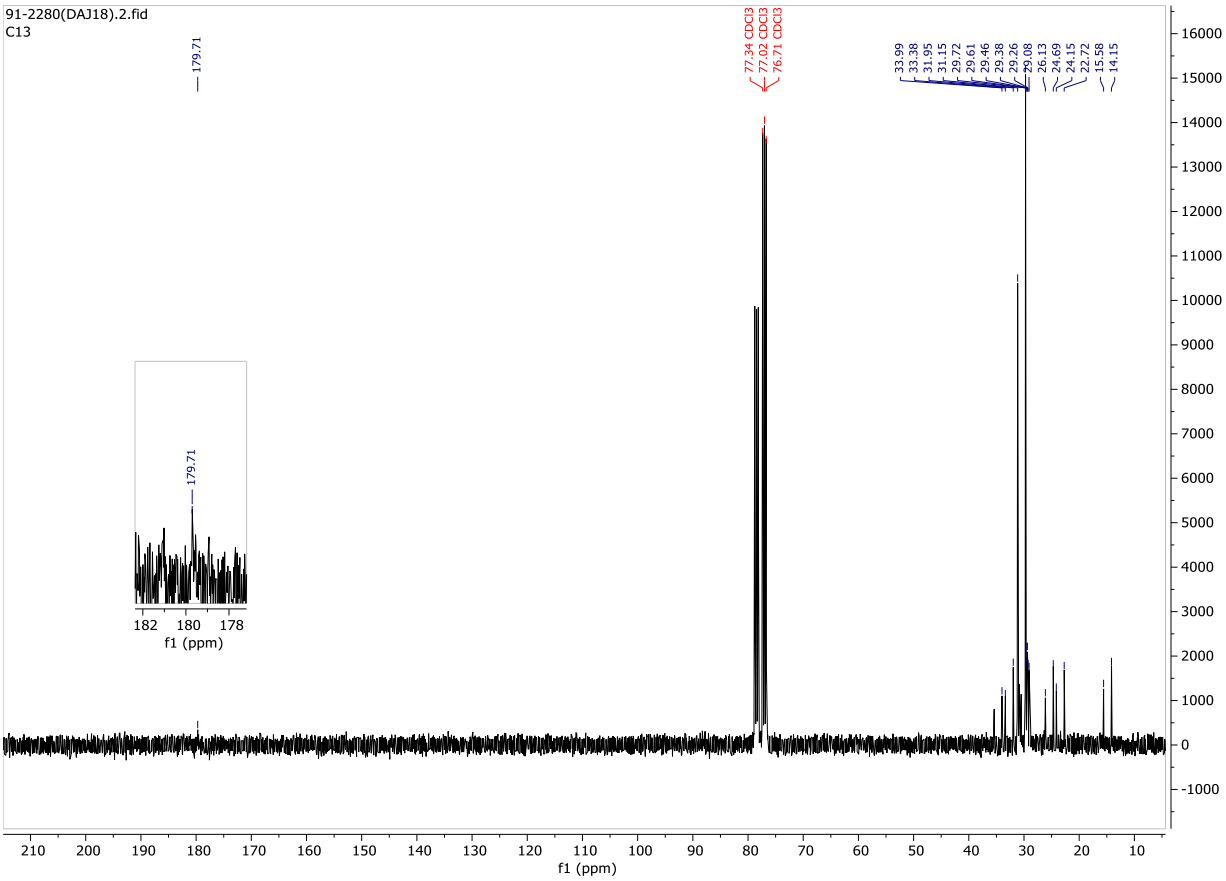

Appendix 15: DEPT-135 spectrum (101 MHz, $CDCl_3$) of compound **49**

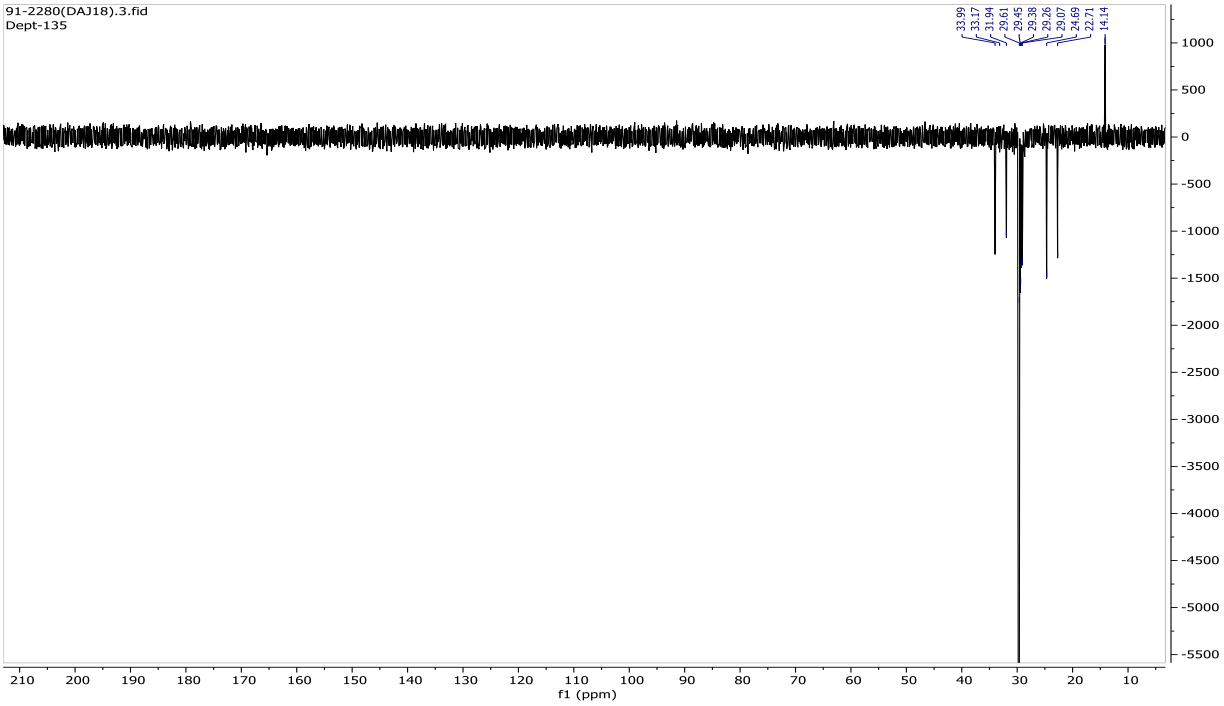

Appendix 16: ^{1}H-NMR spectrum (400 MHz, $CDCl_3$) of compound **50**

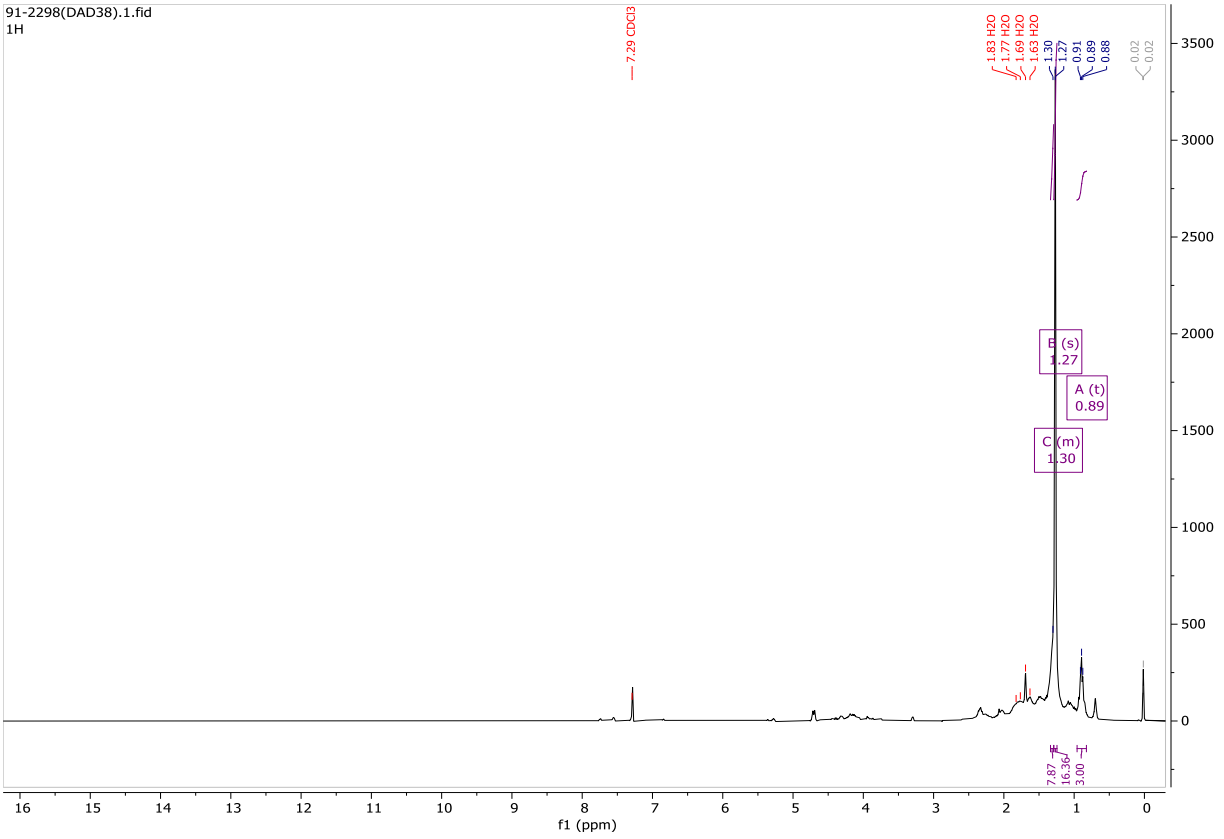

Appendix 17: ^{13}C NMR spectrum (101 MHz, $CDCl_3$) of compound **50**

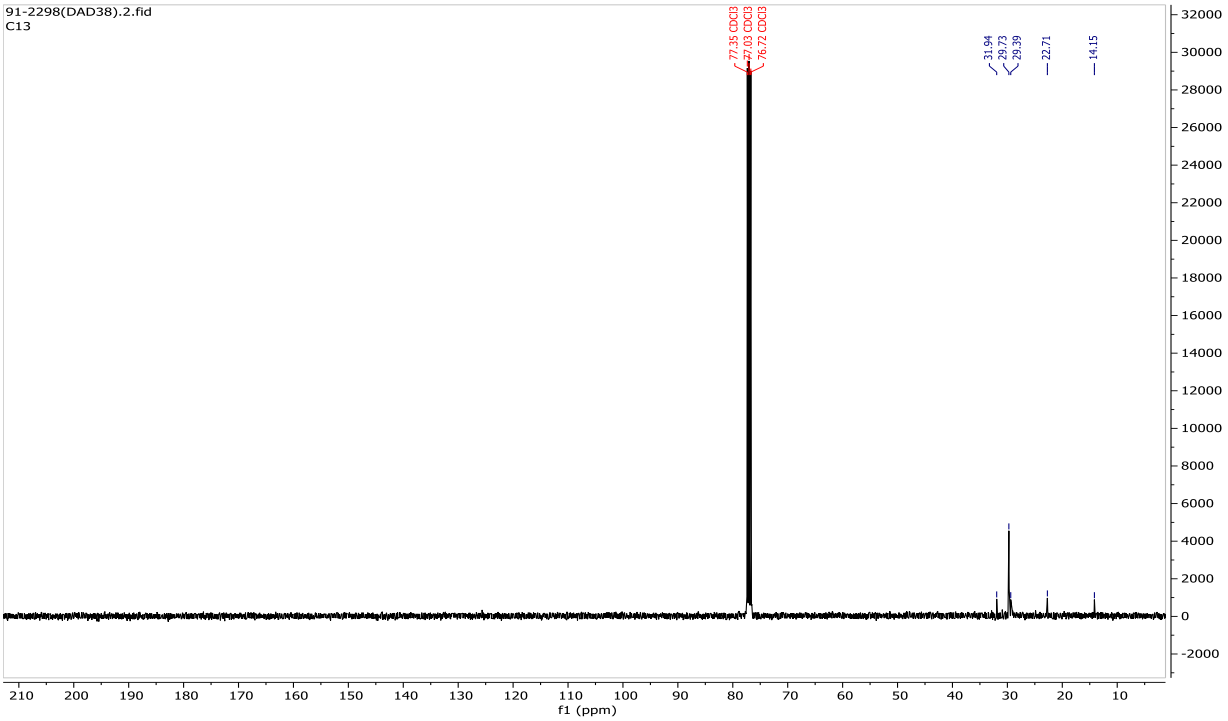

Appendix 18: DEPT-135 spectrum (101 MHz, $CDCl_3$) of compound **50**

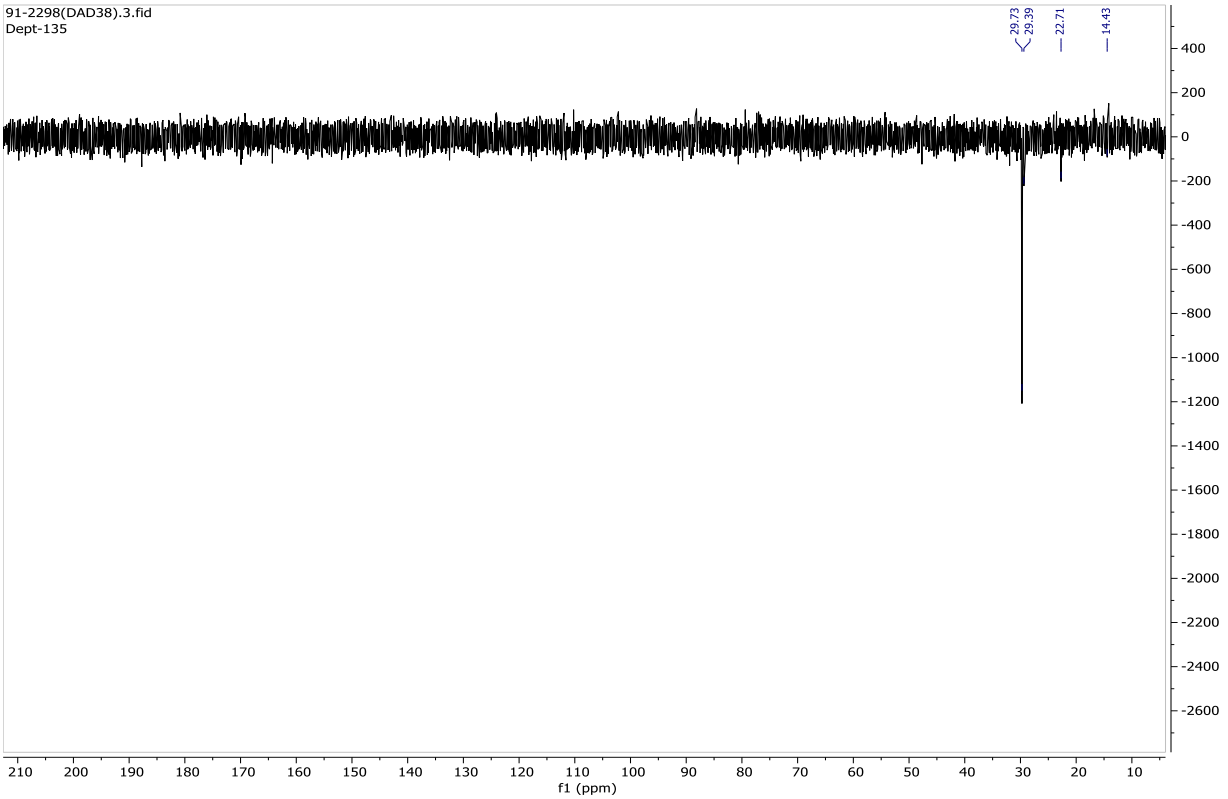

Appendix 19: TLC profile of fractions from the DCM extract (eluent *n*-hexane:EtOAc, 7:3, sprayed with vanillin/H_2SO_4).

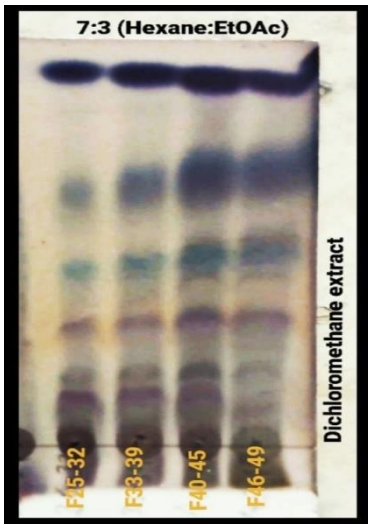

Mobile phase: *n*-Hexane:EtOAc (7:3)

Spraying agent: Vanillin/H_2SO_4

Appendix 20: Phytochemical screening test results of the stem bark extracts of *D. angustifolia*

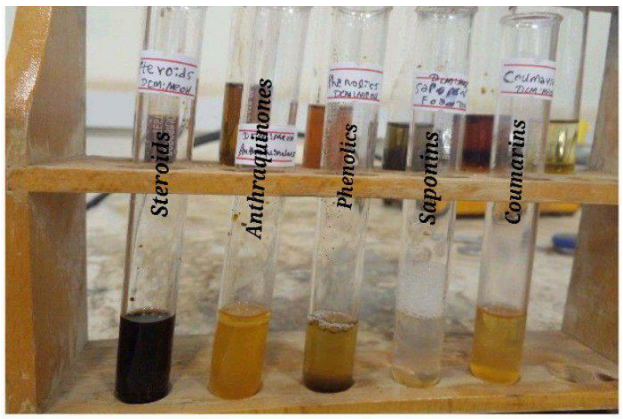

Dichloromethane:MeOH extract

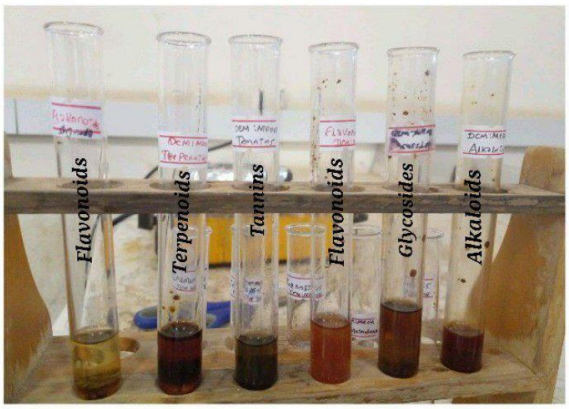

Dichloromethane:MeOH extract

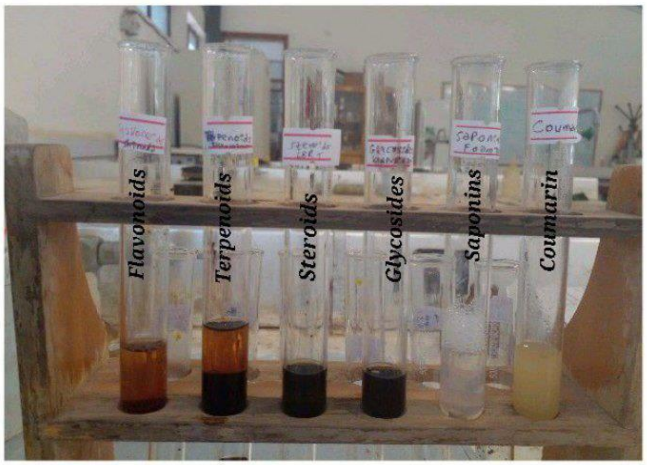

Dichloromethane extract

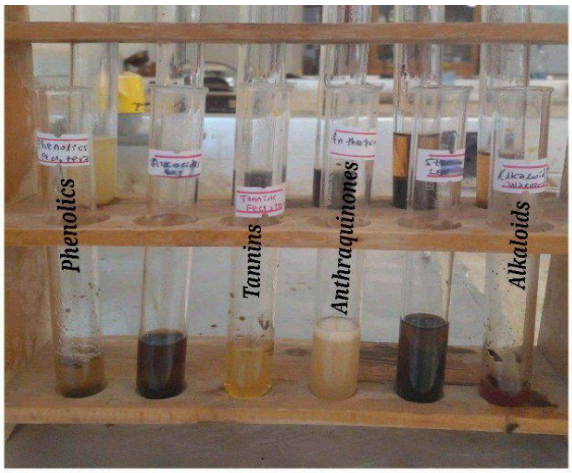

Dichloromethane extract